UTILIZATION OF CURCUMIN AND BIODEGRADABLE POLYMERS IN
INTELLIGENT AND ACTIVE FOOD PACKAGING

A THESIS SUBMITTED TO
THE GRADUATE SCHOOL OF NATURAL AND APPLIED SCIENCES
OF
MIDDLE EAST TECHNICAL UNIVERSITY

BY

EDA YILDIZ

IN PARTIAL FULFILLMENT OF THE REQUIREMENTS
FOR
THE DEGREE OF DOCTOR OF PHILOSOPHY
IN
FOOD ENGINEERING

DECEMBER 2022

Approval of the thesis:

UTILIZATION OF CURCUMIN AND BIODEGRADABLE POLYMERS IN INTELLIGENT AND ACTIVE FOOD PACKAGING

submitted by **EDA YILDIZ** in partial fulfillment of the requirements for the degree of **Doctor of Philosophy** in **Food Engineering, Middle East Technical University** by,

Prof. Dr. Halil Kalıpçılar
Dean, Graduate School of **Natural and Applied Sciences** _____

Prof. Dr. Hami Alpas
Head of the Department, **Food Engineering** _____

Prof. Dr. Gülüm Şumnu
Supervisor, **Food Engineering, METU** _____

Assist. Prof. Dr. Leyla Nesrin Kahyaoğlu
Co-Supervisor, **Food Engineering, METU** _____

Examining Committee Members:

Prof. Dr. Serpil Şahin
Food Engineering, METU _____

Prof. Dr. Gülüm Şumnu
Food Engineering, METU _____

Assoc. Prof. Dr. Halil Mecit Öztop
Food Engineering, METU _____

Assoc. Prof. Özge Şakıyan Demirkol
Food Engineering, Ankara University _____

Assist. Prof. Dr. Nalan Yazıcıoğlu
Department of Nutrition and Dietetics, University of Health Sciences _____

Date: 21.12.2022

I hereby declare that all information in this document has been obtained and presented in accordance with academic rules and ethical conduct. I also declare that, as required by these rules and conduct, I have fully cited and referenced all material and results that are not original to this work.

Name Last name : Yıldız, Eda

Signature :

ABSTRACT

UTILIZATION OF CURCUMIN AND BIODEGRADABLE POLYMERS IN INTELLIGENT AND ACTIVE FOOD PACKAGING

Yıldız, Eda
Doctor of Philosophy, Food Engineering
Supervisor: Prof. Dr. Gülüm Şumnu
Co-Supervisor: Assist. Prof. Leyla Nesrin Kahyaoğlu

December 2022, 205 pages

The main purpose of this study is to produce smart and active packages with curcumin using biodegradable polymers. To fulfill this aim, two different film making methods namely electrospinning and casting were used. Firstly, to take benefit of the halochromic properties of curcumin, it was encapsulated into chitosan/PEO based nanofibers to monitor food freshness. The average diameter of the fibers was found to be between 283 ± 27 nm and 338 ± 35 nm. It was concluded that increasing the chitosan amount in nanofibers decreased the diameter of the fibers. Throughout the storage period, the color change of intelligent packaging film was correlated with the chemical (TVB-N) and microbial deterioration (total mesophilic aerobic bacterial count) of the chicken breast. Curcumin loaded nanofiber satisfied the expectation and enabled to visualize real time monitoring of chicken spoilage. For active food packaging, curcumin was encapsulated into chickpea flour/polyethylene oxide (PEO) nanofibers. The effect of heat treatment (microwave or conventional) on electrospun solution and film characteristics was investigated.

Although microwave treated active films showed an antimicrobial effect against *E.coli* with an inhibition area of 1.62 ± 0.36 cm^2, they did not exhibit any effect towards *S.aureus*. Then, curcumin incorporated chitosan/faba bean flour films were produced by a solvent casting technique. To eliminate the potential drawbacks of biopolymer, different crosslinking agents (glutaraldehyde and citric acid) were incorporated into the film forming matrix at different ratios. Citric acid and gluteraldehyde reduced swelling degree by 75% and 13% compared to the films without cross-linker, respectively. Increasing both crosslinking ratios decreased the water vapor permeability drastically which was more than 110%. At the end of the analysis, it was concluded that citric acid cross-linked films had a more feasible character in terms of swelling degree, water solubility and mechanical properties with respect to the other films containing glutaraldehyde. Moreover, citric acid was utilized as a crosslinking agent to improve the packaging performances of chickpea flour/chitosan/curcumin film. Elongation at break (EAB) value increased from 1.64% ± 0.13%, to 11.1%± 1.21% whereas tensile strength (TS) value decreased from 7.83± 0.08 MPa to 3.58± 0.20 MPa. The film with the highest citric acid concentration showed an inhibitory effect on both *E.coli* (inhibition zone area 5.88 ± 0.49 cm^2) cm and *S. aureus* (inhibition zone area 1.59 ± 0.27 cm^2). Further, it enhanced the shelf life of chicken breast samples up to 9-day. As a result, citric acid crosslinked chickpea flour/chitosan active film can be recommmended to be used in active packaging to extend the shelflives of microbiologically susceptible perishable meat foods..

Keywords: Curcumin, Electrospinning, Casting, Intelligent Packaging, Active Packaging

ÖZ

KURKUMİN VE BİOÇÖZÜNÜR POLİMERLERİN AKILLI VE AKTİF GIDA PAKETLEMEDE KULLANIMI

Yıldız, Eda
Doktora, Gıda Mühendisliği
Tez Yöneticisi: Prof. Dr. Gülüm Şumnu
Ortak Tez Yöneticisi: Dr. Öğr. Üyesi Leyla Nesrin Kahyaoğlu

Aralık 2022, 205 sayfa

Bu çalışmanın temel amacı, biyolojik olarak parçalanabilen polimerler kullanılarak kurkumin içeren akıllı ve aktif ambalajların üretilmesidir. Bu amacı gerçekleştirmek için elektroeğirme ve döküm olmak üzere iki farklı film yapım yöntemi kullanılmıştır. İlk olarak, kurkuminin halokromik özelliklerinden faydalanmak için, gıda tazeliğini izlemek üzere kitosan/PEO bazlı nanoliflere kapsüllendi. Liflerin ortalama çapı 283±27 nm ile 338±35 nm arasında bulunmuştur. Nanoliflerde kitosan miktarının artmasının lif çapını azalttığı sonucuna varılmıştır. Depolama süresi boyunca, akıllı ambalaj filminin renk değişimi, tavuk göğsünün kimyasal (TVB-N) ve mikrobiyal bozulması (toplam mezofilik aerobik bakteri sayısı) ile ilişkili bulunmuştur. Kurkumin yüklü nanolifler beklentiyi karşılamış ve tavuk bozulmalarının gerçek zamanlı görsel olarak izlenmesini sağlamıştır. Aktif gıda paketlemesi için kurkumin, nohut unu/polietilen oksit (PEO) nano liflerine kapsüllenmiştir. Isıl işlemin (mikrodalga veya konvansiyonel) elektroeğirme işleminde kullanılan çözelti ve film özellikleri üzerindeki etkileri araştırılmıştır. Mikrodalga ile işlenmiş aktif filmler, 1.62±0.36 cm²'lik bir inhibisyon alanı ile *E.coli*'ye karşı antimikrobiyal etki göstermesine rağmen, *S.aureus*'a karşı herhangi

bir etki göstermemiştir. Daha sonra, kurkumin katkılı kitosan/bakla unu filmleri, döküm tekniği ile üretilmiştir. Biyopolimerin potansiyel dezavantajlarını ortadan kaldırmak için, film oluşturucu matrikse farklı oranlarda farklı çapraz bağlayıcı maddeler (gluteraldehit ve sitrik asit) eklenmiştir. Sitrik asit ve gluteraldehit, şişme derecesini çapraz bağlayıcı içermeyen filmlere kıyasla sırasıyla %75 ve %13 oranında azaltmıştır. Her iki çapraz bağlama oranının arttırılması, %110'dan fazla olan su buharı geçirgenliğını büyük ölçüde sınırlandırmıştır. Analizler sonucunda sitrik asit çapraz bağlı filmlerin glutaraldehit içeren diğer filmlere göre daha uygun bir karaktere sahip olduğu sonucuna varılmıştır. Analizler sonucunda sitrik asit çapraz bağlı filmlerin glutaraldehit içeren diğer filmlere göre daha uygun bir karaktere sahip olduğu sonucuna varılmıştır. Ayrıca, nohut unu/kitosan/kurkumin filminin ambalaj performansını iyileştirmek için çapraz bağlama maddesi olarak sitrik asit kullanılmıştır. Kopmada uzama (EAB) değeri %1,64 ± %0,13'ten %11,1± %1,21'e yükselirken, çekme mukavemeti (TS) değeri 7,83± 0,08 MPa'dan 3,58± 0,20 MPa'ya düşmüştür. En yüksek sitrik asit konsantrasyonuna sahip film hem *E.coli* (inhibisyon bölgesi alanı $5,88 \pm 0,49$ cm^2) cm hem de *S. aureus* (inhibisyon bölgesi alanı $1,59 \pm 0,27$ cm^2) üzerinde inhibitör etki göstermiştir. Ayrıca, tavuk göğsü örneklerinin raf ömrünü 9 güne kadar uzatmıştır. Sonuç olarak, sitrik asit çapraz bağlı nohut unu/kitosan aktif filminin mikrobiyolojik açıdan hassas bozulabilir et gıdalarının raf ömürlerini uzatmak için aktif paketlemede kullanılması önerilebilir.

Anahtar Kelimeler: Kurkumin, Elektroeğirme, Döküm, Akıllı Paketleme, Aktif Paketleme

To my gradparents, mom and my husband

ACKNOWLEDGMENTS

I am the luckiest child in the world to have such a strong and incredible mom, Tekşen Özer. She always gives me the biggest support, she stands always stronger and more confident. She is the most beautiful example to remind me that I can do everything if I trust myself.

TABLE OF CONTENTS

LIST OF TABLES

TABLES

LIST OF FIGURES

FIGURES

CHAPTER 1

INTRODUCTION

1.1 Active and Intelligent Food Packaging

Traditional food packaging is defined as a passive barrier to prevent adverse influences of the environment on food. On the other hand, modern food packages have different roles, such as retaining the safety and quality of the food. Although traditional food packages are designed to lower the interaction between food and package-environment as much as possible, innovative food packages aim to increase this interaction. Intelligent and active packages are the two main concepts that bring a new meaning to food packaging (Figure 1.1) (Mohammadian et al., 2020). The main difference between these two concepts is that intelligent packaging can help to monitor the condition of the food, whereas active packages change the surrounding environmental conditions of food inside the package to increase the shelf life (Drago et al., 2020)

```
                    ┌─────────────────────────┐
                    │ Innovative food packaging│
                    │        systems           │
                    └─────────────────────────┘
              ┌───────────────┴────────────────────┐
      ┌───────────────┐                    ┌──────────────────┐
      │Active packaging│                    │Intelligent packaging│
      └───────────────┘                    └──────────────────┘
        ┌────┴─────────┐                   ┌────┴──────────────────┐
  ┌──────────┐  ┌──────────┐         ┌──────────────────┐
  │Scavenger │  │Releasing │         │External indicators│
  │systems   │  │systems   │         │      (TTI)        │
  │(Absorbers)│  │(Emitters)│         └──────────────────┘
  └──────────┘  └──────────┘         ┌──────────────────┐
                     │               │Internal indicators│
              ┌──────────┐           │(gas and microbial)│
              │Antioxidant│          └──────────────────┘
              └──────────┘           ┌──────────────────┐
              ┌──────────┐           │Data carriers (RFID,│
              │Antimicrobial│        │     barcode)      │
              └──────────┘           └──────────────────┘
              ┌──────────┐           ┌──────────────────┐
              │ Antifungi │          │     Sensors       │
              └──────────┘           └──────────────────┘
```
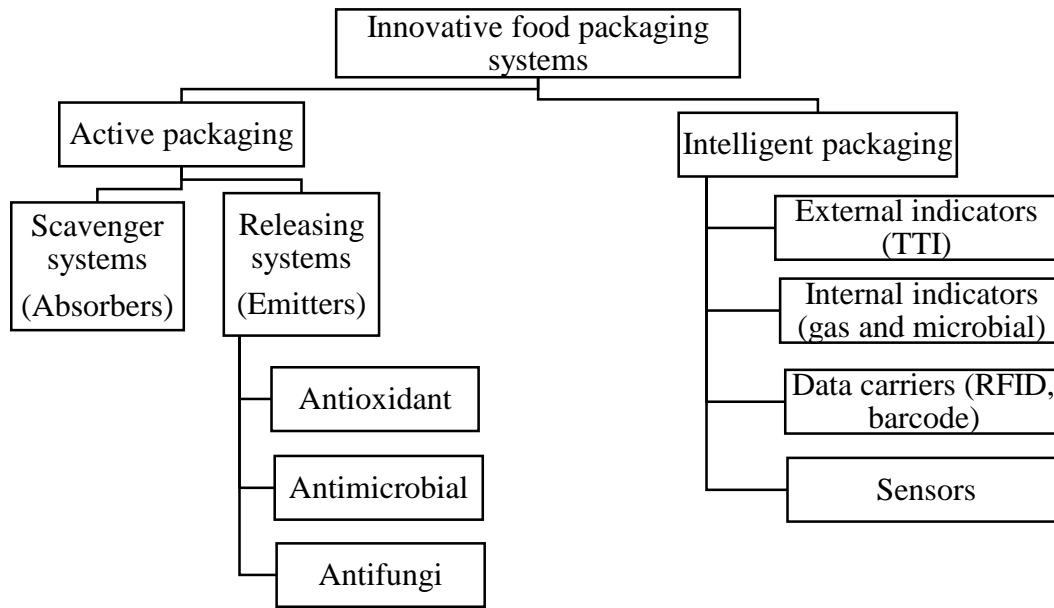
Figure 1.1. Brief categorization of active and intelligent packaging systems

According to European regulation (EC) No 450/2009, active packages are systems based on "deliberately incorporating compounds that can release or absorb components into or from inside the package." Active packaging systems are divided into two sub main categories: active scavenging systems, called absorbers, and active releasing systems, emitters. The active scavenging systems can remove/hold undesirable components from either food or the environment, whereas active releasing systems can introduce compounds to food or headspace (Yildirim et al., 2018).

There are numerous examples of moisture controllers, ethylene scavengers, CO_2 emitters, and oxygen scavengers which are the examples of absorber-based active packages as shown in Table 1.1. Releasing system based packages and their possible alternatives with antioxidant, anti-fungi, and antimicrobial characteristics are also illustrated in Table 1.1.

Table 1.1 Examples of active packaging studies.

	Purpose	Active component	Results	References
Oxygen scavengers	To detect leakage in modified atmosphere package	Leuco dyes (leuco indigo and leuco thioindigo)	An irreversible color change is observed (from pale yellow to deep blue)	(Wilhelm & Wolfbeis, 2011)
Carbon dioxide absorbers and emitters	To detect the excess amount of CO_2 concentration which is higher than critical threshold. CO_2 inside the package causes physiological injuries of the products like banana, cauliflower, and mushroom.	Sodium carbonate Sodium glycinate	The firmnesss values of mushrooms in active packages was closer to its initial value after 5 day storage.	(Hurley et al., 2013a)

Table 1.1 (cont'd)

Moisture controllers	High humidity in the packages promotes moisture condensation which resulted in microbial growth. To control humidity, moisture absorbers are preferred.	silica gel, xylitol, CaCl2, sorbitol, KCl, CaO and bentonite	After 5 day storage, the mushrooms packed with moisture controllers were still marketable.	(Mahajan et al., 2008)
Ethylene scavengers	Ethylene is a hormone that controls ripening, senescence, dormancy. To increase the shelf life of the fresh produce ethylene scavenger is utilized.	Granular-activated carbon (GAC) alone or impregnated with palladium as a catalyst (GAC−Pd).	Tomatoes treated with ethylene scavengers had lower weight loss, and less softening. This treatment also prevented decaying.	(Bailén et al., 2006)

Table 1.1 (Cont'd)

Antioxidant release	To delay lipid oxidation and decrease protein denaturation on a fatty fish species. The maintenance of quality and the extension of the shelf life of frozen fish by packaging systems	BHT	Fish fillets packed in active films had lower TBA and peroxide value which were the products of oxidation..	(Torres-Arreola et al., 2007)
Antioxidant release	To decrease oxidation of soy bean oil	α-Tocopherol	Oxidation products such as proxide value in soy bean oil packed with α-tocopherol film was lower than control.	(Manzanarez-López et al., 2011)

Table 1.1 (Cont'd)

Anti-fungi effect	To delay the fungi contamination of tomato	Oregano essential oil	The active film showed anti fungi effect on tomatoes without any negative sensorial effect.	(Rodriguez-Garcia et al., 2016)

Perishable foods lose their quality during harvesting, transport, and storage or on the market shelves. As can be understood from Table 1, the main reasons for food deterioration are oxidation, spoilage and metabolism of the food. These factors decrease nutritional value and cause rancidity, and color change in the food. Indeed, they affect food quality, safety, consumer decision, consumer health, and the most importantly economy. Furthermore, pathogenic microorganisms threaten human health such that nearly 76 million people in the US are affected by food-borne diseases. This results in increased medical cost, the number of deaths and finally the economic burden (Han et al., 2018). Therefore, all these outcomes emphasize the necessity and importance of active food packages.

To hinder the deterioration of food, either synthetic or bioactive compounds were incorporated into the food packaging matrix. Butylated hydroxyanisole (BHA), ethylenediaminetetraacetic acid (EDTA), butylated hydroxytoluene (BHT) are the most commonly utilized synthetic active compounds. Their antioxidant and antimicrobial activities have been studied many times. For example, the antimicrobial activity of EDTA incorporated zein films was examined on *Listeria*

monocytogenes, *Escherichia coli* O157:H7, and *Salmonella typhimurium* and the packaging performance of the films was tested on ground beef. Active films had antimicrobial activity on all tested microorganisms and they extended the shelf life of foods by inhibiting both microbial growth and retarding lipid oxidation (Ünalan et al., 2011). Different amounts of BHA were encapsulated into the gelatin nanofiber by electrospinning technique. The activity of the fibers was evaluated by the preservation of strawberries. Films showed an antibacterial effect on *S. aureus* and slowed down the growth rate. Furthermore, the films retarded the decay of strawberries by inhibiting four mold genera. The results also highlighted anti fungi effect of the BHA (L. Li et al., 2018). In another study, BHT (0, 8, and 14 mg/g) was added to the LDPE films, and the effects of active films on cheese shelf life were determined at 5ºC during the storage. Although active film containing 8mg/g BHT extended the shelf life of cheese from 20 days to 100 days by retarding lipid oxidation, the amount of BHT diffusing into the cheese exceeded the legal limits for the film containing 14 mg/g BHT (Soto-Cantú et al., 2008). As illustrated in this example, the usage of synthetic compounds is strictly regulated because of their potential toxicity. The researchers are suspicious that these compounds might cause liver damage. The analysis carried out on laboratory animals proved this hypothesis since higher carcinogenic compounds are measured in the blood of these animals (BHA and BHT). Furthermore, these compounds have great potential to make molecular complexes with DNA and damage the helical structure of nucleic acids (Shahidi & Ambigaipalan, 2015).

Because of the potential toxicity of synthetic compounds, natural phenolics extracted from roots, leaves, seeds of fruit and vegetables have attracted attentions. Naturally occurring phenolic compounds can be classified under six groups, namely, phenolic acids, flavanoids, stilbenes, courmarines, lignans and finally tannins (Shahidi & Ambigaipalan, 2015).

Phenolic acids are divided into two main subcategories hydroxycinnamic acid and hydroxybenzoic acid, which possess both antioxidant and antimicrobial characteristics. These compounds have at least one aromatic ring in their structure

and in the aromatic ring, at least one hydrogen is exchanged with a hydroxyl group (Heleno et al., 2015). P- hydroxybenzoic acid, protocatechuic acid, vanilic acid, syringic acid, gallic acid, p-coumaric acid, caffeic acid, ferulic acid, sinapic acid are the most common examples of hydroxycinnamic acid and hydroxybenzoic acid (Shahidi & Ambigaipalan, 2015). Their antioxidant and antimicrobial activities have already been studied many times by researchers. For example, synthesized p-hydroxybenzoic acid-grafted chitosan conjugates showed antimicrobial activity against G (+) (*B. subtilis. S. aureus)* and G (-) (*E. coli, P. aeruginosa)* bacteria. The antioxidant activity of the samples also was proved by the DPPH and ABTS methods (J. Wang & Jiang, 2022). Gallic acid was encapsulated into the lentil flour/PEO nanofibers and walnuts were packaged with these active nanofibers. Accelerated shelf life testing results showed that active nanofibers reduced the oxidation of food samples (Aydogdu, Yildiz, Aydogdu et al., 2019a), grafted chitosan derivatives of vanilic acid and courmaric acid (Chatterjee et al., 2015), cellulose nanofibrils with vanillic and syringic acids (Lakshmi Balasubramaniam et al., 2022), protocatechuic acid grafted chitosan films (Jun Liu et al., 2017) are the other examples of phenolic acid utilization in food packaging area.

Flavonoids, the secondary metabolites of plants, are known as the most dominant part of the phenolic compounds since they comprise nearly two/thirds of phenols. There are more than 6000 types of flavonoids and flavonoids can be classified into the subcategories namely, flavonol, flavanones, flavones, isoflavones, flavanol, flavanonol, and anthocyanidin. The chemical structures of flavonoid subgroups differ from each other due to the variation around the heterocyclic oxygen ring. However, they have the common C3-C6-C3 carbon skeleton (Shahidi & Ambigaipalan, 2015). The metal chelating ability, hydrogen-electron donating potential and finally the delocalization of the unpaired electron with stable phenoxyl radical are three potential mechanisms of flavonoids for antioxidant activity (Musialik et al., 2009; Shahidi & Ambigaipalan, 2015). Because of these promising features, the effects of the flavonoids on the functionality of the food package have been examined. The natural flavonoids, quercetin and catechin, were added into the

8

ethylene vinyl alcohol film to investigate the effect of active film on lipid oxidation of peanut and sunflower oil. The oxidation results showed that the active films were effective especially at the initiation stage. It was hypothesized that the flavonoids quenched the hydroxyl radicals present in the vapor phase inside the peanut packet. In sunflower packaging case, the results were not as promising as in the previous case due to the limited solubility of flavonoids in oil. However, in any case, flavonoids reduced the oxidation reactions (Hurley et al., 2013b). Rutin incorporated pullulan/chitosan active films exhibited antimicrobial activity against *L. monocytogenes* and *E. coli* (Roy & Rhim, 2021). To develop an antioxidant food package, flavonol-rich *Spondias purpurea* L. pulp was added to the cellulose acetate film matrix (Vasconcelos et al., 2021). Nanoemulsion of luteolin, one of the flavones, was added into the chitosan and the potential effect of active agent on the functionality of the films was investigated. As expected, lureolin significantly enhanced the antioxidant activity of the films and authors asserted that films could maintain this activity for up to 10 days in a 95% ethanol stimulant. Furthermore, antimicrobial activity of the films was reported for the tested microorganisms; G (-) (*E. coli, S. typhimurium*) and G(+) (*S. aureus, L. monocytogenes*) (Bi et al., 2021).

Stilbenes, t*rans*-resveratrol and its glucoside, are known for their antitumor, antioxidative and anticarcinogenic features (Shahidi & Ambigaipalan, 2015). Resveratrol is most commonly present in fruits such as mulberries and grapes, edible leaves of plants and peanuts. The antioxidant activity of resveratrol was examined by Gülçin, (2010) and compared with trolox, BHT, α-tocopherol and BHA. The results showed that at the same concentration, resveratrol had a much better performance in inhibiting lipid peroxidation of linoleic acid. Grapevine cane, rich in stilbenes, the agro waste of viticulture, was utilized in thermoplastic starch food packaging. In the study, antifungal and antimicrobial activity were proved and the films were suggested as a potential food package (Díaz-Galindo et al., 2020). Another natural phenolic compound, lignin, is also known for its antioxidant and antimicrobial activity since it has an aliphatic hydroxyl group, low molecular weight, phenolic hydroxyl group. The aromatic ring and highly cross-linked structure make

9

lignin more reactive. In fact, lignin has a similar reaction mechanism with BHT and BHA (Zadeh et al., 2018). Although a study indicated that both antioxidant and antimicrobial activity of the lignin depended on the origin and extracted solvent type, lignin/chitosan films had an antimicrobial effect on *P. fluorescens and B. thermosphacta* (Alzagameem et al., 2019). Although lignin extracted from corn stover showed an inhibitory effect on G (+) (*S. aureus* and *L. monocytogenes*) bacteria, no effect was observed for G (-)(*S.* Enteritidis and *E.coli* O157:H7) (Dong et al., 2011).

Tannins are natural polyphenols that are extracted from many different plant parts and are well known for their antioxidant feature because of phenolic hydroxyl groups in the structure (X. Huang et al., 2022). Further, they are distinguished by their UV-blocking characteristic (Ji et al., 2020). Similar to the other phenols, tannins are recognized as GRAS by FDA so it is safe in direct contact with food (H. Li et al., 2022). In the study of tannic acid incorporated into chitosan/methylcellulose/ gelatin matrix and tested as an active package for the preservation of cherry tomatoes and grapes. The results showed that tannic acid substantially contributed to the antioxidant feature of the film and inhibited the growth of *E. coli* and *S. aureus*. Furthermore, active films preserved the food quality for two- weeks (Halim et al., 2018). Similarly, it was observed that the addition of tannic acid and cellulose nano crystals into the gelatin film, showed microbial inhibition on the same microorganisms (Leite et al., 2021). As seen, natural phenolic compounds had antioxidant and antimicrobial features as much as synthetic ones as illustrated by the examples.

Due to increasing concerns and demands about the natural compounds, one of the polyphenols, curcumin, is utilized in this study as an antioxidant and antimicrobial agent. The features of curcumin will be discussed in upcoming sections.

Food companies conduct mandatory microbial and chemical tests during production to comply with the regulations. However, in most cases food freshness cannot be tracked after delivery to the market as traditional food packaging is designed simply

to provide external protection. In recent years, packaging has evolved from being simple to functional by integrating food safety monitoring systems. Nowadays, packages might monitor food freshness or even extend the shelf life while keeping food safe against adverse effects of ambient conditions (Balbinot-Alfaro et al., 2019). Intelligent packaging systems might also provide great alternatives to the expiration date labels on traditional food packaging to protect consumers against potential foodborne diseases (Ezati et al., 2019). Intelligent packaging is the new generation packaging system, it might provide information regarding the quality/safety status of food through the help of its sensing and communication capabilities.

Time-temperature indicators (TTI) indicate whether the threshold temperature has been exceeded during storage or transportation; if exceeded, TTI estimate approximately how much time has been spent above the critical value (Biji et al., 2015). The most commonly preferred TTI is thermochromic ink which shows the storage conditions of the product. Examples of commercial TTIs can be listed as MonitorMark™, Timestrip®, Fresh-Check®, CheckPoint® and their manufacturers are 3M™, Timestrip Plc, LifeLines, Vitsab, respectively (Kuswandi et al., 2011).

Radio frequency identification systems, RFID, have a critical role in the industry controlling the food supply chain. RFID is mainly composed of chips that store data, readers, and computer systems (Kuswandi et al., 2011). An antenna plays a role in transmitting information between the tag and the reader. The reader is a platform utilized to receive and process information. According to battery requirements, there are two types of RFID: active and passive. In active RFID, a battery is used as a power source; in the passive type, power is generated from the received signals. In RFID systems, low-frequency systems work in the range of 125 kHz–134 kHz, and high-frequency systems operate at approximately 13.56 MHz (Kalpana et al., 2019). Another intelligent packaging example is the integrity indicator. They are preferred to detect possible leakage that disrupts the package's unity. These indicators might be the oxygen indicators which are redox dyes. Their colors change when oxygen concentration fluctuates in the package. Ageless Eye®(Mitsubishi Gas Chemical

11

company) is a commercial example of an oxygen indicator whose color changes from pink to blue when the oxygen level exceeds 0.05% or more (Biji et al., 2015).

Although all these intelligent packaging systems are very useful, these indicators are found in the market very rarely. The main reason for this consequence is the high manufacturing cost. Generally, in the industry, the packaging accounts for 10% of the product cost. However, intelligent packages cost almost 50%- 100% of the product. Therefore, it is not financially sustainable (Müller & Schmid, 2019). Furthermore, power source (battery) and communication with the reader are other handicaps of these systems.

One of the perishable food, meat, has a very short shelf life since it is susceptible to the growth of microorganisms and enzymes. Spoilage detection cannot be possible by the human eye and nose (Cao et al., 2019). Therefore, it is necessary to carry on chemical analysis i.e. gas chromatography (GC) or other analytical techniques such as electronic tongue, and nose (F. Kong & Singh, 2011). These are known as destructive test methods and similar to the FRID technique, it requires high instrumentalization and professional operators. Therefore, it is not feasible for consumers. A low-cost, non-destructive, rapid and real time sensing systems become a necessity. At this point, colorimetric intelligent packages have gained the attention of both researchers and consumers (Cao et al., 2019). Meat products being protein rich are highly perishable. Food freshness decreases over time due to microbial and biochemical spoilage of foods. Proteins can be broken down into amino acids as a result of proteolytic activity of microorganism (Balamatsia et al., 2007). Free amino acids can be involved in oxidative deamination, decarborboxylation and desulfurization reactions leading to the formation of metabolic gases such as total volatile basic nitrogen (TVB-N) compounds and carbon dioxide (Rukchon et al., 2014). Thus, high levels of TVB-N content, including mainly of ammonia, dimethylamine and trimethylamine, can be used as a microbiological spoilage indicator of protein rich foods indirectly by monitoring pH change in the package headspace.

The synthetic dyes utilized in intelligent packaging systems such as bromophenol blue, bromocrosol green, boromocrosol purple, cresol red threaten consumer health and are regarded as carcinogenic because of their potential toxicity (Balbinot-Alfaro et al., 2019).

Similar to the active packaging, there is a trend in the use of natural coloring agents in these packages due to their low cost, non-toxicity, biodegradability, pollution-free, renewable and available characteristics (Mohammadian et al., 2020). Anthocyanins, chlorophyls, curcuminoids and betanins are the main coloring agents are utilized in intelligent packaging applications (X. Luo et al., 2022).

Betalains are the water-soluble pigments that can be extracted from cactus pear, purple pitaya and amaranth flower. The main subgroups of betalains are (i) red-purple betacyanins and (ii) yellow orange betaxanthins. The color of betacyanins is pink-red at acidic to neutral pH however it turns yellow at alkaline conditions. This feature makes betacyanins one of the coloring agents for intelligent packaging (X. Luo et al., 2022). Betacyanins extracted from dragon fruit were used to produce PVA- glucomannan based intelligent package to monitor fish freshness. TVB-N results of the sample showed parallel results with the color response of the films and the films were suggested as a promising indicator (Ardiyansyah et al., 2018). Moreover, different concentrations of red pitaya peel extract were added in the polyvinyl alcohol/ starch films and the sensitivity of the film to ammonia was measured. Depending on the response, the most appropriate one was selected for the freshness monitoring of shrimp. At 20 °C storage conditions, the sample spoiled at the end of 2-days and the color of the films changed from pink to yellow (Y. Qin et al., 2020). Another study compared the impact of betacyanin source on the color change of starch/PVA films. The results showed that the red pitaya flesh extract had a more distinguishable color change compared to globe amaranth flower extract, red beetroot extract and prickly pear fruit extract when monitoring shrimp spoilage (X. Yao et al., 2021). Finally, starch based film with extract of paper flower betalains was also successful in detecting fish spoilage (Naghdi et al., 2021).

The key component photosynthesis, chlorophylls, one of the most widely distributed in the environment (Echegaray et al., 2022). In the study of X. W. Huang et al., (2014) the color change performances of different pigments were compared. The order of the materials from the most successful one to the least was as follows black rice (anthocyanins,) red radish (anthocyanins,) winter jasmine (carotenoids) and spinach (chlorophyll). This difference was attributed to the different chemical structures of the components. Although anthocyanins have carbonyl and hydroxyl groups which make interactions with amines, the presence of alkyl group rather than hydroxyl and carbonyl groups makes carotenoid and chlorophyll less sensitive (X. W. Huang et al., 2014). In another study, different than the meat spoilage studies, lipid oxidation of sesame oil was detected by the chlorophyll/wheat gluten film (Chavoshizadeh et al., 2020).

The most widely utilized natural coloring agent, anthocyanins, is a water-soluble pigment and one of the sub group of flavonoids (Becerril et al., 2021). Structurally, anthocyanins are the glucoside form of anthocyanidins and have a typical C6–C3–C6 skeleton. This skeleton is composed of two aromatic rings named A and B (Figure 1.2). These two aromatics rings are separated from each other by six-membered heterocyclic (C) ring containing oxygen (Yong & Liu, 2020).
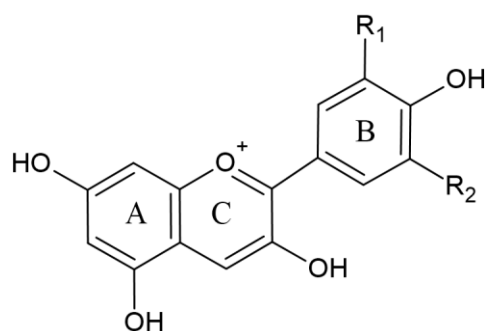
Figure 1.2. Structure of the anthocyanins

Anthocyanins are a large family and have approximately 500 members. The differences between members come from hydroxylated group, number/ nature of

14

bonded sugars and finally the position of aliphatic or aromatic carboxylates linked to sugar moieties (Becerril et al., 2021). Further, they have a wide range of colors from red, blue and orange to violet, and are present in many plants (Becerril et al., 2021). Bayberry (Yun et al., 2019), red cabbage, black bean seed coat (Prietto et al., 2017), blackberry (Nogueira et al., 2019), black carrot (Moazami Goodarzi et al., 2020), black chokeberry (S. Kim et al., 2018), black plum (Xin Zhang et al., 2019), blood orange (Jridi et al., 2019), grape pomace (Stoll et al., 2016) purple carrot (Akhtar et al., 2012) are only few examples of anthocyanin sources.

The color changes of anthocyanins depend on the source and composition. In general, the color of anthocyanins changes from red to blue/ purple, and finally colorless/ yellow (Yong & Liu, 2020). At low pH (pH<3), flavylium in the structure of anthocyanins become protonated and flavylium cations are formed. Between pH 3-5, flavylium cation is converted to neutral quinonoids. Until pH 7, quinonoids become predominant in the structure. Further increasing pH until 9, quinonoids are deprotonated and form anionic quinonoids (L. T. Wu et al., 2021). Therefore, they are very suitable components for intelligent packaging systems and were utilized to test the deterioration of different food products such as milk (Pereira et al., 2015), pork meat (Choi et al., 2017), shrimp (Merz et al., 2020), fish (H. zhi Chen et al., 2020).

Since anthocyanins have a wide range of applications, they have been incorporated in many different polymer matrixes PVA/chitosan (Pereira et al., 2015), bacterial cellulose (Kuswandi et al., 2020), κ-carrageenan (Jingrong Liu et al., 2019), agar potato starch (Choi et al., 2017), gelatin/PVA (Zeng et al., 2019).

As can be understood from these examples, due to the wide color change spectrum, extensive source, and water soluble characteristic and non-toxic features, anthocyanins have been extensively studied.

In this thesis, curcumin was utilized as a coloring agent.

1.1.1   Film making methods

1.1.1.1   Electrospinning Method

Electrospinning is a simple film-forming method that provides nanofibers from either polymer solutions or melts. It comprises three main components: voltage source, nozzle, and collector (De Vrieze et al., 2009).

A voltage source charges the polymer solution during the electrospinning process, and a pump controls the volumetric flow rate. When the electrical field achieves a critical value, where electrical force overcomes the surface tension, the polymer solution starts to elongate through the plate at the same time solvent starts to evaporate. Finally, nanofibers are collected the surface of the plate (De Vrieze et al., 2009, Park, 2010).

The morphology and diameter of electrospun nanofibers are affected by many parameters, which can be divided into three main categories; solution properties (conductivity, viscosity, concentration and surface tension), processing parameters (distance between needle and collector, applied voltage, volumetric flow rate) and environmental factors (temperature and relative humidity).

The sample's viscosity, which is generally determined by the molecular weight of the polymer and concentration, should be high enough to obtain smooth, uniform nanofibers but low enough to get continuous jet formation. Low viscosity causes the formation of beads on the nanofibers, while high viscosity obstructs the ejection of solution from the tip and causes the formation of larger fiber size. Surface tension and conductivity are the two main counteracting forces on the solution. To start the electrospinning, electrostatic forces should overcome the surface tension. A solution with a lower surface tension generally favors the beadless nanofiber formation, but it does not mean that low-surface tension solutions are always spinnable.

Electrical conductivity is correlated to the charge density of the solution. Higher electrical conductivity generally supports the formation of thinner fiber, but after a

certain level, it can cause bending instability and non-smooth fiber formation. The distance between the needle and the collector is another crucial parameter for fiber morphology. This distance should be in balance with the conductivity, flow rate, and voltage of the system to provide enough time for the evaporation of the solvent. Temperature modifies the solvent evaporation rate and jet solidification. Since the solvent evaporates quickly and the polymer mixture does not elongate high enough, thicker fiber formation is more commonly observed in the high-temperature process. Finally, relative humidity should be well adjusted to get homogenous fiber formation. In highly humid environments, solvent evaporation cannot occur, and bead formation on the fibers can be observed (Rahmati et al., 2021) (Rostamabadi et al., 2020).

The electrospinning method is widely used in numerous areas such as air filtration (Thavasi et al., 2008), wound dressing (Powell et al., 2008), drug delivery carrier (Xie & Wang, 2006), cosmetics (Camerlo et al., 2013) and immobilization of enzyme (Fazel et al., 2016). In addition to all these areas, due to high encapsulation efficiency and high surface-to volume ratio (Castro Coelho et al., 2021), electrospinning methods is commonly preferred in food systems to encapsulate active agents. Since electrospinning is a non-thermal process, the thermally sensitive compound can easily be encapsulated with this method, also. The electrospinning process is based on the evaporation of the solvent, therefore it decreases the possibility of solvent residue in the film. All these favored properties make electrospinning one of the most desired techniques for developing food packaging. For example, in the study of Aydogdu, Yildiz, Aydogdu, et al., (2019b), gallic acid was encapsulated into PEO, lentil flour nanofibers. In the study, to increase the solubility of lentil flour proteins, the solution was prepared at pH 1 and pH 10. This variation affected both solution properties such as viscosity, conductivity, and fiber characteristics including morphology and thermal properties. At the end of the research, it was reported that gallic acid loaded lentil flour/PEO nanofibers extended the shelf life of walnuts by reducing the lipid oxidation. In another study, tea polyphenol was encapsulated into the poly(vinyl alcohol)/ethyl cellulose nanofibers. The results showed that the

conductivity and viscosity of the solutions were dependent on the tea polyphenol concentration in the solution and different concentrations of active compounds also decreased the water contact angle of the nanofiber films and increased the radical scavenging activity. Furthermore, films having antimicrobial activity against *E.coli* and *S. aureus* also extended the shelf life of pork by 3 days (Y. Yang et al., 2021). Yet in another study, carvacrol was encapsulated in to soluble potato starch and at different concentrations. The average fiber size of nanofilms was between 73 to 95 nm. Thermogravimetric analysis (TGA) showed that the encapsulation process increased the thermal stability of the carvacrol. The active films had an antimicrobial activity on *Listeria monocytogenes, Salmonella* Typhimurium and this activity of the films was maintained for approximately 1 month against *S. aureus.* In the end films were suggested as a potential antimicrobial and antioxidant food package (Fonseca et al., 2019). In the study of Sun et al., (2021), blueberry-extracted anthocyanins was incorporated into the poly-l-lactic acid (PLLA) to monitor freshness of mutton. The color of the films changed from pink to light pink and finally the colorless when the concentration of ammonia increased. Finally, the freshness of the mutton and the color of the films showed parallel changes and the film was suggested to be used in intelligent packaging applications. Yet another research, zein nanofibers with alizarin was produced as an alternative intelligent packaging. The freshness of the fish fillets was observed with the alizarin-zein nanofibers. The total bacterial load, pH, and TVB-N of the fillets were measured during the storage period at 4°C. Color changes of the nanofibers and biochemical changes showed a parallel pattern (Aghaei et al., 2020). Black carrot anthocyanin was encapsulated in bacterial cellulose nanofibers and these nano films were utilized as an intelligent package to monitor fish freshness. Films showed distinct color changes between pH 2 and 11. Finally, the results proved the positive correlation between the microbial load of the sample and the color changes of the films (Moradi et al., 2019).

Despite all these great potentials, the low productivity of electrospinning restricts the wide range of application. Furthermore, the utilization of natural polymers i.e.

polysaccharides and proteins is in trend though the high rigidity of these polymers results in difficulty in processing (C. Zhang et al., 2020).

1.1.1.2   Casting Method

The solvent casting method is one of the most common techniques in laboratory-scale film formation. It can be basically described as spreading polymeric solution to the surface and then air-drying sample at a suitable time and temperature. The final film characteristic is mainly affected by the composition of the solution and drying conditions (temperature, humidity, time) (Ribeiro et al., 2021). Drying is the challenging stage of the casting process since inaccurate drying conditions can introduce some defects such as cracks and blisters, which significantly lower the quality of the film. The drying process mainly assists in molecular assembly, interaction, and crystallization. The solvent evaporation efficiency is mainly influenced by temperature, which affects film characteristics such as mechanical properties. For example, increasing the processing temperature from 30°C to 50°C increased tensile strength and decreased water vapor permeability. This result was due to the more compact network formation at higher temperatures (C. Li et al., 2019).

In addition to the main constituents forming the polymeric film matrix, another critical factor affecting film properties is the plasticizer, which is generally responsible for the integrity of the film (Thakur et al., 2019). Extensive interaction between biopolymer units which causes rigid and brittle structure, can be eliminated by introducing plasticizers in the formulation. The plasticizers, small molecules with low volatility, have a position between polymer units to decrease interaction between chains and increase their mobility. The effect of plasticizers on film characteristics is most commonly observed on solubility, permeability, and mechanical properties. Introducing plasticizers generally increased these parameters. Furthermore, releasing of active agents becomes more accelerated because of more flexible chain

movements (Ribeiro et al., 2021)**.** In the literature, glycerol and sorbitol are one of the most commonly used plasticizers.

Similar to the electrospinning methods, there have been various studies on active film production by casting method. In a recent study by Chen & Chi, (2021), different concentrations of tea polyphenol were encapsulated into the carboxylated cellulose nanocrystal/pullulan film-forming matrix. The incorporation of tea polyphenols enhanced the barrier, mechanical and thermal properties of the film. Furthermore, tea polyphenol addition enhanced antioxidant activity and films with the appropriate amount of tea polyphenol had an antimicrobial activity on *E.coli* and *S. aureus* (F. Chen & Chi, 2021). In another study, different active agents namely, curry, kesum, thymol oils were incorporated into the PLA matrix and their effects were compared. Kesum oil added films had higher thermal stability compared to the other active films and regardless of the oil type, the permeability values of films improved with the addition of oil. Although films had antimicrobial activity on *S. aureus*, they did not show any effect on *E.coli*. Finally, to simulate a real food package, chicken fillets packed with active films, which extended the shelf life of the food sample three more days (Mohamad et al., 2020). Coconut shell extract and sepiolite clay were incorporated into the corn starch-polyvinyl alcohol film matrix to modify film characteristics and improve the antioxidant capacity of the films. The results showed that the elasticity of the films improved with the addition of sepiolite clay and the incorporation of extract negatively affected permeability values. The antioxidant activity of the films significantly increased, in fact, the oxidative stability of soy bean oil increased when packed with the active film (Tanwar et al., 2021). In an edible active film study, germinated fenugreek seeds were utilized as an active agent in semi-refined κ-carrageenan film matrix. As expected, the antioxidant and antimicrobial activity of the film enhanced depending on the active compound. Furthermore, films caused microbial reduction in chicken breast during 7- day storage period compared to the control sample (Farhan & Hani, 2020). Finally, despite the easy processing and simplicity, high economic cost because of low

production capacity and difficulties in the scaling of the industry is the most important drawback of the solvent casting method (Ochoa-Yepes et al., 2019).

Considering all the positive and negative aspects of these two film making methods, in the literature, some studies compared the film performance of these two. For example, in the study of S. Wu, Qin, & Li, (2014), cellulose acetate nanofibers had higher thermal stability, in other words, decomposition temperature, compared to casting cellulose acetate film. Furthermore, electrospun nanofiber had higher contact angle (127.2°) than casting film (74.4°). This result pointed out that electrospun nanofibers were more hydrophobic surfaces than the casting film, which was explained by the orientation of the hydrophobic groups to the air/solid interface. Furthermore, the other reason for this consequence was higher crystallinity of the electrospun nanofibers.

Similar to the previous example, gelatin/zein nanofibers had more hydrophobic surfaces than gelatin/zein casting film showing a lower contact angle. A higher single melting point of gelatin/zein nanofibers suggested newly formed hydrogen bonding between components more successfully stabilized nanofibers than casting the film. Finally, nanofiber film showed higher solvent resistance than casting film due to heterogeneous dispersion of components (Deng, Kang, et al., 2018).

Antibacterial test of PVA/chitosan electrospun and casting films exhibited that due to higher surface roughness and nanofiber structure, electrospun films were more effective on *S.aureus* and *E.coli* (Nokhasteh et al., 2019).

Despite all these positive attributes, Wang et al., (2020) investigated that casted gelatin films had significantly higher elastic modulus and tensile strength than electrospun fiber.

1.1.2   Film Modification Methods (Crosslinking)

Nowadays, biodegradable and eco-friendly components have drawn attention because of increasing environmental concerns about petroleum-based packaging

materials. To replace traditional packaging, natural biopolymers such as polysaccharides, proteins, and lipids have been regarded as possible alternatives(Lin et al., 2019). Although films made from polysaccharides show good oxygen and carbon dioxide barrier properties due to their tightly packed network structure, they are generally permeable to water vapor due to their hydrophilic nature (Mohamed et al., 2020).

On the other hand, proteins provide better mechanical features to the produced films compared to polysaccharides. However, the hydrophilic nature of proteins also leads to poor water vapor barrier characteristics with the films (Rajeswari et al., 2020). Crosslinking these compounds to modify film structure is one of the promising solutions to eliminate the potential drawbacks of these biopolymer films.

For example, sodium trimetaphosphate (STMP) (Aydogdu et al., 2020) and sodium sulphate crosslinking agents (Kalaycıoğlu et al., 2017) were used in guar gum/orange oil emulsion and chitosan antimicrobial film, respectively. Further, the effect of graphene oxide (Grande et al., 2017) on crosslinking chitosan films and UV-induced crosslinking (J. Zhou et al., 2008) on corn starch films were also analyzed.

Rather than these crosslinking agents, citric acid (CA) is a bio-based tricarboxylic acid and is commonly used due to its low-cost, non-toxic nature. The carboxyl group of citric acid might react with the hydroxyl and amino groups of different biopolymers (Nataraj, Sakkara, Meghwal, & Reddy, 2018; Yang, Peng, Wang, & Liu, 2010). Thus, CA was utilized to modify film characteristics in the studies. For example, different concentrations of CA were utilized as a crosslinking agent in the potato starch-chitosan film matrix. Increasing CA concentration in the film matrix caused a reduction in water solubility while increasing hydrophobicity, and decreasing permeabilities. Finally, CA improved the antimicrobial activity of the films against both G(+) and G(-) bacteria (H. Wu et al., 2019a). In the cassava starch film study, CA was incorporated into the film forming solution and this solution was heated at different temperatures (75°C and 85°C). The results showed that the permeability and moisture content of the films significantly reduced. Films became nearly insoluble in dimethyl sulfoxide (DMSO). Although crosslinking slowed down

the degradation of the films, they were still biodegradable (Seligra et al., 2016). Similarly, the characteristics of the polyvinyl(alcohol)/starch/graphene nanocomposites were improved by the addition of CA as a crosslinking agent. The incorporation of CA led to increasing thermal stability, tensile stress and elasticity of the film. Finally, FTIR results supported the enhanced interaction between hydroxyl group of PVA and starch due to crosslinking (Jose & Al-Harthi, 2017). In another study, the effect of heat treatment and catalyst on CA crosslinked wheat straw hemicellulose films were analyzed. The results revealed that crosslinking reaction decreased the permeability of the film and enhanced water resistance. The heat treatment and the catalyst did not affect significantly the film properties (Azeredo et al., 2015).

On the other hand, glutaraldehyde is one of the most commonly preferred crosslinking agents for proteins and polyhydroxyl compounds. Because it has a rigid chemical structure without any hydrophilic group, the addition of glutaraldehyde decreases the water sensitivity of the material. The carbonyl group of glutaraldehyde reacts with the amino group (chitosan) and the hydroxyl group of polysaccharide molecules (Gonenc & Us, 2019).

1.1.3   Utilization of polymers and biocomposites in food packaging

Although most of the packaging materials in the marketplace are petroleum-based due to their relatively low price and desirable properties, their non-biodegradable and non-renewable properties stand out as the biggest challenge. Only in the US, more than 30 million tons of these materials are wasted annually. Furthermore, less than 3% of these petroleum-based polymers are recycled due to technical and economic difficulties (Mohamed et al., 2020).

Therefore, nowadays, biodegradable and eco-friendly components have drawn attention. In this sense, to replace traditional package material, in addition to natural biopolymers including polysaccharides, proteins, and lipids, synthetic

biodegradable polymers such as PEO have been regarded as possible alternatives (Lin et al., 2019). Therefore, the utilized materials in this study will be discussed further in upcoming sections.

1.1.3.1   PEO (polyethylene oxide)

PEO, a synthetic polymer, is produced by the polymerization of ethylene oxide with the help of a metallic catalyst. PEO is composed of flexible linear macro chains and repeating units of carbon, hydrogen, and oxygen ($-CH_2-CH_2-O-$). Since it is a semi-crystalline polymer, the melting point ranges between 63 °C and 67 °C, and the glass transition temperature is between −50 and −57°C. In its natural state, PEO is generally in the form of a regular helix structure, whereas in an aqueous solution, PEO modifies its structure as a random coil (Hassouna, Morlat-Thérias, Mailhot, & Gardette, 2007; Ma, Deng, & Chen, 2014).

PEO is a biocompatible, hydrophilic, non-toxic polymer, and it also has good compatibility and mechanical properties such as high elongation and good orientation ability (Grkovic et al., 2017). In the literature, studies mainly reported the difficulties of electrospinning natural polymers such as alginate and chitosan due to their failure in jet instability. To overcome these handicaps, natural polymers are commonly mixed with PEO as a carrier polymer. The alginate electrospinning exemplified this situation. A tightly overlapped form of rigid and extended conformation of alginate caused ineffective chain entanglement in the electrospinning process. Due to this insufficiency, mechanical strength, which endured electrical force, lowered and prevented stable jet formation (Cui et al., 2016).

The first positive effect of PEO is a charge-counteracting effect on these polyelectrolyte polymers. The second one is related to the chain entanglement of PEO and biopolymers. It was hypothesized that the molecular weight of PEO should be high enough to promote electrospinning (Vega-Lugo & Lim, 2012).

24

Due to these benefits, PEO is utilized in different areas such as solar cell production (Md Shariful Islam et al., 2019), and metal ion adsorption (Shariful et al., 2018). It is also frequently preferred in food packaging applications i.e. HPMC, PEO, gallic acid active nanofilm (Aydogdu, Sumnu, et al., 2019), rutin encapsulated cellulose acetate/PEO nanowebs (B. Li & Yang, 2020) aloe vera agrowaste incorporated PEO nanofibers (Solaberrieta et al., 2020).

1.1.3.2   Chitosan

Chitosan, (1-4)-2-amino-2-deoxy-β-D- glucan, (CS) is a cationic polysaccharide with a typical acetylation degree of 20%. It was commercially produced from the fishery by-products. It is one of the most widely used biodegradable, biocompatible, and antimicrobial polymers. These characteristics make it a frontrunner compound for biomedical practices, tissue engineering, and food packaging (Grkovic et al., 2017).

Protonation of amino groups makes chitosan soluble in an acidic solution and positively charged. An increasing number of hydrogen bonding at high concentrations results in sharply increasing viscosity of the solution. Because of that, during electrospinning, the CS concentration becomes a vital parameter in moving the solution from the tip of the needle to the plate (Tsai et al., 2015).

Furthermore, electrospinning of pure CS solution is very difficult because of high repulsive forces between ionic groups. Cationic characteristics and high charge density cause a homogeneous splitting of jets. To improve the spinnability of CS, it is blended with other natural or synthetic polymers (Ahmed et al., 2020). Incorporation of CS into the electrospun solution caused drastic changes in both solution properties, film morphology and film characteristics. For example, in the study of Koosha & Mirzadeh, (2015) chitosan was blended with poly(vinyl alcohol) (PVA) at different ratios. In addition to the solution properties, the effect of blend ratio on fiber morphology and mechanical properties was examined. The research

showed that the highest blending ratio of CS:PVA (100:0) solution was not suitable for electrospinning. This was the consequence of the high viscosity of chitosan solution which prevented stable jet formation. Furthermore, SEM results supported that increasing CS ratio in the polymer mixture decreased average fiber size of nanofibers due to increasing conductivity values. Finally, incorporation of CS with the PVA lowered the ductility of nanofibers compared to pure PVA nanofibers (Koosha & Mirzadeh, 2015). In another study, chitosan was blended with pullulan at different ratios to obtain fast dissolving oral nanofibers. The viscosity of the solution increased with an increased chitosan ratio in the solution, similar to the conductivity values. SEM images proved that the average fiber size of nanofibers strongly depended on the CS ratio of the polymer mixture, and the average fiber size of nanofibers was measured between 134±77nm (CS/Pullulan 0/100) and (CS/Pullulan 60/40) 51±12nm. The thermal stability of the nanofibers increased with increasing CS which indicated hydrogen bonding between chitosan and pullulan (Z. yu Qin et al., 2019). In the food packaging area, chitosan is frequently utilized because of its natural antimicrobial and antioxidant activities. The antimicrobial activity of chitosan is related to the three main elements (i) microorganism (cell age, species), (ii) characteristics of chitosan (molecular weight, concentration, and deacetylation degree) and (iii) environment (temperature, pH, ions) (Confederat et al., 2021). The effect of chitosan molecular weight on antimicrobial activity has been studied and results revealed that chitosan with lower molecular weight is more effective on G (-) bacteria, and the reverse case is valid for G (+) bacteria. The main suggestion about this outcome was that lower molecular chitosan could more easily attach on G (-) cell wall whereas higher molecular weight of chitosan acted as a barrier around the G(+) bacteria by hindering nutrient absorption (Fernandes et al., 2008). Another factor, deacetylation degree, is related to the positively charged density of the chitosan. Therefore, more positively charge density means stronger electrostatic interaction and better antimicrobial activity (Confederat et al., 2021). Since chitosan has a pKa value around pH 6.5, it becomes positively charged at pH values lower than pKa. Therefore, chitosan has a better inhibitory effect when it is

26

cationic (Younes & Rinaudo, 2015). Because of this unique feature, chitosan has been utilized in food packaging. For example, different concentrations of chitosan (1%, 3%, 5%) were incorporated into the low density poly ethylene (LDPE) to develop antimicrobial food packages and the effect of these packages on the shelf life of Tilapia steaks was investigated. Films with 3% and 5% concentrations of chitosan caused a 100% reduction of *E.coli* after 96 h and these films extended the shelf life of fish up to 15 days (Reesha et al., 2015). In another study, the chitosan/guar gum active film results showed that films containing 85% chitosan had antimicrobial effects on both *E.coli* and *S.aureus* (Rao et al., 2010). On the other hand, the inhibitory effect of gelatin-chitosan edible films was reported only for *E. coli*, clear zone was not observed for *L. monocytogenes* (Pereda et al., 2011). To improve the antimicrobial effect of chitosan, it was also blended with other antimicrobial compounds. For example, *Sonneratia caseolaris* (L.) Engl. leaf extract was incorporated into the chitosan film matrix at different concentrations and the films were effective on G (+) (*S.aureus*) and G(-) (*Pseudomonas aerugino)* bacteria (Nguyen et al., 2020). Moreover, the incorporation of rosemary essential oil (0.5, 1.0 and 1.5% v/v) into chitosan film increased antimicrobial efficiency against *S. agalactiae, E. coli, L. monocytogenes* (Abdollahi et al., 2012).

Although the antioxidant activity of the chitosan was attributed to the amino and hydroxyl groups on the structure, the studies suggested that the antioxidant activity of the chitosan depended on the molecular weight. Chitosan can interact with free radicals and metal ions by donating a hydrogen atom or lone pair of electrons (Oladzadabbasabadi et al., 2022). The results of kefiran-chitosan films proved the antioxidant feature of chitosan since the highest DPPH scavenging activity was observed for the films with the highest amount of chitosan (Sabaghi et al., 2015). However, it should be noticed that chitosan is more commonly utilized for its antimicrobial activity rather than its antioxidant feature.

In addition to these inherent characteristics of chitosan, it is also relatively hydrophobic and has better barrier properties than other natural macromolecules such as starch (Luchese et al., 2018). However, the practical application is still

limited because of susceptibility to moisture, and mechanical properties should be improved (Oladzadabbasabadi et al., 2022).

1.1.3.3   Flour

As mentioned, over the last decade, natural and renewable polymers have attracted the attention of both researchers and the industry. These materials are not only considered potential food package materials but are also preferred in different fields such as scaffold tissue engineering (Malafaya et al., 2007).

In food science, to obtain environmentally friendly films, researchers generally either extract or purify biopolymers such as starch and protein, then mix these biopolymers to achieve desirable film structure, and eliminate some undesirable characteristics of these biopolymers. For example, films made from polysaccharides show good oxygen and carbon dioxide barrier properties due to their tightly packed network structure. However, they are generally permeable to water vapor due to their hydrophilic nature. In addition, proteins provide better mechanical features to the produced films than polysaccharides. However, the hydrophilic nature of proteins also leads to poor water vapor barrier characteristics with the films (Mohamed et al., 2020).

To eliminate extraction and purification processes and to handle possible disadvantages of each biopolymer, flour, a bio-composite material, and the natural mixture of protein, starch, and lipids can be considered an attractive solution (Valderrama Solano & Rojas de Gante, 2014).

For that purpose, for example, Yildiz, Bayram, et al., (2021) developed pea flour-based gallic added active films and analyzed the effect of film on lipid oxidation; Riveros, Martin, Aguirre, & Grosso, (2018) studied the effects of peanut flour package efficiency on the preservation of sunflower oil quality while Tapia-Blácido, Sobral, & Menegalli, (2005) characterized the film-making ability of amaranth flour.

Among different flour types, faba bean, also known as the broad bean, filed bean, and horse bean (Multari et al., 2015) is a good source of proteins and carbohydrates. The protein content of faba bean is higher than other high protein flours such as pea flour (Yildiz, Bayram, et al., 2021) and lentil flour (Aydogdu, Yildiz, Aydogdu, et al., 2019b). In addition, faba bean contains high amounts of secondary metabolites, that is, phenols and flavonoids which enrich their antioxidant activity (Millar et al., 2019). Up to now, faba bean flour has been mostly utilized in gluten-free pasta (Rosa-Sibakov et al., 2016) and protein enriched gluten free bread (Sozer et al., 2019). No study has investigated so far in the film formation performance of faba bean flour.

Like faba bean, chickpea is a good carbohydrate source, including dietary fiber and protein. Chickpea proteins are mainly composed of globulins, albumin, glutelin, and prolamin, whose isoelectric point is between pH 4-6. Starch is the primary carbohydrate source, and 30-35% of starch is amylose. The gelatinization temperature of the amylose is approximately 64–73 °C. In addition to its good emulsifying, pasting, and foaming properties, as an antioxidant, bioactive compound in chickpea was also reported (Olga et al., 2019).

The effect of pH (7-10) and plasticizer concentration (1% or 3% w/v) on the film-forming performance of chickpea flour was investigated. For this purpose, the permeability, solubility, and mechanical and thermal characteristic of the films were analyzed. WVP of the films significantly increased with increasing plasticizer concentration due to enhanced free volume and less dense film structure. Tensile strength and elastic modulus of the films declined, whereas elongation at break value increased with increasing plasticizer concentration. This result was explained by the limitation of cohesive forces between polymer chains caused by the plasticizer and higher moisture content of the films (Olga et al., 2019).

Another study aimed to produce gallic acid-loaded chickpea flour films and similarly analyzed the influence of pH (9 and 11) and plasticizer (1 and 3% w/v) concentration. The results suggested that films produced at pH 11 had higher antioxidant activity.

Higher plasticizer concentration resulted in a more flexible and hydrophilic film. Furthermore, gallic acid incorporation had a decreasing effect on the WVP of the films (Kocakulak et al., 2019).

However, there is no research in the literature examining chickpea flour-based nanofibers as an active food package.

1.1.4   Active Agent-Curcumin

Curcumin (Figure 1.3), 1,7-bis (4-hydroxy-3-methoxyphenyl)-1,6-hepadiene-3,5-dione, is a natural compound having a molecular weight of 368.385 g/mol, extracted from Curcuma longa and it is in solid form at room temperature (Roy et al., 2022). Although curcumin is poorly soluble in water which limits application and bioavailability, it is highly soluble in polar solvents such as ethanol. Furthermore, analysis has shown that higher processing temperatures speed up the degradation rate of curcumin (Aliabbasi et al., 2021).

Since the bioactive characteristics of curcumin are well known, it is widely used in numerous areas such as wound healing (Alven et al., 2020), prevention of antimutagenicity (Fernández-Bedmar & Alonso-Moraga, 2016) and cancer (Duvoix et al., 2005).

The utilization of curcumin is not limited to these areas. Since curcumin is accepted as GRAS (generally recognized as safe) by FDA (Food and Drug Administration) (X. Luo & Lim, 2020) it is widely preferred by researchers to alter food packaging characteristics.

Curcumin is incorporated into film formulations to take advantage of its hydrophobic characteristics. In the study of curcumin-added carbohydrate-based films, the water solubility of agar films significantly decreased from 41.7 ± 3.9 % to 33.9 ± 3.8% (Roy & Rhim, 2020d). The water contact angle of guar gum-based film increased from 38.83 ± 0.29 º to 40.89 ± 0.37º (Aydogdu et al., 2020). Finally, the WVP of carboxyl methyl cellulose films reduced from 2.12 ± 0.1 to $1.82 \pm 0.1 \times 10^{-9}$

g.m/m^2.Pa.s with the incorporation of curcumin (Roy & Rhim, 2020a). In addition to these, another reason for researchers to prefer curcumin in food packaging is its antimicrobial activity. The antimicrobial activity of curcumin is based on the deactivation of FtsZ protein, which is critical to initiate cell division. Although the mechanism and the interaction of FtsZ - curcumin is not clear yet, the methoxy group, phenolic group and two carbonyl groups of curcumin potentially interact with the active site of FtsZ by hydrogen and/or hydrophobic bonds. When the polymerization of FtsZ and formation of Z- ring are interrupted by curcumin, the viability of the bacteria becomes compromised (Roy & Rhim, 2020b).
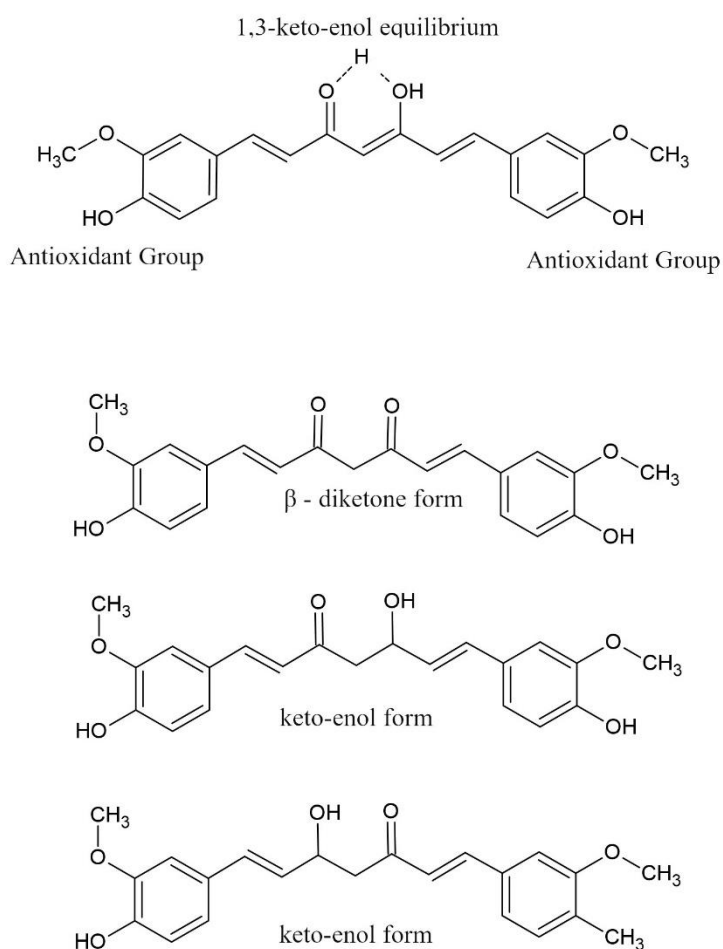
Figure 1.3. Structure of curcumin

Because of this feature, the antimicrobial activity of curcumin has been tested by different studies with different polymer matrices. For example, curcumin was incorporated into the carrageenan, chitosan and agar films and their antimicrobial activities were tested on *E.coli* and *L. monocytogenes*. As expected, except for chitosan film, neat carrageenan and agar film did not show any bactericidal activity. Although the addition of curcumin brought all films antimicrobial features, the presence of chitosan accelerated bacterial destruction (Roy & Rhim, 2020d)**.** Although the antimicrobial activity of curcumin is a well-known fact, its concentration is a determiner factor for the bactericidal effect. Increasing curcumin concentration from 1% to 5% in the cellulose based film resulted in the increase of inhibition zone from 0.7 cm to 2.3 cm for *E.coli* (N. Luo et al., 2012). The result of PLA/curcumin film also showed that there was a positive correlation between the increasing antimicrobial activity of the films and curcumin concentration (Roy & Rhim, 2020c). The gelatin- curcumin study pointed out that antimicrobial films were more effective on G(-) (*E.coli*) than G(+) *L. monocytogenes* bacteria. The films significantly inhibited the growth of *E.coli* whereas slightly reduced the growth rate of *L. monocytogenes* (Roy & Rhim, 2020b). Contrary to these results, the activity of curcumin was tested on 100 pathogen strains coming from 19 species and the results indicated that curcumin was more effective on G(+) bacteria than G(-) bacteria (Adamczak et al., 2020). Therefore, the antimicrobial activity of curcumin was also dependent on the type of test bacteria and the strain. As an example of food packaging application, curcumin functionalized chitin and glucan complexes were tested on chicken breast samples. The quality of food sample both packed with cling film and film with the highest amount of curcumin was assessed by total viable bacteria count technique. The results showed that the active film extended the shelf life of the chicken breast meat up to 10 days (Kaya et al., 2022). The phenolic hydroxyl and single methylene groups of curcumin contribute to the antioxidant activity which is measured by various methods such as DPPH (Roy & Rhim, 2020b) reducing power assay, ABTS radical scavenging (Taghavi Kevij et al., 2020).

Similar to the antimicrobial activity, the nature of the film forming material has also an influence on the antioxidant activity of the curcumin. The same amount of curcumin was added into the films made by the different molecular weights of chitosan (15 kDa, 50 kDa, 500 kDa, 850 kDa, 1700 kDa, 4150 kDa) and the bacterial cellulose. The results of both ABTS and DPPH scavenging rates of the films suggested that the molecular weight of chitosan might influence the antioxidant activity. The films made from 500 kDa and 850 kDa molecular weight of chitosan had slightly higher antioxidant activity compared to the other films (Xu et al., 2021). In addition, curcumin was encapsulated into the glucomannan and zein matrix by electrospinning technique. Films had higher antioxidant capacity when zein concentration was higher in the spinning solution (L. Wang et al., 2019a). Curcumin (0% - 5%) was also incorporated into the tara gum/ polyvinyl alcohol film matrix. As expected, the antioxidant activity of the films increased with increased curcumin concentration. The study also investigated the temperature (25°C, 35°C and 45°C) dependency of the releasing behavior. Since chain mobility increased and film compactness was modified at higher temperatures, curcumin exhibited a higher release rate (Q. Ma, Ren, et al., 2017).

Actually, the antioxidant activity of curcumin is also related to the releasing environment. Among the different mediums (0%, 25%, 50%, 75% and 95% ethanol), curcumin release increased with increasing ethanol concentration (Xu et al., 2021). Since 95% ethanol illustrates fatty food systems, curcumin containing active films might be more effective on lipid oxidation and in high-fat content foods. Curcumin added thermoplastic starch/poly(butylene adipate-co-terephthalate) films were produced by extrusion technique and the antioxidant efficiency of films was tested on packaging of chia oil. Authors reported a decrease in concentration of oxidation products when oil was packaged with active film. However, they also emphasized that the color of the oil turned to yellowish during the release of curcumin into the oil (Mücke et al., 2021). Since the solubility of curcumin is very low in hydrophilic environments, to make it more functional and to increase bioavailability, curcumin was encapsulated in the inclusion of complexes. For this reason, β-

cyclodextrin/curcumin complexes were incorporated into the gelatin film forming matrix. To delay the oxidative browning, apple juice was packed with the gelatin-cyclodextrin/curcumin film. The results revealed that the polyphenol content of all samples decreased during storage. However, the lowest change was reported for the samples packed with the highest curcumin content (J. Wu et al., 2021). As in this case, curcumin became soluble in a hydrophilic environment and bioavailable when encapsulated in the inclusion complex.

Besides its antioxidant and antimicrobial characteristics, curcumin is also favorite as a dye due to its chromogenicity. As mentioned before, some dyes used in producing pH indicators are synthetic, toxic, and unsuitable for food packaging applications (Prietto et al., 2018). Due to their low toxicity, pollution-free, renewable features and easy preparation characteristics, natural dyes are good candidates for substitution of chemical reagents (Xiahong Zhang et al., 2014). It is well known that under alkaline conditions, diketone groups of curcumin are shifted to keto-enol form, which is responsible for color change from yellow to orange/red (X. Luo & Lim, 2020) and this property makes curcumin an excellent pH indicator candidate.

In intelligent film applications, casting technique was the most commonly preferred method rather than electrospinning. Although electrospinning has an increasing popularity for both active and intelligent packaging because of its superior characteristics which were discussed previously, there are still limited studies on nanofiber intelligent packaging. Although there are some examples of electrospinning intelligent packaging, polymers that completely change film characteristics and applications are different. The application of intelligent packaging films was mostly focused on the storage of sea foods such as shrimp. For example, in the study of Wu et al., (2019), chitosan curcumin casting film was designed to be used for shrimp, at the end of day 5, TVB-N value of the samples was measured as 54.25 mg/100 g and TVB-N value exceeded the limits. The color change of pectin based curcumin films was observed for the shrimp at the end of 36h, at 25°C storage conditions (Ezati & Rhim, 2020). Similarly, the freshness of the shrimp

34

was detected by κ-carrageenan / curcumin casting film. The other seafood freshness monitoring examples were also listed in Table 1.2.

The articles studied on chicken storage were different from this thesis by both the packaging method and the dye, for example, PVA/ gelatin/amaranthus leaf extract (Kanatt, 2020), cassia gum /cellulose fiber /bromothymol blue (Cao et al., 2019), bacterial cellulose/ methyl red (Hurley et al., 2014), methylcellulose and hydroxypropyl methyl- cellulose/ bromothymol blue/ methyl red/bromocresol green/ phenol red (Rukchon et al., 2014).

Table 1.2 Examples of curcumin based intelligent packaging.

Material	Packaging Method	Application	References
Tara gum/polyvinyl alcohol / curcumin	Casting	Shrimp	(Q. Ma, Du, et al., 2017)
bacterial cellulose/cotton fiber/ curcumin	Casting	Soaked in the different pH solution	(X. Ma et al., 2020)
Low density polyethylene (LDPE) / curcumin	Extrusion	Meat	(Zhai et al., 2020)
Pectin / curcumin	Casting	Shrimp	(Ezati & Rhim, 2020)
Gelatin/ curcumin	Casting	Soaked in the different pH solution	(Musso et al., 2017)
κ-carrageenan / curcumin	Casting	Shrimp	(Jingrong Liu et al., 2018)
Ethylcellulose, PVP, PEO / curcumin	Electrospinning	Exposed on ammonium vapor and suggested to be used as intelligent packaging	(X. Luo & Lim, 2020)
Polyvinyl alcohol/cellulose / curcumin	Casting	shrimp	(Ding et al., 2020)
Chitosan/ curcumin	Casting	Shrimp	(C. Wu et al., 2019)
Agar and polyvinyl alcohol / curcumin	Casting	Shrimp	(J. Zhang et al., 2021)
Bacterial Cellulose / curcumin	Casting	Shrimp	(Kuswandi et al., 2012)

1.2   Objectives of the study

Packaging is not only necessary to ensure food integrity but also critical for product advertising. Besides keeping food safe from ambient conditions and preserving quality during transportation and storage, nowadays, packages have an essential role in providing innovative solutions for increasing shelf life and guiding consumers about the freshness of food.

Intelligent packaging is the next-generation packaging system capable of sensing, detecting, recording, communicating, and providing information about the state of food through the supply chain. Although traditional packages give info about food origin, theoretical expiration date, and composition, intelligent packages significantly reduce food waste and upgrade traceability. Because of this reason, these packages have a great potential to reduce food waste. Active packages, on the other hand, are another innovative trend in the industry that include a variety of agents that retard the deterioration of food.

Solvent casting is one of the most commonly used techniques in film fabrication due to its simplicity and cost-effectiveness. On the other hand, electrospinning offers the fabrication of polymeric nanofibers with superior flexibility, porosity, surface area, and surface functionality characteristics.

Due to increasing environmental concerns about the disposal of plastics, studies have started to focus on new materials such as natural combinations of protein, lipids, carbohydrates, and fibers to obtain biodegradable, bio-based food packages from natural sources. Chitosan, a natural polysaccharide obtained from chitin, is one of the most commonly used biopolymers for food packaging applications owing to its non-toxicity, biodegradability, biocompatibility, and antioxidant and antimicrobial activities. PEO (polyethylene oxide) is one of the most common co-spinning agents to facilitate the electrospinnability of natural biopolymers due to its biocompatibility and high elongation ability. Flours contain carbohydrates, lipids, and proteins together. Therefore, they have been an excellent source for producing food packages.

36

Since faba bean and chickpea flour have a high amount of protein compared to the other flours, they might be considered a promising bio-composite as a food packaging material. Curcumin is one of the most valuable ingredients in turmeric and has been long used in different fields due to its anticancer, antioxidant, antimicrobial, and anti-arthritic character. Furthermore, it can be utilized as a halochromic dye, a natural pH-responsive agent. Therefore, curcumin is one of the best candidates for utilizing intelligent packages.

The risk of food contamination by packaging materials becomes the most significant challenge against the commercialization of intelligent packaging films. Although chemical compounds were utilized in intelligent packaging, there is a literature gap on producing natural dye-containing biopolymer-based electrospun nanofibers to be used as intelligent packaging. Furthermore, most of these sensors were tested on seafood samples and there are limited number studies on the application of intelligent packages on chicken packaging. Moreover, in the literature, there is no study about the application of legume flour based and curcumin containing active films produced by electrospinning. Apart from these, in general, to eliminate the drawbacks of biopolymers, different crosslinking agents such as glutaraldehyde, a well-known toxic chemical, have been frequently used. From this perspective, no study is aimed at comparing the performance of different crosslinking agents in the production of a curcumin-added active films. Furthermore, this study compares the performances of faba bean and chickpea flour based active films.

The main aim of this study was to obtain biopolymer-based (chitosan, faba bean and chickpea flour) and curcumin incorporated intelligent and active packaging materials by using electrospinning and casting methods. In the intelligent packaging part, chitosan/PEO was used as an external support matrix for halochromic curcumin. First, the conductivity and viscosity of film-forming solutions were studied. Additionally, nanofiber films were characterized in terms of morphology (SEM), thermal analysis, water vapor permeability and sensitivity to volatile ammonia. Then, the relationship between the concentration of volatile compounds and the color change of intelligent packaging was systematically analyzed. In the second part of

37

the study, chickpea flour and PEO were preferred as support matrix materials due to their nontoxic and biodegradable characteristics. The effects of curcumin and heating methods (conventional and microwave) on solution and film properties were investigated. The antioxidant and antimicrobial activity of the active films were also analyzed. In the third part of the study, the possibility of replacing glutaraldehyde (GLU) with citric acid (CA), a nontoxic compound, was questioned in film formation. In addition to film characteristics, antioxidant, antimicrobial analysis, and biodegradation behavior of the film were also carried out. Based on the results of the previous part, CA cross-linked chickpea flour/chitosan films were obtained and antimicrobial activity was tested on chicken breast storage.

CHAPTER 2

MATERIALS AND METHODS

2.1 Materials

PEO (M.W. 900 kDa) was obtained from Sigma- Aldrich (St. Louis, MO). Curcumin (1,7-bis (4-hydroxy-3-methoxyphenyl)-1,6-hepadiene- 3,5-dione), mediummolecular weight (75–85% deacetylated) chitosan and ethanol were purchased from Merck (Darmstadt, Germany). MgO (magnesium oxide), boric acid, bromocresol green-methyl red mixed indicator solution, hydrochloric acid solution (32–36%), sodium hydroxide pellets, DPPH, Polyoxyethylene sorbitan monooleate (Tween 80) (density: 1.064 g/cm3, viscosity: 400–620 cps at 25 °C) were obtained from Merck (Darmstadt, Germany). Chickpea flour was obtained from Değirmencibaşı Gıda (Turkey). Faba bean flour was purchased from Havancızade Gıda (İstanbul, Turkey). For antimicrobial analyses, nutrient broth, and plate count agar were purchased from Condalab.

2.2 Methods

2.2.1 Preparation of film forming solutions

2.2.1.1 Preparation of curcumin/CS/PEO electrospun solution

A homogeneous PEO stock solution (4% (w/v)) was prepared using a magnetic stirrer (MaxTir 500, Daihan Scientific, Seoul, Korea). Similarly, chitosan (CS) solution (1%, w/v) was prepared by dissolving 1 g of CS powder in 100 mL of acetic

acid (80%, v/v). Then, PEO stock solution and CS solution were mixed at different weight ratios (PEO: CS (w/w); 8.5: 1.5, 8:2, 7.5:2.5). In the meantime, 0.05 g curcumin was dissolved in 10 mL ethanol to prepare curcumin stock solution. Later, 5 mL of curcumin stock solution was mixed with the polymer solutions (10 mL) of PEO and CS to prepare the electrospun solutions. The solubility of curcumin in ethanol was taken directly as the value on the specification sheet provided by the Sigma Aldrich. Herein, all the mixture was stirred at 1500 rpm for 10 min at 25 °C and no precipitation was observed after mixing.

2.2.1.2   Preparation of curcumin/PEO/chickpea flour electrospun solution

PEO (2.5% w/v) was prepared by using a magnetic stirrer at 750 rpm (Daihan Scientific Co, KR) at room temperature for 24 h. Chickpea flour (3% w/v) (CF) was added to PEO solution and homogenized by high speed homogenizer (IKA T25 Digital Ultra-Turrax, Staufen, Germany) at 10200 rpm for 2.5 min. Then, the pH of the solution was adjusted to 10.2 ± 0.2 by adding 0.6 M NaOH. It was heated in the water bath (GFL, Type 1086, Germany) to prepare a conventionally-heated solution until its temperature reached 80 °C. Subsequently, after the solution was transferred to the magnetic stirrer at 750 rpm to keep it at 80 °C for 2 h, it was cooled down to room temperature. Tween 80 was added (2 % w/v) as a surfactant and it was stirred again at 750 rpm for 30 min. To prepare microwave-heated sample, the PEO/chickpea flour mixture, whose pH was adjusted in advance, was directly heated by a microwave oven (Kenwood, New Jersey, USA) for 2.5 min at 416 W until the solution temperature reached 80 °C. The power level was determined by IMPI 2-L test. Then, the procedures of cooling and addition of Tween 80 were conducted in the same way as conventional heating. Curcumin (0.05 ± 0.005 g) was dissolved in 5 mL ethanol to prepare a curcumin stock solution. It was subsequently added to 10 mL of chickpea flour/PEO solution. All solutions were stirred at 1500 rpm for 10 min at 25 °C to ensure homogeneity before electrospinning. The films were labeled as C/CON, CUR/CON, C/MW, CUR/MW. In labeling, the curcumin added films

were symbolized by an abbreviation of CUR while the control films without curcumin were represented as C. The latter part of the labels referred to the heating treatments of polymer mixtures, that is, CON for conventional heating and MW for microwave heating.

2.2.1.3   Preparation of curcumin/faba bean/chitosan casting film

Chitosan (2 % w/v) (CS) was dissolved in acetic acid solution (2% v/v) overnight at 45 °C by using a magnetic stirrer at 750 rpm (MaxTir 500, Daihan Scientific, Seoul, Korea). A slurry of faba bean flour (4%, w/v) was prepared by stirring at 750 rpm and at 80 °C for 45 min to complete starch gelatinization and protein denaturation. After cooling down the slurry to 45 °C, chitosan and flour slurry were mixed in equal volumes. Then, 0.4 % (w/v) glycerol was added to the solution as a plasticizer. Curcumin (0.05 g) was dissolved in 10 mL ethanol and added into film-forming solution (FFS) was obtained. Films without any crosslinking agent were regarded as a control (FC-C). To prepare citric acid (CA) cross-linked films (FC-0.5C, FC-1C, FC-1.5C), CA was added to the FFS in different ratios (0.5 %w/v, 1% w/v, 1.5% w/v). To obtain glutaraldehyde (GLU) (FC-30GLU, FC-60GLU, FC-120GLU) cross-linked films, GLU were included in the FFS in different ratios (0.03% v/v, 0.06 v/v, %0.12 v/v). Films were symbolized according to the presence of crosslinking agents and ratio. The nomenclature was given in Table 2.1. FFS was stirred at 1200 rpm for 45 min and then degassed using an ultrasonic bath (Lab Companion, Jeiotech, Seoul, Korea) at 37 kHz for 25 min.

Table 2.1 Nomenclature of the faba bean flour-chitosan- curcumin films (FC)

Nomenclature	Citric acid (CA) % (w/v)	Glutaraldehyde (GLU) % (v/v)
FC-C	-	-
FC-0.5C	0.5	-
FC-1C	1.0	-
FC-1.5C	1.5	-
FC-30GLU	-	0.03
FC-60GLU	-	0.06
FC-120GLU	-	0.12

2.2.1.4 Preparation of citric acid cross-linked curcumin/ chickpea flour/ chitosan casting films

The solvent casting method was employed to produce CA cross-linked CUR/CF/CS active films. Chitosan (2 % w/v) was dispersed in acetic acid solution (2% v/v) overnight, at 45°C by using a magnetic stirrer at 750 rpm (MaxTir 500, Daihan Scientific, Seoul, Korea). A solution of chickpea flour (4% w/v) was prepared in DI water, and stirred at 80 °C for 45 min to obtain a chickpea flour slurry as a result of protein denaturation and starch gelatinization. When the chickpea flour slurry was cooled down to room temperature, chitosan solution and flour slurry were mixed in equal volumes. Next, glycerol (0.4% w/v) was introduced into the solution as a plasticizer. Curcumin (0.05 g) was dissolved in 10 mL ethanol and added in to film forming solution (0-CUR/CF/CS). Eventually, CA was added at different concentrations 0.5%w/v (0.5-CUR/CF/CS), 1% w/v (1-CUR/CF/CS), 1.5% w/v (1.5-CUR/CF/CS) to film forming solution and the final mixture was mixed once

more for 45 min at 1200 rpm to make it homogenous. This procedure was followed by degasification at 37 kHz for 25 min by using an ultrasonic bath (Lab Companion, Jeiotech, Seoul, Korea).

2.2.2 Characterization of solution properties

2.2.2.1 Spectral characteristics of curcumin solution for intelligent packaging

The color and spectral changes in curcumin solution at different pH values were measured by colorimeter (KonicaMinolta CR-5 Osaka, Japan) and UV/VIS spectro-photometer (UV 2450, Shimadzu, Columbia, USA), respectively. In this experiment, curcumin solution was added to different pH solutions varying from 2 to 13 and scanned in the range of 300–600 nm. To calculate ΔE^* values (Equation 1) initial values L^*, a^*, b^* of curcumin were used.

L_0^*, a_0^*, b_0^* are the color values of standard curcumin solution.

$$E^* = \sqrt{(L_0^* - L_0)^2 + (a_0^2 - a_0)^2 + (b_0^* - b_0)^2} \qquad \text{(Equation 1)}$$

2.2.2.2 Rheological properties

The rheological behavior of the solution was measured using a controlled strain rheometer (Kinexus dynamic rheometer, Malvern, UK) with a cone (4° cone angle) and plate (40 mm diameter) geometry at 25 ± 1 °C. After placing the solution, the edges were trimmed. For flow measurement, shear stress values of the sample were recorded between 0.1 s−1–100 s−1 shear rates. Then, obtained data were fitted to the Power Law Model equation (Equation 2).

$$\tau = K(\dot{\gamma})^n \qquad \text{(Equation 2)}$$

where τ is the shear stress (Pa), $\dot{\gamma}$ is the shear rate (s^{-1}), k is the consistency index (Pa.s) and n is the flow behavior index.

2.2.2.3   Solution conductivity

The electrical conductivity of samples was measured using a conductometer (WTW LF95, Germany) at 25 °C.

2.2.3   Electrospinning of solutions

The electrospinning process was carried out using Nano-Web 103 (Mersin, Turkey). Polymer solutions were placed in 5 mL syringes having 21gauge steel needle with 11.58 mm inner diameter. After placing the syringe horizontally in front of the aluminum foil covered stationary collector, electrodes were connected to the collector plate. The collector is a square (Each size is 16 cm). The distance between the syringe and collector was 30 cm. Relative humidity is 30–40% in the electrospinning cabinet. The flow rate and voltage were 0.6 mL/h -12 kV and 0.6 mL/h- 15kV for CS/PEO and chickpea flour/PEO solutions, respectively.

2.2.4   Casting Film production

Solutions of 15 g were poured into LDPE Petri plates and dried in a 55ºC oven (Binder ED 115, Tuttlingen, Germany) for 6.5 h. Films were stored in a climate chamber (52% RH, at 20 ºC) at least for 48 h before analysis.

2.2.5 Film characterization

2.2.5.1 Morphological analysis of nanofibers

Morphological characterization of curcumin loaded nanofibers was carried out with Field Emission Scanning Electron Microscopy (FESEM) (JEOL, Japan). After samples were stuck on metal stubs and coated with gold palladium (10 nm), surface images were obtained. Diameters of randomly selected 100 fibers were measured using Image J software (Maryland, USA).

2.2.5.2 Ammonia sensitivity of curcumin/CS/PEO nanofilms

To demonstrate the response of curcumin loaded films toward a real food system, nano films were exposed to ammonia vapor (Ezati & Rhim, 2020). Flask was filled with 80 mL of 0.8 M ammonia solution, and the top (4.90 cm^2) was covered with a colorimetric film. The distance between the solution and the nanofiber film was adjusted to 1cm. Color changes of films were recorded by colorimeter (PCE-CSM 3) in terms of L*, a*, b*, then it was converted to RGB color scale by MATLAB 9.0 (R 2016a). Data were taken every 3 minutes for 30 minutes. The sensitivity of the indicator was calculated using equation (3) (Zhang et al., 2019)

$$S_{RGB} = \frac{(R_a - R_b) + (G_a - G_b) + (B_a - B_b)}{R_a + G_a + B_a} \times 100 \qquad \text{(Equation 3)}$$

S_{RGB} refers to sensitivity value, subscript 'a' shows initial values, and 'b' indicates colors after exposing ammonia.

2.2.5.3 DPPH radical-scavenging activity of films

DPPH activity of the films was measured by the method described by Prietto et al., (2018) and Aydogdu, Yildiz, Ayhan, et al., (2019a). Some amount of nanofibers (0.05 g) was dissolved in ethanol solution and centrifuged at 10000 rpm for 3 min.

A diluted sample was mixed with DPPH (50 ppm) solution and the absorbance value (UV 2450, Shamadzu, Columbia, USA) was measured at 517 nm after 30 min. Then DPPH scavenging activity, and antioxidant activities were calculated by using equation (4) and (5);

$$\text{DPPH scavenging activity (\%)} = \frac{A_{control} - A_{sample}}{A_{control}} \times 100 \qquad \text{(Equation 4)}$$

$A_{control}$ and A_{sample} are the absorbance of the DPPH solution with and without sample.

$$\text{DPPH Activity (mg DPPH/ g dry weight of sample)} = \frac{C_1 - C_2}{W_{sample}} \times V \qquad \text{(Equation 5)}$$

2.2.5.4   ABTS radical scavenging activity of the films

To prepare the ABTS analysis, potassium persulfate (2.6mM) and ABTS (7mM) were mixed and stored at room temperature in the dark. The diluted sample was mixed with ABTS solution and incubated at room temperature for 30 min. The absorbance of the solution was measured by a spectrophotometer at 734 nm. (Roy & Rhim, 2020e). ABTS scavenging activity of the samples was calculated according to the equation (6) below,

$$\text{ABTS scavenging activity (\%)} = \frac{A_{control} - A_{sample}}{A_{control}} \times 100 \qquad \text{(Equation 6)}$$

$A_{control}$ and A_{sample} are the absorbances of the ABTS solution with and without the sample.

2.2.5.5   Differential scanning calorimeter of the films

Thermal analysis of films was performed by using a differential scanning calorimeter (Pyris 6 DSC, PerkinElmer, Massachusetts, USA). A sample of 5 mg was placed in an aluminum pan and heated with a heating rate of 10 ºC/min from 25 °C to 350 ºC. For each measurement, an empty pan was used as a reference. The experiment was replicated twice for each sample.

2.2.5.6 Thermogravimetric Analysis (TGA) of the films

Thermogravimetric analysis of the samples was carried out using a thermo-gravimetric analyzer (Perkin Elmer Pyris 1). A sample of 5 mg was heated from 30 °C to 600 °C at a rate of 10 °C/min and a nitrogen flow rate of 30 mL/min.

2.2.5.7 Mechanical Properties of the films

Tensile strength and percentage elongation at break were measured by a texture analyzer (Brookfield, Ametek CT3, Middleboro, MA, USA, TA- DGA tension probe). The test was carried out using 0.4 N load cell at a test speed of 0.40 mm/s.

2.2.5.8 Water vapor permeability of the films

The thickness of the films was measured from six different random points with a handheld digital micrometer (LYK 5202, Loyka,). Cups with 40 mm internal diameter were filled with 35 mL water to adjust internal relative humidity to 100%. Then, the film was placed on top of the cup and fixed by using rubber joints. Cups were placed in the desiccator which was filled with silica gels. During the experiment, relative humidity and temperature were recorded by humidity/temperature logger (EBI20-TH1, EBRO, Ingolstadt, Germany). Weight changes of the cups were recorded over 12-hour period at 1 h intervals. WVP of the cups was calculated using the equation below (7)

$$\text{WVP} = \frac{WVTR \times (\Delta x)}{(\frac{R_1 - R_2}{100}) \times P_{sat}}$$ (Equation 7)

Water vapor transmission rate (WVTR) can be calculated from weight changes versus time graph ($\text{g m}^{-2}\,\text{s}^{-1}$), Δx is the thickness of the nano films (m), relative humidity inside and outer side of the cups were represented by R_1 and R_2 respectively. Finally, the P_{sat} (Pa) is the saturated water vapor pressure at room temperature.

2.2.5.9   XRD analysis of the films

Crystalline properties of the films were analyzed by X-ray diffractometer (Rigaku Ultima-IV, USA) using copper (Cu) irradiation with 30 mA current and 40 kV energy. Samples were scanned at an angular range of 5° and 70° scanning range with a 2°/min scanning rate.

The crystallinity degree of the samples was determined by using Equation (8), based on the method described by Demirkesen, Campanella, Sumnu, Sahin, & Hamaker, (2014).

$$Total\ Crystallinity\ (T_C) = \frac{I_c}{I_c + I_a} \hspace{3cm} \text{(Equation 8)}$$

Where I_c is integrated intensity of crystalline phase and I_a is the integrated intensity of amorphous phase.

2.2.5.10   Antimicrobial activity of the active films

The bacterial cultures of Gram (-) Escherichia coli (ATCC 11229) and Gram (+) Staphylococcus aureus (ATCC 43300) were provided by Public Health Institution of Turkey, from culture collection and preserved at the Department of Food Engineering, METU. The antimicrobial activity of films was tested according to the method described by Janani, Zare, Salimi, & Makvandi, (2020). Lyophilized each bacterial culture was revived by incubating one bead in 9 mL nutrient broth for 24h, 37 °C. At the end of the period, *E.coli* and *S.aureus* microbial suspensions were transferred to the selective media agar namely Chromogenic *E.Coli*, Baird Parker Agar and incubated at 24h, 37 °C. Then, colonies from each microbial strain were incubated in the nutrient broth at 37 °C overnight. The optical density of each medium was read at 625 nm, and absorbance was set at nearly 0.1 with a final cell density of approximately 1.5×10^8 CFU/mL. Bacterial suspensions (100 µL each) were transferred into the corresponding agar medium. The films were cut into a disc shape of 0.8 mm diameter and placed on previously inoculated Petri plates. After

diffusion of the active compound (at 37 °C for 24 h) into the medium, the diameter of inhibition zones was measured.

2.2.6   Chicken Analysis

2.2.6.1   pH measurement of the chicken breast

After placing 10 ± 0.1 g of chicken breast in the petri dish, it was sealed with PVC film. Petri dishes were stored in the refrigerator at 4 ºC for 8 days. pH of the chicken breast was measured every 24 h interval with pH probe (Hanna Lab, FC2022, USA).

2.2.6.2   TVB-N measurement

Chicken of 10 g was homogenized by with 100 mL of water using a sterile blender (Waring Commercial, USA). The homogenized chicken sample was centrifuged at 10000 rpm for 10 min. The corresponding supernatant was made alkaline by adding an equal volume of MgO solution (1 % w/v). Steam distillation method was performed. The distillate was collected in a flask containing 25 mL of (20 g/L) boric acid and a few drops of methyl red/ bromocrosol green indicator. Finally, the obtained solution was titrated with 0.1 M HCl solution until a color change from green to pink was observed (J. Hu et al., 2019). The TVB-N content of the samples was calculated with the following equation (9);

$$\text{TVB-N (mg/100g)} = \frac{(V_1 - V_2) \times c \times 14}{m \times 10/100} \times 100 \qquad \text{(Equation 9)}$$

where V_1 and V_2 are the titration volumes (mL) of the sample and the blank, c is the concentration of HCl, (mol/L) and m represents the weight of the sample (g).

2.2.6.3 Application of colorimetric films on the food package and microbiological analysis

Chicken samples were prepared by cutting the into the pieces with 1 g and placed into the sterile petri dish and sealed with PVC film. Colorimetric nano fibers were placed near the meat. Samples were stored at 4 ºC. Color changes of films were recorded by colorimeter (PCE-CSM 3) in terms of L^*, a^*, b^*. Data were taken every 24 h.

The microbial experiment was carried out according to the method described by Mohammadalinejhad, Almasi, & Moradi, (2020) with some modifications. Daily, 10 g of chicken breast was transferred to the stomacher bag containing 90 mL of 0.1% peptone water and homogenized for 2 min to obtain a stock solution. Serial dilutions were carried out and 100 µL of each was spread onto the plate count agar (PCA) plates. The aerobic mesophilic microbial count was carried out by counting the number of colonies after 24h incubation at 37 °C and results were shown in terms of $\log_{10}$CFU/g.

2.2.6.4 Application of citric acid cross-linked curcumin/ chickpea flour/chitosan films on chicken breast

The chicken breast meat was bought from a local market in Ankara, Turkey and aseptically cut into 10 g- pieces. Chicken samples were completely wrapped by 0-CUR/CF/CS and 1.5-CUR/CF/CS active films and stored at 4ºC. The microbiological quality of the samples was evaluated 0, 1, 3, 5, 7 and 9 days of storage.

To carry out the analysis, chicken samples (10 g) were transferred aseptically to a stomacher bag containing 90 mL of 0.1% peptone water and blended in a Stomacher (WiseMix, WES- 400, DAIHAN) for 2.5 min.

Samples were diluted serially using 0.1% peptone water. Total aerobic mesophilic counts were determined using the plate count agar technique. The microbiological analysis was carried out in duplicate and the results were expressed based on log (CFU/g) (Konuk Takma & Korel, 2019).

2.2.7 Statistical analysis

All experiments were performed in duplicate. All statistical analysis was performed using MINITAB (version 16). Analysis of variance (ANOVA) with Tukey's multiple comparison test was used for the statistical evaluation of experimental data ($p < 0.05$).

CHAPTER 3

RESULTS AND DISCUSSION

3.1 Fabrication of curcumin loaded CS/PEO nanofibers

To find the optimum concentration and to decide electrospinning parameters of curcumin CS/PEO nanofibers, preliminary experiments were carried out. Increasing concentration of chitosan resulted in increasing conductivity which obstructed smooth fiber formation. Although homogenous fibers were obtained at different concentrations of PEO (4%, 5%, and 6% (w/v)), the lowest concentration was chosen.

3.1.1 Conductivity of the electrospun solutions

The conductivity of electrospun solution plays a crucial role in the production of bead-free uniform fibers. For this reason, the solution conductivity at different CS/PEO ratios was investigated. In this study, CS was dissolved in aqueous acetic acid (80%, v/v) before mixing with PEO and curcumin. CS has amino groups on its backbone with the pKa value of 6.3 (Silva-Weiss, Bifani, Ihl, Sobral, & Gómez-Guillén, 2013) and thus, at a pH below its pKa value, CS becomes readily soluble as a result of the electrostatic repulsion between protonated backbone amino groups (Kriegel et al., 2009a). These positively charged amino groups on the backbone would also be held responsible for the observed trend that the conductivity of the resulting electrospun solutions increased with the amount of CS added in Table 3.1. In another words, when the ratio of charged CS to the uncharged PEO was increased in the electrospun solution, the conductivity increased as expected.

3.1.2   Rheological behavior of the electrospun solutions

Rheological behavior of the polymer solution is the main indicator for intermolecular interaction between polymer chains. Molecule interactions play a major role in both the solution spinnability and the fiber morphology (Dilamian et al., 2013). As seen in Table 3.1, the flow behavior index (n) and the consistency index (k) of the electrospun solutions with different chitosan and PEO ratios followed the power law with a high coefficient of determination values (r^2=0.996). The flow behavior indices of all the investigated electrospun solutions were less than unity with a non-Newtonian shear-thinning flow profile and showed no significant difference among the samples. Shear thinning polymer mixtures were also used previously to produce nanofibers of alginate/PEO (Rošic et al., 2012), HPMC/ PEO (Aydogdu, Sumnu, et al., 2018), maltodextrin/soy protein isolate, maltodextrin/ whey protein (Kutzli et al., 2019), in the literature.

There was no significant change in the consistency index values of polymer mixtures prepared at different CS/PEO ratios (Table 3.1). When the rheological properties of sole CS/PEO blends were investigated previously in the literature, increasing CS ratio was reported to cause a more viscous polymer blend with greater consistency index values (Surendhiran et al., 2020). The increase in the solution viscosity was attributed to higher repulsive forces between protonated amine groups of the CS molecules leading to an expansion of hydrodynamic volume (Pakravan et al., 2011). On the other hand, when CS is dissolved in acetic acid concentrations greater than 50-wt%, the viscosity of CS stays constant as amine groups exist entirely in the fully protonated form at this concentration and above (Pakravan et al., 2011). In this study, CS before blending with PEO was dissolved in 80% (v/v) leading to the complete protonation of backbone amine groups. This explains no difference in the solution viscosity and, thereby the consistency index values at different CS/PEO ratios. Besides, curcumin stock solution in ethanol was directly introduced to the polymer mixture just after blending of CS and PEO to prepare the final electrospun solutions. Ethanol in this case might act as a diluent by loosening the interaction between

chitosan and PEO, which might provide more free space for polymer motion. CS-PEO hydrogen bonding might be replaced by CS-ethanol and PEO-ethanol hydrogen bonding. For this reason, molecules might have become more freely orientated in the movement direction during constant shear rheology measurement. Therefore, the increase in consistency index behavior with chitosan concentration might not be observed in our study as expected.

Table 3.1 Conductivity, flow behavior index (n) and consistency index (k) and average fiber size of the electrospun solutions;

Chitosan /PEO	Conductivity (µs/cm)	k (Pa s^n)	n	Fiber diameter (nm)
1.5/8.5	283$\pm$2.64[c]	1.265$\pm$0.01[a]	0.891$\pm$0.04[a]	338$\pm$35[a]
2.0/8.0	296$\pm$4.58[b]	1.177$\pm$0.03[a]	0.918$\pm$0.01[a]	304$\pm$28[b]
2.5/7.5	311$\pm$ 1.0[a]	1.188$\pm$0.04[a]	0.913$\pm$0.01[a]	283$\pm$27[c]

Columns having different letters are significantly different ($p \leq 0.05$).

3.1.3 Nanofiber morphology

FESEM images of nanofibers were shown in Figure 3.1. Continuous and smooth high quality beadless nanofibers are hard to produce due to strong intramolecular and intermolecular hydrogen bonds between hydroxyl and amino groups of CS when CS is used as a bare polymer in the electrospun solution (Deng, Taxipalati, et al., 2018). In this respect, copolymers such as PEO can be used to improve the spinnability of chitosan. The addition of PEO might interfere with the self-association of CS chains and induce the hydrogen bond formation between hydroxyl and amino groups of CS molecules and ether groups of PEO (Surendhiran et al., 2020). In the present study, chitosan and PEO were blended at different ratios to ensure homogenous and reproducible fiber formation.

Viscosity and conductivity of the electrospun solution control the fiber morphology significantly. Solutions with high viscosity undergo a longer relaxation time after ejection from the needle tip and consequently cause an increase in fiber diameter. On

the other hand, the solution with higher conductivity values may lead to electrospun fibers with smaller diameters due to higher elongation of the solution jet through the collector (Erdem & Akalın, 2015). As shown in Table 3.1, diameters of electrospun fibers decreased significantly with increasing chitosan concentration in the solution. As solutions showed similar rheological behaviors, the differences in fiber diameters might be attributed to the increase in solution conductivity with chitosan concentration. In other words, solutions with higher conductivities might elongate more that even a small change in chitosan concentration in solution might result in completely distinct fiber sizes. For instance, changing chitosan/PEO ratio from 1.5/8.5 to 2.5/7.5 resulted in a significant decrease in average fiber diameter from 338.66 ± 35.57 to 283.18 ± 27.83 nm, respectively.
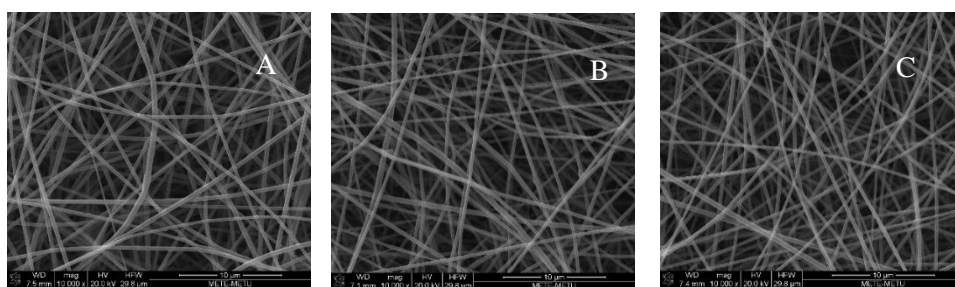
Figure 3.1. SEM images of curcumin loaded electrospun fibers (A) chitosan/PEO ratio: 1.5/8.5, (B) chitosan/PEO ratio: 2/8, (C) chitosan/PEO ratio: 2.5/7.5

3.1.4   pH response of the solutions

UV-Vis spectra of the solutions at different pH values were represented in Figure 3.2a. The absorption maximum of curcumin solution was observed at 432 nm between pH 6 and 10 and the intensity of this peak decreased upon the increase in the solution pH. When the solution became more alkaline (pH>10), the absorption peak at 432 nm was shifted to 470 nm. Such a red shift of the absorption spectrum could be related to pH-induced changes in the chemical structure of curcumin.

Curcumin has a structure of bis-α,β- unsaturated β-diketone, which can be at the equilibrium with its enol tautomeric form (R. A. Sharma et al., 2005).
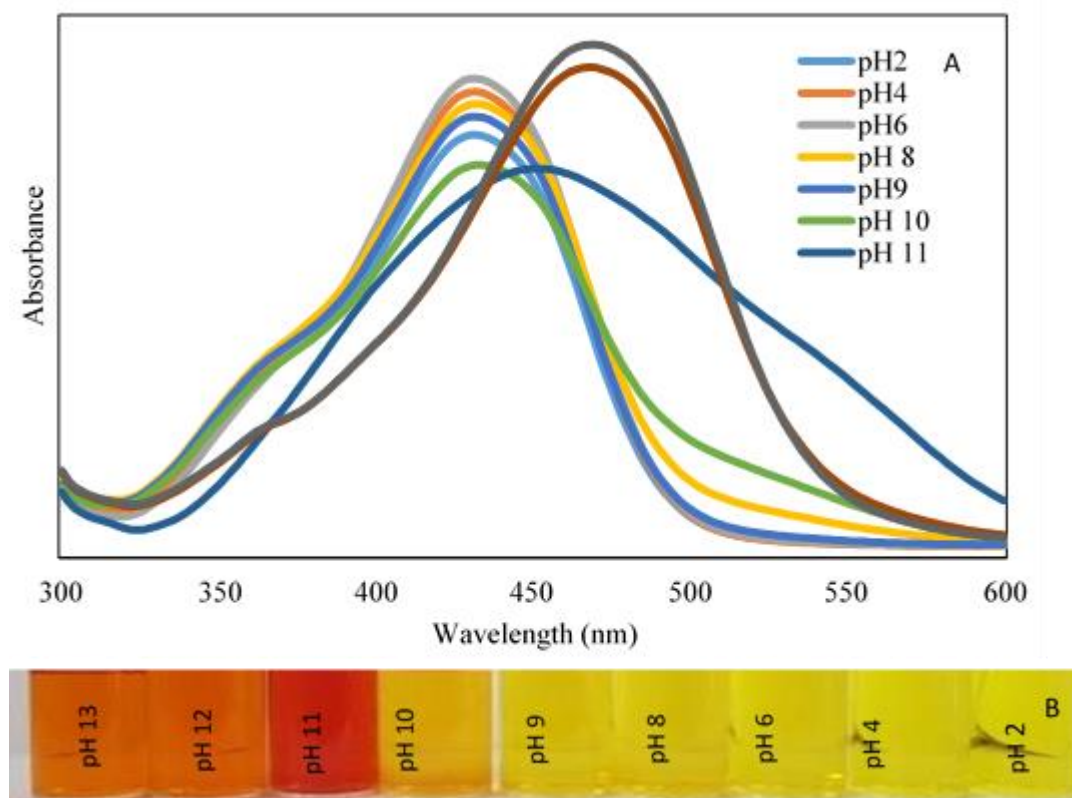
Figure 3.2. (a) UV-vis spectra and (b) picture of color variations of curcumin solution at different pH

Under acidic pH (between 3 and 7), curcumin acts as a hydrogen atom donor because of its dominant bis-keto structure. The peak at the acidic environment, therefore, is attributed to the electron excitation from the π-π* transition of curcumin. On the other hand, its enolate structure becomes predominant, and curcumin stands out as an electron donor under alkaline conditions. The peak at the alkaline environment is ascribed to the fully deprotonated structure of curcumin (L. Kong & Ziegler, 2014). Further, the color change of curcumin solutions was analyzed in terms of CIELAB color scale. The color of curcumin solution changed from bright yellow to dark-red orange from acidic to basic pH (Figure 3.2b). Drastic value change was observed at 'a*' scale of the samples with increase in pH value (Figure 3.3). ΔE*

results were mostly shaped under the effect of 'a*' value, and followed a very similar trend. Therefore, color change of the curcumin solution might be easily distinguished after pH 10. Thus, curcumin might serve as a promising visual indicator in CS/PEO nanofibers to monitor the freshness of chicken breast samples.
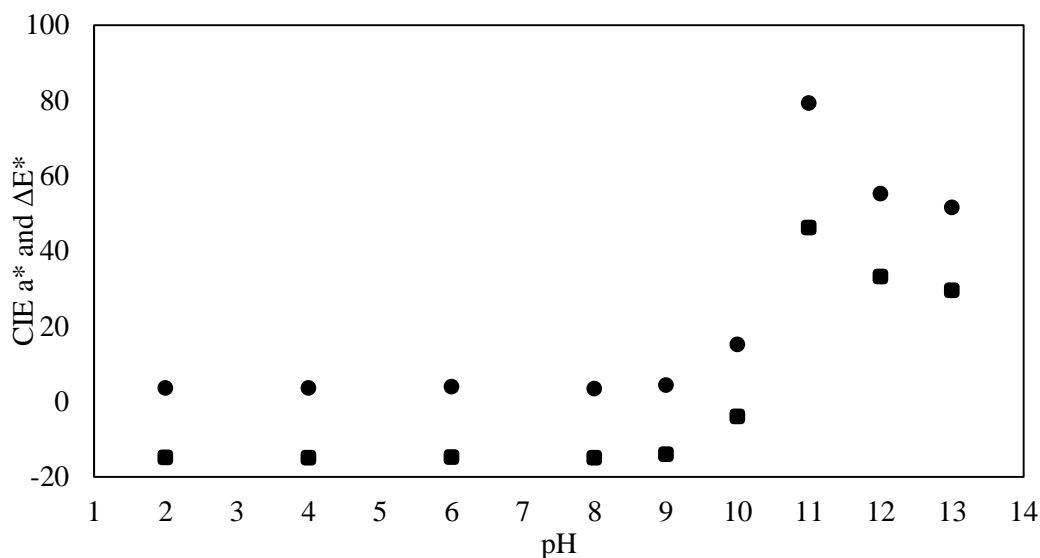
Figure 3.3. Change in a* and ΔE^* values of curcumin solutions with respect to pH, ●: ΔE^*, ■: a*

3.1.5   Ammonium response of the fibers

CUR/CS/PEO nanofiber films were subjected to 0.8 M ammonium vapor to monitor the color change. Herein, ammonium vapor was selected to mimic volatile nitrogen compounds i.e., TVB-N, which are produced during spoilage of protein-rich foods and used as a freshness indicator. In this respect, sensitivity of the films to ammonium vapor for 30 min was monitored using the changes in the RGB values (Figure 3.4). Air humidity promotes the reaction between ammonia and water to form ammonium and hydroxide ions. The phenolic hydroxyl group of curcumin might give an acid-base reaction with hydroxyl groups of ammonia to form phenolic oxygen anion in the curcumin structure (Q. Ma, Du, et al., 2017) which was mainly responsible for the color change of the films.
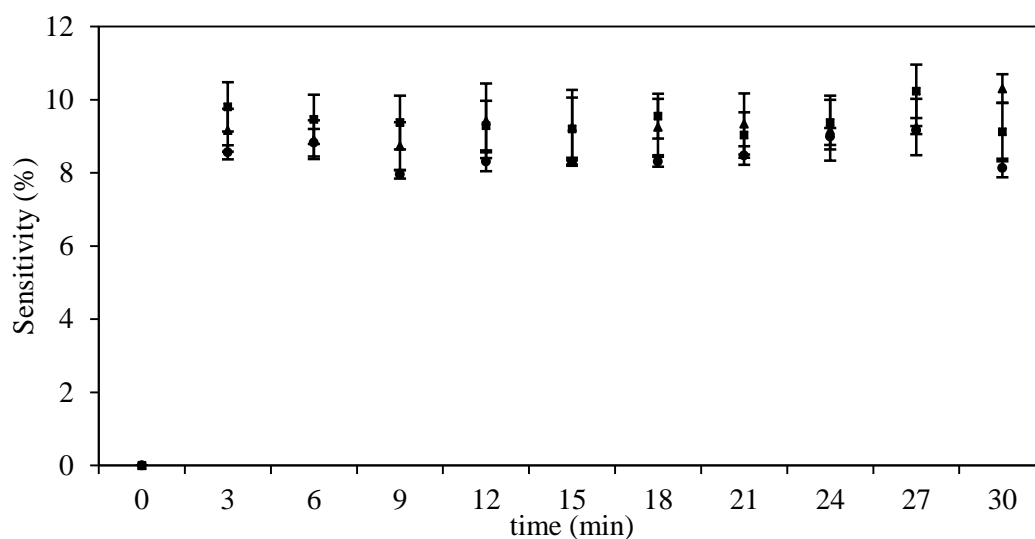
Figure 3.4. Sensitivity of curcumin loaded chitosan/PEO films to ammonia vapor.
■:1.5/8.5, ●: 2.0/8.0, ▲: 2.5/7.5.

Curcumin content and average fiber size diameter might be considered as two important factors affecting the ammonium gas response of the films. Gas molecules diffuse faster through nanofibers with smaller diameters (Avossa et al., 2019). Thus, thinner nanofibers are expected to show better gas sensing performance with their higher specific surface areas (Zhang et al., 2018). However, fiber diameter by itself would not be a good indicator of sensitivity when recognition molecules are doped into nanofibers. In that sense, antioxidant activity was used here to determine the active amount of curcumin embedded into the nanofibers indirectly. When ammonium response of the films (Figure 3.4) was analyzed, the sensitivity of all films at time 3 min (initially) and 30 min (at the end) was not markedly different. On the other hand, films with CS/PEO ratio of 1.5/8.5 had a higher antioxidant activity with the highest fiber size diameter while the films with chitosan/PEO ratio of 2.5/7.5 showed the lowest fiber size diameter and the lower antioxidant capacity. Thus, an inverse relationship between fiber size diameter and antioxidant activity was found. In short, none of the films gained an advantage over the other films in terms of sensitivity due to this inverse relationship between two variables.

3.1.6   Differential scanning calorimetry (DSC) analysis and Thermogravimetric analysis (TGA) of the nanofibers

In DSC measurements of the fibers, pure chitosan, curcumin, PEO were used as controls (Table 3.2). Despite of its crystalline structure, crystalline melting temperature (T_m) of CS cannot be extracted from DSC analysis. This behavior is attributed to the rigid polymer backbone of CS with strong interchain or intrachain hydrogen bonding (Lee et al., 2000). However, there was a peak located at 150.14°C in DSC thermograms of CS. A similar endothermic peak has been reported to occur and associated with the dissociation of interchain hydrogen bonding of CS (Chuang et al., 1999). Further, T_m of pure PEO was measured to be 71.6°C. On the other hand, the presence of CS depressed the T_m of the system at all ratios of CS/PEO. The melting point depression is a good indicator of polymer miscibility and thereby, pointing out the miscibility of CS/PEO blends and curcumin in this study.

The melting temperature depression might be related to the disruption of PEO crystallinity due to its interaction with CS. Similar findings were also reported for nanofibers of PEO/HPMC (Aydogdu, Sumnu, et al., 2018) and PEO/CS (Kriegel et al., 2009a) fibers. The T_m values of PEO/HPMC nanofibers were also found to be lower than that of pure PEO (Aydogdu, Sumnu, et al., 2018). At higher PEO ratios, PEO crystals extended and hold each other tightly. However, increasing chitosan ratios in polymer blending disrupted PEO-PEO interactions and destabilized PEO crystallinity and lowers the temperature (Erdem & Akalın, 2015). As can be seen in Table 3.2, samples with a higher chitosan amount had a lower melting point than the pure PEO. This might be evidence of disruption of PEO crystallinity by the chitosan through hydrogen bonding between chitosan (-NH2) and PEO (etheric oxygen).

Table 3.2 DSC and WVP results

	T_m (°C)	ΔH_m (J/g)	T_d (°C)	ΔH_d (J/g)	WVP ($\times 10^{-11}$) (g m^{-1} s^{-1} Pa^{-1})
PEO	71.6	163.27	-	-	
Chitosan	-	-	150.14	140.37	
Curcumin	178.38	115.54			
1.5/8.5	63.47	95.14	-	-	14.27±0.05[a]
2.0/8.0	62.91	106.76	-	-	13.03±0.01[a]
2.5/7.5	61.67	95.29	-	-	7.30±0.06[b]

Columns having different letters are significantly different ($p \leq 0.05$). Curcumin loaded chitosan/PEO films: 1.5/8.5, 2.0/8.0, 2.5/7.5. T_m- melting temperature, ΔH_m (J/g)- melting enthalpy, T_d- denaturation temperature, ΔH_d (J/g)- denaturation enthalpy of

Another reason of this melting point depression might be the working principle of electrospinning. During electrospinning, polymer chains are stretched by electrical force and remain in noncrystalline state mostly upon rapid solidification (Md Shahidul Islam & Karim, 2010). This change in the highly crystalline structure of PEO as a result of electrospinning might also contribute to the observed melting point depression. Similar to the decreasing trend of T_m in Table 3.2, the melting enthalpy of nanofibers shifted gradually to the lower values as the CS content in the electrospun solution was raised, possibly due to the same reasons listed above. Furthermore, T_m of crystal curcumin was found to be 178 °C. However, DSC curves of nanofibers did not show any endothermic peaks associated to the T_m of curcumin. The absence of the peaks shows that curcumin crystals are amorphized as a result of

the molecular interaction with polymeric chains (Nascimento da Silva et al., 2019) that might be an evidence of the successful incorporation of coloring agent curcumin into CS/PEO matrix.

TGA is a measurement of weight change of materials as a function of temperature, which indicates the thermal stability. The weight loss versus temperature curve of polymers and fibers was shown in Figure 3.5. Chitosan showed two stage degradation. The first step of weight loss was observed just after heating of samples initiated that might be due to loss of absorbed moisture. Similar behavior was also observed in studies by Deng, Taxipalati, et al., (2018). The second stage of chitosan degradation started approximately at 255°C. A similar decomposition temperature of chitosan was reported in a previous study of CS/PEO nanofibers (Surendhiran et al., 2020). On the other hand, PEO has one degradation step with an onset temperature of around 350°C and almost 4% of sample weight remained at the end of the experiment. Compared to CS and curcumin, curcumin loaded CS/PEO nanofibers achieved higher thermal stability with a degradation temperature shifted by nearly 25°C (to 280 °C). One of the reasons might be relatively higher PEO content of the films as compared to chitosan and curcumin. Furthermore, strong intermolecular forces between PEO, CS and curcumin might also improve the thermal stability of the fibers. Comparable outcomes were also observed with the study on gallic acid loaded lentil flour based nanofiber (Aydogdu, Yildiz, Aydogdu, et al., 2019b). Finally, this improvement might also be linked to the presence of curcumin with a radical scavenger ability. Radicals generated during the thermal degradation might also be captured by curcumin. The onset degradation temperature of composite films with low-density polyethylene and curcumin had higher than that of pure LDPE. The difference was attributed to the presence of curcumin in the study (Zia et al., 2019). The second degradation of nanofiber films started and accelerated faster at around 360°C. Even though the degradation of the nanofiber films was a little faster than pure PEO, it was slower than pure chitosan and curcumin.
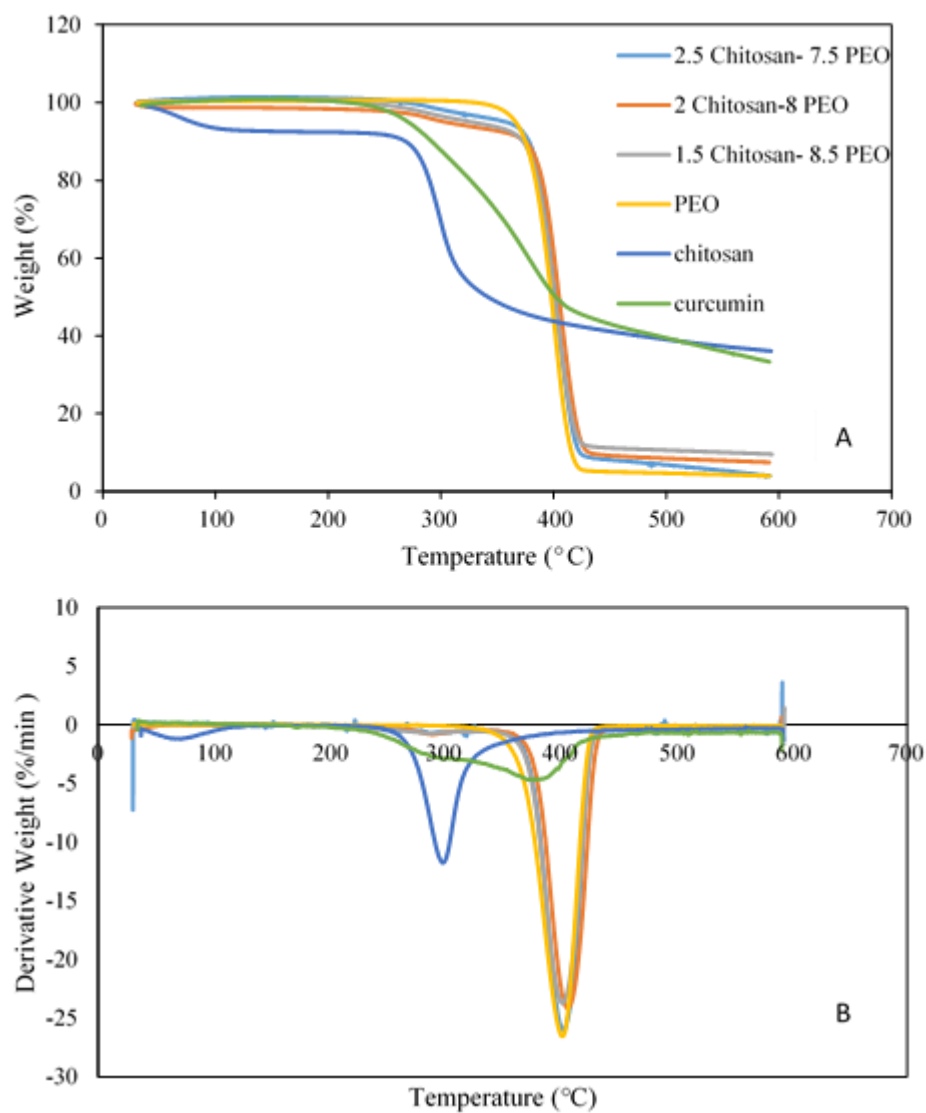
Figure 3.5. (A)Thermo-gravimetric curves and (B) DTG curve of pure components and nanofiber films

3.1.7   Water vapor permeability of the films

High permeability values of hydrophilic polymer films pose a great challenge to their use in practical packaging applications. One of the problems related to hydrophilic polymer films is their high water vapor permeability (WVP). In this study, although both CS and PEO can be categorized as hydrophilic polymers, permeability values of nanofibers (Table 3.2) were relatively lower than those with similar compositions. To illustrate, permeability values of the curcumin loaded CS/PEO nanofibers were in the range of 7.3 ± 0.06 and $14.27 \pm 0.05 \times 10^{-11}$ g m^{-1} s^{-1} Pa^{-1}. However, the results of CS and sodium caseinate films made by casting method were between 12.8 ± 0.22 and $101.3 \pm 1.10 \times 10^{-11}$ g m^{-1} s^{-1} Pa^{-1} (Z. Yang et al., 2008). The main reason behind this difference might be closed packaging of curcumin loaded chitosan/PEO films with nano size and three dimensional fiber networks. Furthermore, the presence of curcumin in the intelligent package formulation might have an impact on lower WVP values. Hydrophobic nature of benzene rings, and long carbon chain of curcumin hindered the transfer of water vapor from one side of the film to another by creating torturous pathways (Wu et al., 2019). Bulky benzene ring group might also interfere with chain mobility and thereby, decrease the rate of water vapor transfer. Similar results were also revealed by tara gum/polyvinyl alcohol based nanofibers. The outcomes were justified with hydrophobic character of curcumin (Ma, Du, et al., 2017). Besides, strong intermolecular interactions between all compounds might decrease available hydrogen for hydrogen bonding with water molecules. By this way, low affinity of nano fiber films towards water vapor might result in lower permeability (Siripatrawan & Harte, 2010). Further, there might be a relationship between fiber size and WVP. Increasing fiber size diameter brought about an increase in the permeability of the films with a correlation coefficient 0.892 ($p < 0.05$).   The decrease in fiber size diameters might cause tightly packed fibers with a compact network that might retard the migration of water vapor through a resulting torturous pathway.

3.1.8 Mechanical properties of curcumin loaded CS/PEO nanofibers

Tensile strength (TS), and elongation at break (%EAB) values of the CS/PEO/curcumin films are shown in Table 3.3. The highest TS value was recorded as 4.69±0.48 MPa for 2.5/7.5 chitosan/PEO sample whereas the lowest TS was measured as 2.42±0.08 MPa for 1.5/8.5 chitosan/PEO nanofiber. TS of the films enhanced with increasing chitosan concentration which was attributed to the rigid and stiff structure of chitosan (Surendhiran et al., 2020). These structural attributes of chitosan were expected to decrease EAB values of the films as stated in the study of Surendhiran et al., (2020). Although films with CS/PEO ratio of 2.5/7.5 had the lowest EAB (%) value, nanofiber formulated with 2/8 CS/PEO ratio showed the highest EAB (%). Therefore, it might be concluded that there was an optimum blending ratio for samples. The results of another chitosan/PEO blending nanofiber study supported that idea since the elasticity of the films did not significantly change until PEO ratio reached 75% (J. Li et al., 2010).

Table 3.3 Mechanical properties of CS/PEO nanofilm

Chitosan/PEO	Tensile strength (TS) (MPa)	Elongation at break (EAB) (%)
1.5/8.5	2.42±0.47[b]	17.88±1.37[ab]
2.0/8.0	4.16±0.03[a]	27.95±5.07[a]
2.5/7.5	4.69±0.08[a]	14.86 ±0.99[b]

Columns having different letters are significantly different ($p \leq 0.05$).

3.1.9 Changes in TVB-N and surface pH of the chicken breast during storage period

Highly perishable chicken can deteriorate easily even under refrigeration conditions. The reason behind this deterioration seems to be different types of microorganisms

such as Shewanella *putrefaciens*, *Pseudomonas* spp. and yeasts, the initial microbial load of carcasses is another important factor (Hurley et al., 2014). In this study, surface pH of chicken breast samples was measured in 24 hours intervals (Figure 3.7). Sample pH was nearly stable in the first 3-day period around 6.2. In the literature, pH value of 6.3 and 6.5 was reported as the onset of deterioration for chicken breast (D. Kim et al., 2017). Thus, starting from day 5, pH value of sample was at the edge of the unacceptable level. At the end of 8 days of storage, pH values started to increase and reached a value of 6.75 ± 0.06.
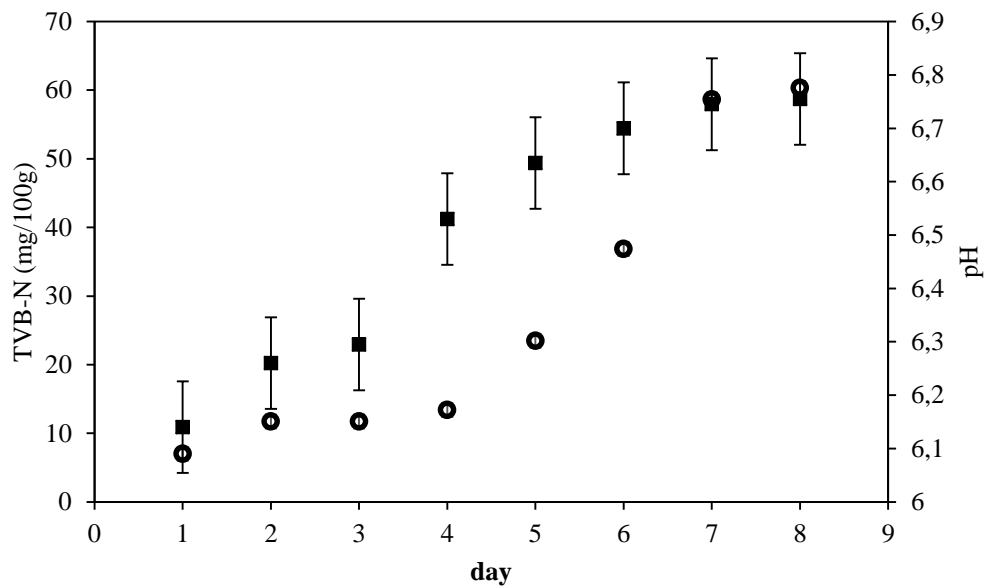
Figure 3.6. pH and TVB-N changes in the chicken breast and nanofiber film during storage time. ○: TVB-N, ■: pH

The amount of TVB-N in perishable food was commonly used to determine freshness, spoilage, in other words, shelf life of food. Since biogenic amines, including trimethylamine (TMA) and total volatile basic nitrogen (TVB-N), are the markers of growth of decarboxylase-positive microorganisms such as *Enterobacteriaceae*, and certain lactobacilli, enterococci and staphylococci (Hurley et al., 2014). The changes in TVB-N concentration of chicken breast samples were shown in Figure 3.6. In the beginning, TVB-N values of samples were recorded as 7.01 (mg/100g). In the literature, acceptable TVB-N value was generally accepted

66

as 20 - 30 mg/ 100 g for chicken meat which was supported by sensorial experiments (Hurley et al., 2014). As illustrated in the Figure 3.6, TVB- N concentration values remained nearly the same during 4 days of storage. After day 4, TVB-N concentration started to increase gradually until the end of the storage time. Samples exceeded the specified limit values at the end of day 6 (36.85 $\pm$ 3.35 mg N/ 100 g). TVB-N and pH increase showed a parallel increase and therefore both two analyses pointed out the unacceptable consumer level in a comparable timeline.

3.1.10   Changes in total aerobic mesophilic bacteria in chicken breast during storage

The change in aerobic mesophilic microbial count (log cfu/g) in chicken breast was observed during 8 days of storage, at 4°C and the results were shown in Figure 8. The number of colonies started to increase from the first day gradually until end of day 3 from 1.97 to 2.85 log CFU/g. Similar to pH change pattern (Figure 3.7), drastic population growth was seen on day 4, reaching 4.97 log CFU/g. Samples reached the spoilage threshold (6.7 log CFU/g) (Soysal et al., 2015) at the end of day 7. This meant that samples were no longer suitable for consumption. TVB-N content in the headspace was correlated to microbial population in the sample. Although chicken breast reached microbiological unacceptable limits at end of the day 7, TVB-N amount in samples achieved the threshold value earlier (day 6) than microbial limitations.
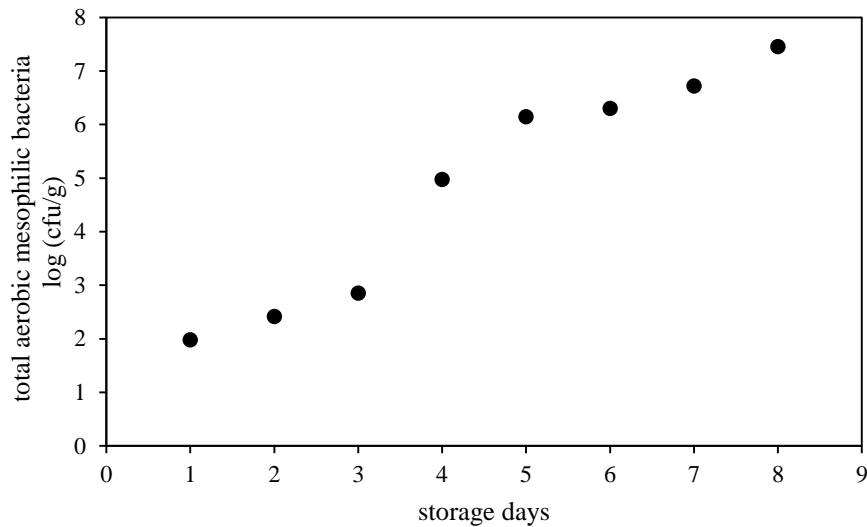
Figure 3.7. Total aerobic mesophilic bacteria (log cfu/g) through storage

3.1.11 Application of nanofiber films on chicken breast

Films formulated with 2.5/7.5 CS/PEO ratio showing the lowest fiber size and water vapor permeability, with the acceptable color response to ammonium treatment were chosen to demonstrate the potential food application. Even though nanofibers had an intense yellow color initially, the color changed as a result of the physicochemical changes in chicken breast over time (Figure 3.8). The CIE a* and b* results of the samples remained nearly constant at the first 3 day of the experiment. Starting from day 4, a* values followed an increasing trend which was opposite to the trend of b* values. In other words, yellowness of the films decreased while the redness of the indicator increased and became dominant over time. Observed trends of a*and b* values were ascribed to a strong alkaline environment as a result of an increase in TVB-N concentration at the headspace.
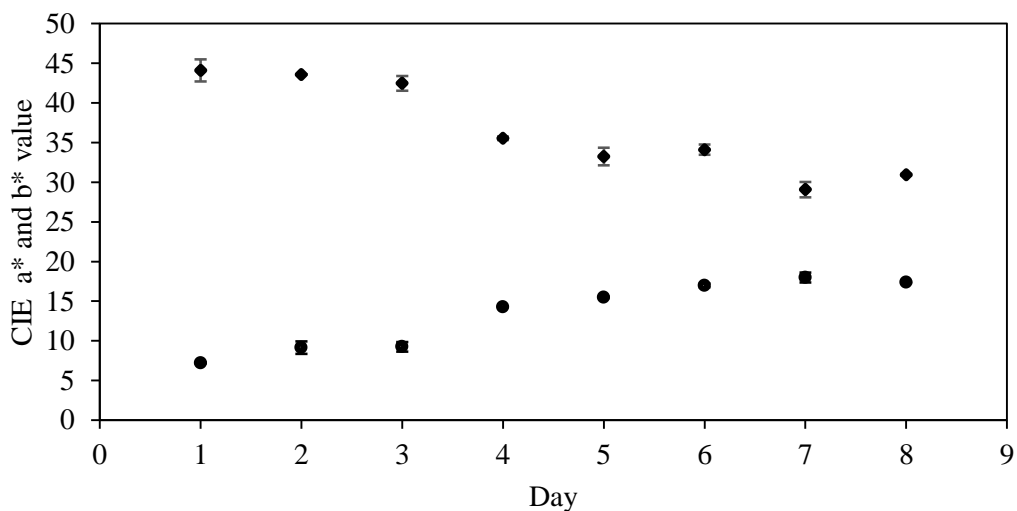
Figure 3.8. CIE a* and b* values of the films through the storage period, ●: a*, ♦: b*

In general, the overall color change of the solution might be evaluated by ΔE* values. When ΔE* is below 1, the observer cannot differentiate the color change visually. When ΔE* is between 1 and 2, only the trained observers can detect the change. When it comes to the values between 2 and 3, inexperienced observers start to differentiate the color variation. As soon as ΔE* reaches a value between 3-5, color variation becomes evident. Finally, any observer can certainly differentiate two different colors when ΔE* is higher than 5 (Silva et al., 2019). In this study, color change of curcumin loaded chitosan/ PEO nanofibers in parallel to the deterioration could be detected by the observer easily (Table 3.4). Even though a very low amount of curcumin was used in the nanofiber preparation, the reason behind achieving strong and intense change might be the film preparation method, electrospinning. The high surface area, and porous structure of nanofiber film might enhance the color change. The result of red cabbage extract loaded polyvinyl alcohol nanofilm sensors correlates well with this hypothesis (Maftoonazad & Ramaswamy, 2019). Taking TVB-N and pH levels, and the color change of the nanofiber films into consideration, the shelf life of the chicken breast stored at refrigerator temperature was estimated to be 5 days. In short, the color response of pH and TVB-N responsive nanofiber

correlated well with food deterioration and thereby, proved its validation as a promising intelligent packaging application

Table 3.4 Variation in in CIE ΔE* values and color of the film with respect to time

Day	ΔE*	Color
1	0	
2	3.09±0.74	
3	3.50±0.45	
4	11.83±1.19	
5	13.95±0.34	
6	14.49±0.18	
7	18.60±2.26	
8	17.33±0.98	

3.2   Fabrication of curcumin loaded chickpea flour /PEO nanofibers

To find the homogenous nano fibers, firstly, different concentrations of chickpea flour (3%, 4% (w/v)) and PEO (2%, 2.5% and 3% (w/v)) were mixed and electrospunned. At 2%(w/v) PEO concentration, homogenous nanofibers were not obtained. In addition, increasing chickpea flour concentration resulted in increasing the addition of NaOH amount to the solution which affected conductivity adversely. Therefore, 3% (w/v) chickpea flour and 2.5% (w/v) PEO concentration were utilized to produce electrospun nanofibers

3.2.1 Conductivity of electrospun solution

Conductivity charges the out layer surface of the droplet and provides an essential driving force to initiate the movement of solution from the tip of the nozzle to the collector. By the way, it affects jet behavior (Aydogdu, Yildiz, Ayhan, et al., 2019b).

In the literature, it was reported that electrospinning of proteins extremely difficult due to their compact secondary and tertiary structure. It limits the physical interaction between carrier polymer and protein. To make them spinnable, different denaturation methods including heating, pH adjustment, were applied. Protein unfolding provides an opportunity to allow protein–carrier polymer chain entanglement (Vega-Lugo & Lim, 2012). Alkali treatment, the addition of NaOH, is generally responsible for the conductivity of the solutions. Furthermore, proteins have an electrical charge when they are far away from their isoelectric point. Therefore, charged proteins also had an impact on the conductivity of the solutions.

Conductivity should be high enough to overcome surface tension and to provide stretching ability to the polymer mixture. However, there is a critical value after which increasing further the solution conductivity leads to bending instability during electrospinning as a result of the overwhelming effect of repulsive forces. (Aydogdu Emir et al., 2021). Furthermore, the amount of electrolyte, mobility of ions, and conductivity of solvents might affect the charge density of electrospun solution (Aydogdu, Yildiz, Ayhan, et al., 2019b). As illustrated in Table 3.5, the electrical conductivity of polymer solutions decreased almost two times after adding curcumin. The conductivity of C/CON was measured as 684 ± 4.24 µs/cm whereas that of CUR/CON was 323.5 ± 6.36 µs/cm. Since NaOH treatment was applied to all samples, this deviation was probably due to significantly different conductivity of ethanol (nearly zero) and water (10.28 ± 1.1 µs/cm). Therefore, the addition of curcumin-ethanol mixture to the solution drastically decreased the conductivity of the solution. Further, a declining trend was also observed between the samples processed with different heat treatments (C/MW< C/CON and CUR/CON< CUR/MW). This decreasing trend might be coming from the mobility of ions.

Polymer mixtures with higher viscosity are expected to restrict the mobility of the ions and thereby, in our case, restricted mobility might result in the reduction of solution conductivity.

3.2.2 Rheological behavior of the electrospun solution

The rheological behavior of the polymer solution affects electrospinnability, fiber size and even morphology. Table 3.5 showed that flow behavior indices (n) of all chickpea flour solutions were less than 1.0, indicating a non-Newtonian, shear-thinning behavior. A decrease in n value generally pointed out the polymer entanglement, which was regarded as a pre-condition of obtaining nanofibers with electrospinning (Kriegel et al., 2009b). Although the heating method and amount of curcumin were different between the polymer solutions, n values only varied from 0.84±0.01 to 0.89±0.02, which did not cause any significant changes. On the other hand, heat treatment and curcumin addition significantly changed the consistency index (K) of polymer mixtures which generally gives an idea about the degree of solution thickening which is in correlation with the apparent viscosity. The highest K value corresponded to the highest entanglement and could be attributed to the strongest interaction between components (Aydogdu, Yildiz, Ayhan, et al., 2019b). As can be seen, K of C/CON and C/MW was 0.6 ± 0.00 (Pa s^n) and 0.91 ± 0.02 (Pa s^n), respectively. Similarly, in curcumin incorporated samples microwave treatment increased the consistency index. This difference in K values between different heating methods might originate from the different working principles of microwave and conventional heating. Although conventional heating promoted the surface gelatinization of the starch granules present in the chickpea flour, the microwave could destroy them completely by affecting water molecules in the crystalline region of starch and intensifying the rupturing effect (Xie et al., 2013). The study investigating the physicochemical changes of starch under microwave heating showed that even 10 s microwave treatment caused loss of birefringence of half of the starch molecules. Furthermore, under the consequence of vibrational motions of

72

polar molecules, starch might gradually break down into smaller fragments of low molecular weights. Therefore, rupturing the crystalline region in a short time period and relatively smaller fragments might increase the number of available bonding sides for other molecules, in particular for water and thereby, leading to a higher water holding capacity (Xie et al., 2013). Increased possibility of entanglement and reinforcing interactions with water would be the explanation for the highest K value of C/MW among all electrospun solutions. Similar results were also observed in the study of Uygun et al., (2020). The viscosity of MW treated carob bean flour/starch/PEO polymer mixture was 0.239 ± 0.005 (Pa.s) while that of conventionally operated ones was 0.146 ± 0.001 (Pa.s).

Curcumin-added samples had a lower K as compared to their control groups. Curcumin was dissolved in ethanol completely before the addition of it to the polymer solution. This might have resulted in dilution of curcumin added samples with a reduction in the interaction between polymer chains and in turn, caused a decrease in K values. As can be seen, the K value of C/MW was 0.91 ± 0.02 (Pa s^n); however, that of CUR/MW was only 0.63 ± 0.04. A similar trend was also observed between C/CON and CUR/CON samples. The study outcomes related to gallic acid encapsulated lentil flour/PEO nanofibers were also very consistent with these results. In that study, adding gallic acid to the solution decreased K value from 2.12 ± 0.05 to 1.03 ± 0.03(Pa s^n) (Aydogdu, Yildiz, Aydogdu, et al., 2019b).

Table 3.5 Consistency index (K), flow behavior index (n), conductivity of the electrospun solutions and average fiber size the nanofiber film

	K (Pa s^n)	n	Conductivity	Average fiber size (nm)
C/CON	0.60 ± 0.00^b	0.89 ± 0.02^a	684.00 ± 4.24^a	273.80 ± 65.85^{bc}
CUR/CON	0.46 ± 0.01^c	0.84 ± 0.01^a	323.50 ± 6.36^c	332.10 ± 65.67^a
C/MW	0.91 ± 0.02^a	0.86 ± 0.01^a	636.00 ± 2.82^b	258.71 ± 54.28^c
CUR/MW	0.63 ± 0.04^b	0.89 ± 0.02^a	294.50 ± 3.53^d	285.30 ± 53.39^b

Columns having different letters are significantly different ($p \leq 0.05$).

3.2.3 Nanofiber morphology

SEM images (Figure 3.9) showed that chickpea flour/PEO nanofibers with/without curcumin had a smooth and bead-free morphology, so curcumin was successfully incorporated into the fibers. The average fiber size of the samples were shown in Table 3.5. The fiber size changed due to the conductivity and apparent viscosity of the solutions. The addition of curcumin to the electrospinning solution changed the average fiber size of the nanofibers significantly. The consistency indices of curcumin solutions (CUR/MW, CUR/CON) were lower than their control groups (C/MW, C/CON) which promoted the thinner fiber formation. However, the conductivities of CUR/MW and CUR/CON were lower than their control groups which paved the way for thicker fibers. Under these contradictory circumstances, it seemed that average fiber size was affected predominantly by conductivity. CUR/MW fibers had an average fiber size of 332.1±65.67 nm, while C/MW achieved that of 258.7± 54.28 nm. Similarly, the electrospinning of curcumin added conventionally treated samples (CUR/CON) resulted in much thicker fibers compared to control samples (C/CON) due to significantly low conductivity value. Furthermore, the polyphenols have been classified as natural cross linkers for

proteins due to the possibility of hydrophobic interactions and hydrogen bonding (Alehosseini et al., 2019). As reported, chickpea flour contains a high amount of protein, so in the presence of curcumin, they might be cross-linked and increased the average fiber size.
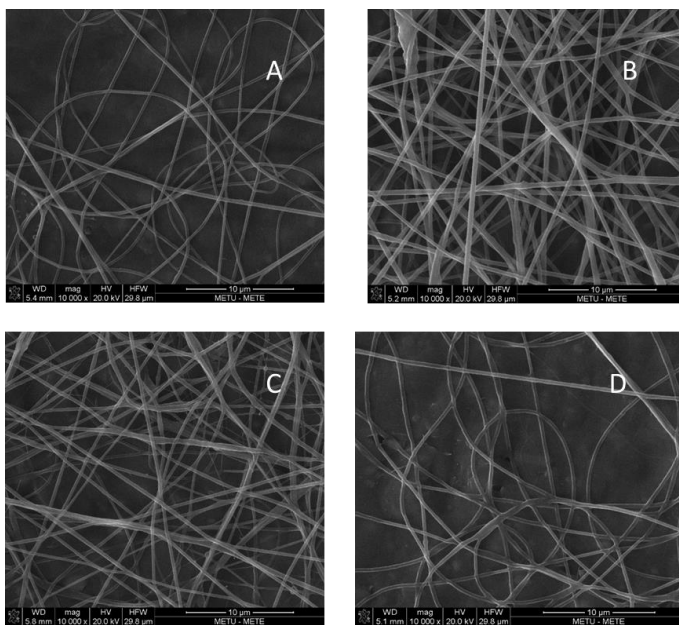
Figure 3.9. SEM images and fiber size distribution (FSD) of nanofibers. (A) C/CON, (B) CUR/CON, (C)C/MW, (D)CUR/MW

3.2.4   Water vapor permeability of the films

WVP is one of the key parameters for food package applications which is correlated with the ability of the material to manage moisture transfer between food and the environment. As expected, packages with the lowest WVP are preferred during the application process, but it is hard to achieve it with the biopolymer films. Although some common strategies were applied to enhance film WVP attributes, i.e. using hydrophobic compound, crosslinking (Aydogdu et al., 2020), film preparation method (casting or electrospinning) has also strongly influenced the properties of the films. In this manner, electrospinning might be one of the possible alternatives to decrease WVP (Aydogdu, Sumnu, et al., 2018).

However, not only the processing methods but also the polymer mixture are effective in final product characteristics. For example, in the study of Hajikhani, Emam-Djomeh, & Askari, (2020), PLA was electrospun on gluten casting film to improve barrier properties. WVP of these samples was approximately between 9.5 and 7.5 $\times 10^{-6}$ g/Pa×s×m. On the other hand, WVP of chickpea flour/PEO electrospun nanofibers ranged between 1.89± 0.05 and 1.28 ±0.37 10^{-10} g/Pa×s×m (Table 3.6). Therefore, lower WVP of chickpea flour/PEO nano fibers suggested that utilization of natural biopolymers without purification might be a better option to obtain better barrier properties. Similarly, instead of the combination of two techniques, a single technique, electrospinning, might provide better film performance with a proper polymer combination.

It has been reported that the permeability of nanofiber film depends on the porosity of the fiber (Aydogdu, Sumnu, et al., 2018) and hydrophobic/hydrophilic ratio of the nanofiber components (Zhou et al., 2020). For the first reason, the films with larger fiber diameters (curcumin incorporated ones) might form larger junction zones while films with smaller fiber diameters (control samples) might have a more torturous path for water vapor diffusion. In both cases, WVP is expected to decrease, however, there was no significant difference among WVP values of the samples (Table 3.6). For the second hypothesis, the polymers used in the electrospinning process are hydrophilic in nature while curcumin is highly hydrophobic. Therefore, there might be an expectation related to decreasing trend on WVP with adding a hydrophobic compound, curcumin. As expected, a decreasing trend in WVP of films was observed upon the addition of the curcumin after both heating treatments. Overall, it did not cause a significant difference among samples. Therefore, it seemed that the amount of curcumin in the electrospun solution might not be sufficient to alter the hydrophilic/hydrophobic ratio in the nanofiber films.

Table 3.6 WVP, Mechanical property (TS, EAB) of nanofiber films

	WVP$\times 10^{-10}$ (g m^{-1} s^{-1} Pa^{-1})	TS (MPa)	EAB (%)
C/CON	1.54±0.27[a]	0.88±0.08[b]	39.53±0.43[a]
CUR/CON	1.28±0.37[a]	0.38±0.00[c]	33.63±4.25[a]
C/MW	1.89±0.05[a]	2.02±0.11[a]	47.02±4.53[a]
CUR/MW	1.47±0.41[a]	0.53±0.07[c]	32.94±1.03[a]

Columns having different letters are significantly different ($p \leq 0.05$).

3.2.5 Mechanical properties

Tensile strength (TS) and elongation at break (E%) of both control and curcumin-loaded nanofibers have been investigated and the results were summarized in Table 3.6. As can be seen, TS of control nanofibers is significantly affected by the type of heat treatment. Tensile strength (TS) term has been associated with binding force between molecular chains (Lan et al., 2019). TS of C/MW nanofibers was 2.02 ± 0.11 (MPa) while that of C/CON nanowebs was 0.88±0.08 (MPa). This result indicates that microwave caused stronger bond formation between polymer chains than conventional heating during polymer preparation. The consistency index of the solutions has already been proved this outcome. As mentioned earlier, C/MW reached the highest K value (Table 3.5) which was interpreted as the highest entanglement and the strongest interaction between molecules. Since fibers with smaller fiber size diameter (C/MW) had larger contact areas and denser structures the tensile strength of the film increased (Yao et al., 2022).

On the other hand, TS of CUR/MW and CUR/CON samples were 0.53±0.07 (MPa) and 0.38 ± 0.00 (MPa), respectively. As can be seen, the addition of curcumin to the formulation drastically declined tensile properties regardless of the heat treatment. Curcumin might interrupt the interaction between polymer chains and might weaken their interactions (Suriyatem et al., 2018). It reduced the toleration toward applied

stress during tension and resulted in lower TS (Subtaweesin et al., 2018). Elongation has been correlated with molecular chain movement (Lan et al., 2019). Unlike TS, neither heat treatment type nor curcumin in the formulation affected stretching ability of fibers underdrawing force, so EAB values were not statistically different for the samples.

In the literature, the tensile strength of the PEO nanofibers varied between 0.2 MPa and (Bianco et al., 2013), 1.2 MPa (Lu et al., 2006). Furthermore, TS of starch based nanofibers was approximately 0.10 MPa (Fonseca et al., 2019). According to conventional standards, TS of food package should be higher than 3.5MPa. The reason for lower mechanical properties is the high probably natures of the polymers (PEO and chickpea flour including mainly starch, protein), nanofiber density, average fiber size, and fiber defects (Mutlu et al., 2018). Although the mechanical properties of chickpea flour/PEO nanofibers were not satisfactory, these nanofibers had relatively better performance than their single electrospinning mat. This outcome suggested that combining these materials caused more stable bond formation between chains than their native forms.

Apart from these, in the literature, generally, it has been observed that nanofibers have relatively lower mechanical properties compared to films made by casting method or extrusion. One of the mean reasons for this consequence might be difference between processing conditions. For example, in electrospinning, the solidification time of polymer equals the time required for solution to the ejection of the tip of the needle to collect on the metal plate which is much less than drying time of casting (Aydogdu, Kirtil, et al., 2018). In addition to that, operation temperature of electrospinning and /or other film methods such as extrusion is significantly different. Electrospinning process is most commonly carried out at room temperature whereas the process temperatures of extrusion are between 90º and 120ºC (Mücke et al., 2021). Therefore, these two main differences might be responsible for the higher mechanical characteristic of casting and extrusion film compared to nanofiber.

3.2.6 Differential scanning calorimetry (DSC) analysis and Thermogravimetric analysis (TGA) of the nanofibers

TGA and DTG curves of chickpea flour, PEO, curcumin, control (C/MW, C/CON) and curcumin-loaded samples (CUR/MW and CUR/CON) were shown in Figure 3.10. The first stage degradation peak of all samples was around 100°C, which was due to moisture evaporation (Yao et al., 2022).

The main thermal degradation of chickpea flour and PEO occurred in another step, and their temperature peaks were located at approximately 300°C and 400°C, respectively (Figure 3.10). Curcumin had a wide range of mass loss diagram from 200 °C to 500 °C.

The nanofibers followed both chickpea flour and PEO degradation patterns and their second and third stage degradation peaks were also observed at similar temperatures.

DTG graph of samples was also an indication of the successful incorporation of curcumin into the polymer matrix. As in the first stage of degradation, the weight loss of CUR/CON samples was approximately 0.29% while that of C/CON was nearly 2.76% at 100°C. Both weight losses were attributed to moisture loss. This result was linked with the replacement of water molecules by curcumin between hydrophilic polymer network formed by PEO and different constituents of chickpea flour. The successful embedding of curcumin into the structure resulted in reduced water content of fibers and the indicator of interaction between curcumin and polymer network (Celebioglu & Uyar, 2020).

Although the presence of curcumin did not affect the degradation pattern other than adding an extra peak, it influenced the degradation rate and thermal stability of samples. As seen in DTG curves, the lower weight loss rate was observed for CUR/MW samples as compared to C/MW and it became distinct at the third degradation peak. A similar conclusion can be drawn from the conventionally treated samples (CUR/CON and C/CON). Furthermore, in DTG curves, regardless form the curcumin and heat treatment type, the third degradation peak temperatures of

nanofibers shifted by approximately 15°C, compared to PEO (~400°C) diagram which was the indicator of higher thermal stability of nanofibers and stronger intermolecular interactions.
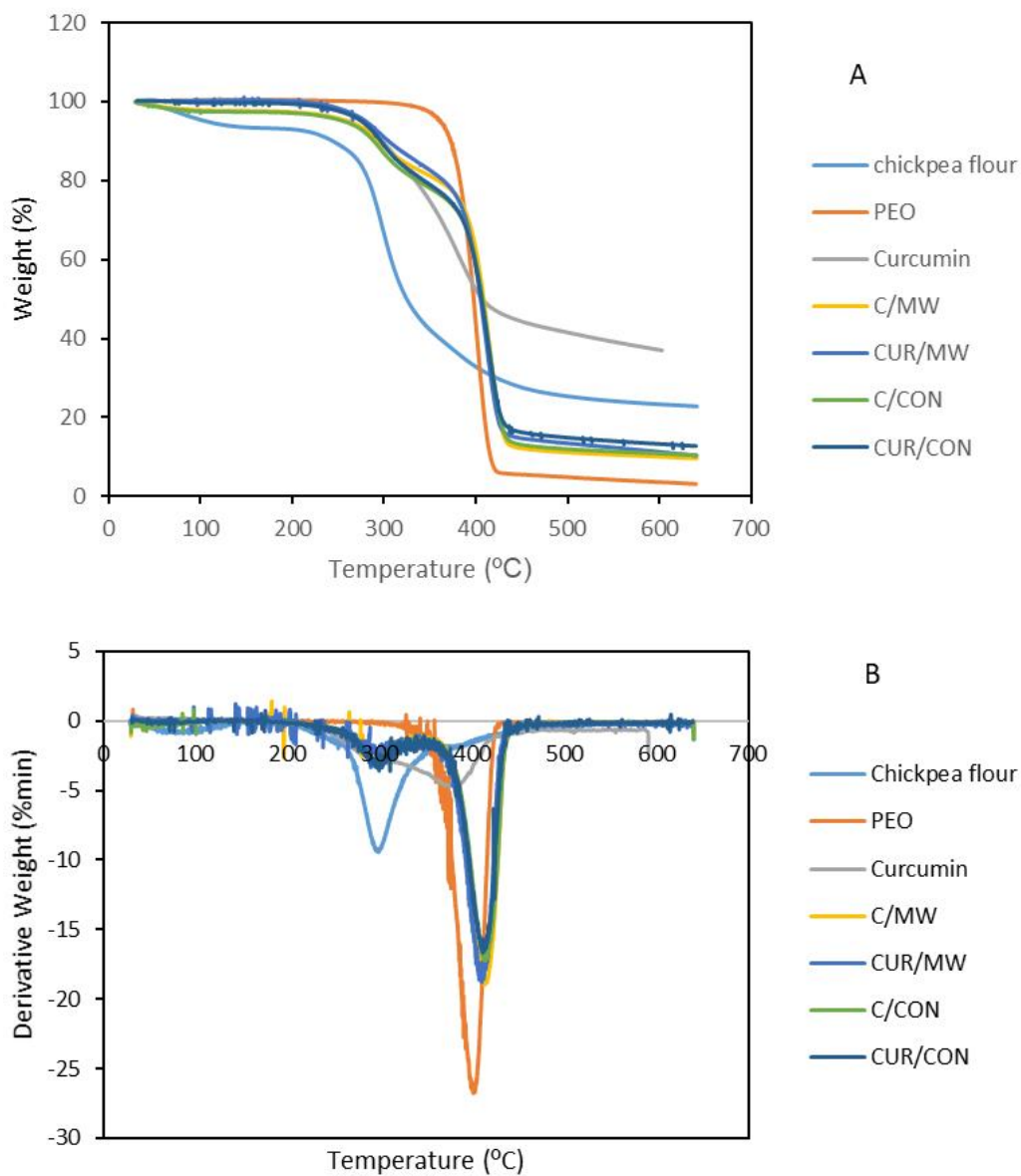
Figure 3.10. (A)Thermo-gravimetric curves and (B) DTG curve of pure components and nanofiber films

To understand the effect of different heat treatments on thermal stability of fibers, the onset degradation temperatures of the samples ($T_{5\%}$) were compared (Sánchez-

Safont et al., 2021). Temperatures at which 5% weight loss occurred for C/MW and C/CON were recorded approximately at 261.7 °C and at 256.83°C, respectively. Although microwave-treated samples required slightly higher temperatures to achieve the same weight loss, their thermal stability seemed comparable. Similarly, the onset degradation temperatures of CUR/MW and CUR/CON were also reported at nearly 280.3 °C and 276.27°C, respectively. Thermal stability of curcumin incorporated samples was also not significantly different from each other. However, as seen, the curcumin incorporated samples had higher thermal stability due to successful incorporation of polymer matrix and strong intermolecular interaction between polymer matrix and curcumin.

DSC results of the fibers, chickpea flour, PEO and curcumin were listed in Table 3.7. Curcumin demonstrated an endothermic peak around 178°C, which was corresponding to the melting of crystal form. The melting peak temperature of PEO was around 70 °C whereas that of nanofibers was between 58 and 61 °C. One reason for the decreasing trend in T_m was correlated to disruption of the crystalline structure of PEO with interaction between other components. Similar results were also reported in the study of PEO-HPMC electrospun nanofiber (Aydogdu, Sumnu, et al., 2018). T_m of CUR/MW and CUR/CON samples was 59.87±0.01°C and 58.95±0.07°C however, that of C/MW and C/CON was measured as 61.51±0.45°C and 61.04±0.30°C. The addition of curcumin into the formulation caused a further reduction in T_m, which was considered an indication of curcumin embedding into the structure. During the electrospinning process, polymer chains are stretched under the effect of electrical force and remain in a non-crystalline state, mostly due to the rapid solidification process. This might be another reason for melting point depression. For the same reasons, the melting enthalpy of CUR/MW and CUR/CON shifted gradually to lower values than that of C/MW and C/CON (Table 3.7). Furthermore, heat treat treatment type did not significantly affect the melting enthalpy and melting temperature of samples.

Table 3.7 Thermal property of nanofibers

	Tm (°C)	ΔHm (J/g)
C/CON	61.04±0.30[a]	53.03±1.87[a]
CUR/CON	58.95±0.07[b]	46.43±1.88[bc]
C/MW	61.51±0.45[a]	51.42±1.12[ab]
CUR/MW	59.87±0.01[ab]	40.76±0.49[c]

Columns having different letters are significantly different ($p \leq 0.05$). T_m (ºC), and ΔH_m (J/g)) of nanofiber films, Tm- melting temperature, ΔH_m (J/g)- melting enthalpy

3.2.7 XRD

PEO is a semi-crystalline polymer and showed sharp diffraction peaks at 19.2° and 23.4° (Figure 3.11). Although the intensity of these characteristic peaks declined, they were still observed in the diffraction patterns of all samples. The reduction in the melting enthalpy of pure PEO (163.27 J/g) compared to nanofibers (between 53.03 ±1.87 and 40.76±0.49 J/g) supported disruption of PEO crystallinity. Stretching and rapid solidification during electrospinning and intermolecular interaction between compounds were mainly responsible for this result. Curcumin is a crystalline solid and its diffraction peaks are positioned at 8.89°, 12.96°, 14.61°, 17.49°, 18.26°, 19.61°, 21.28°, 23.39°, 24.74°, 25.83°, 27.56°, 29.10 ° (Figure 3.11). Almost none of the characteristics peak of curcumin, except 17.49° and 23.39°, was found in curcumin loaded nanofibers (CUR/MW, CUR/C), probably because of the transition of the crystal structure of curcumin to amorphous and encapsulation of curcumin with the polymer matrix. However, the small diffraction peaks indicated the existence of non-entrapped curcumin molecules of the crystalline form (Celebioglu & Uyar, 2020). The contribution of these curcumin crystallinity peaks

(17.49° and 23.39°) to the total crystallinity was higher for CUR/CON (%54.79±0.57%) than for CUR/MW (%44.45 ±0.35) samples, which pointed out that curcumin more successfully encapsulated in microwave treated sample (CUR/MW) (Table 3.8). The results of both DPPH and ABTS activities of CUR/CON and CUR/MW samples also proved this hypothesis, which will be discussed in the upcoming section.
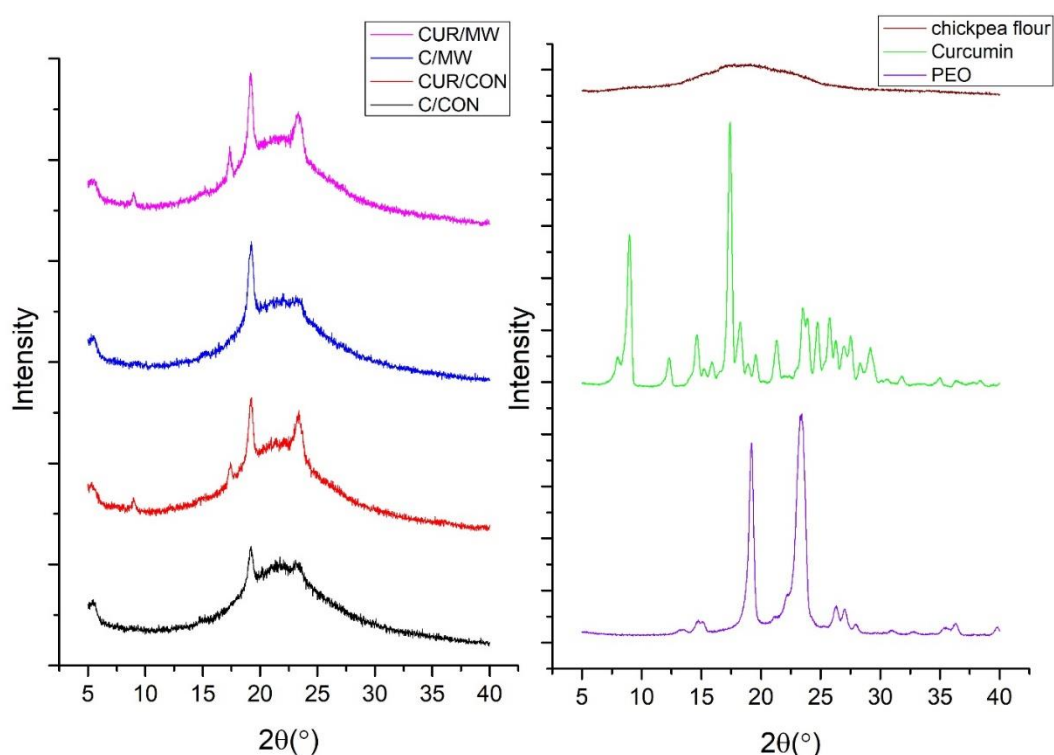
Figure 3.11. X-Ray Diffraction (XRD) Pattern of spins pure components and nanofiber films

3.2.8 Antioxidant activity (DPPH& ABTS)

To analyze the antioxidant activity of the chickpea flour/PEO based nanofibers, ABTS and DPPH radical scavenging activity methods were preferred. Table 3.8 shows the antioxidant activity of nanofibers. ABTS scavenging activity of control fibers lied between 4.86±0.15% (C/MW) and 10.85±0.07% (C/CON) whereas

83

DPPH actives were between 5.93±0.39% (C/MW) and 2.42±0.15% (C/CON). Phenolic acids including protocatechuic acid, vanillic acid, caffeic acid, and ferullic acid were mainly responsible for the antioxidant activity of control nanofiber samples (Sreerama et al., 2010). Although the control nanofibers (C/CON and C/MW) exhibited very low antioxidant activity, after curcumin incorporation, as expected, both ABTS and DDPH activity of the films enhanced significantly. Although the hydrogen atom donation ability of phenolic hydroxyl group (Roy & Rhim, 2020a) was mainly responsible for the antioxidant ability, methylene group of β-diketone moiety also contributes to the antioxidant activity of curcumin. ABTS and DPPH scavenging activities of CUR/CON were reported as 49.78±3.51% and 20.08±0.78%, whereas these of CUR/MW were measured as 87.47±1.98% and 45.50±1.56%, respectively. Different heat treatments caused significant differences in the antioxidant activity of the films. Microwave treatment influenced both the physical and chemical structure of the starch granules. As described previously, the pressure inside the granule caused rapid expansion; however, granule hydration might not be as quick as granule expansion which resulted in stress induced collapse and rupture of granules. The general term for this process is gelatinization. After this process, cooling of starch starts and disordered chains undergo re-association through hydrogen and hydrophobic interactions (Zhao et al., 2019; Siriamornpun et al., 2016). A more disordered structure of starch in microwave heating might increase the interaction between starch and curcumin molecules, called a non-inclusion complex, so, curcumin might be entrapped into the polymer network more (Remanan & Zhu, 2021). This resulted in higher antioxidant activity of the microwave treated (CUR/MW) sample than conventionally treated one (CUR/CON). The findings of XRD and TGA also confirmed the result of more successful incorporation of curcumin into the microwave treated sample (CUR/MW) by a relatively lower crystalline contribution of curcumin and slightly higher thermal onset degradation ($T_{5\%}$), respectively (Table 3.8, Figure 3.11).

Table 3.8 Crystallinity and antioxidant scavenging activity (DPPH, ABTS) results of nanofibers

	DPPH (scavenging activity %)	ABTS (scavenging activity %)	RDC (%)	CUR-RDC
C/CON	2.42 ± 0.15^c	10.85 ± 0.07^c	9.92 ± 0.52^c	-
CUR/CON	20.08 ± 0.78^b	49.78 ± 3.51^b	16.69 ± 0.47^a	54.79 ± 0.57^a
C/MW	5.93 ± 0.39^c	4.86 ± 0.15^c	7.61 ± 0.21^d	-
CUR/MW	45.50 ± 1.56^a	87.47 ± 1.98^a	14.95 ± 0.30^b	44.45 ± 0.35^b

RDC: relative degree of crystallinity, CUR-RDC: Curcumin crystallinity contribution to RDC

3.2.9 Antimicrobial activity of nano fibers

CUR/MW film was selected for measurement of antimicrobial activity of film due to its higher antioxidant activity than other films. C/MW film was also applied as control of CUR/MW. Antibacterial activity of CUR/MW and C/MW film was measured by disc diffusion methods by measuring the clear zone diameter. To test that activity of the film, *S. aureus* (Gram positive) and *E.coli* (Gram negative), the most common foodborne pathogens, were selected. As shown in Figure 13 (A2- B2) and C/MW did not show any inhibitory zone for neither *E.coli* nor *S.aureus* which proved that control films had no effects on growth inhibition. However, curcumin incorporation into the formulation influenced the antimicrobial activity of the film against *E.coli* significantly. As seen Figure 13 (A1), released curcumin from the nanofiber diffused into the agar, suppressed activity of *E.coli* and inhibition zone diameter were recorded as 1.62 ± 0.36 cm^2. As supported by the previous analysis, crystal structure of the curcumin changed from crystal to amorphous form. Amorphous solids had higher solubility and dissolution rates than crystalline

counterparts which was observed in Figure 13 (A1). A similar result was also reported in the study of curcumin encapsulation in gelatin (Gómez-Estaca et al., 2017). Apart from *E.coli* result, no inhibition zone was observed for *S. aureus* sample (Figure 13 (B1)). The first reason for the different zone sizes might be due to the differences in the diffusion rates (Suppakul et al., 2003) of curcumin into selective media (Baird Parker Agar, Chromogenic *E.Coli*). The second reason might be the difference between the cell wall structures of *E.coli* (outer phospholipidic membrane) and *S. aureus* (outer peptidoglycan layer) and their possible interactions with curcumin (Bhawana et al., 2011). Although some studies showed that curcumin has better antimicrobial activity against *S. Aurues* as compared to *E.coli* (H. Wang et al., 2017), some other researchers showed the opposite case (L. Wang et al., 2019b). The different strains in each experiment and their resistance to curcumin might be responsible for these contradicting results in the literature.
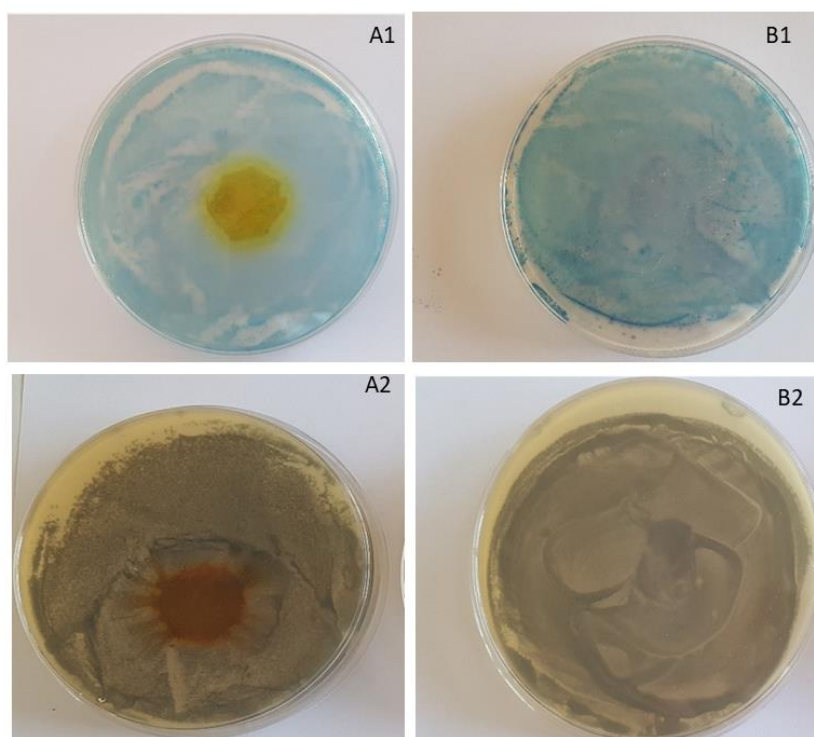
Figure 3.12. Images of bacterial culture plates incubated with (A1) CUR/MW, (B1) C/MW against *E.coli*, and (A2) CUR/MW, (B2)C/MW against *S.aureus*.

86

3.3 Fabrication of curcumin faba bean flour/chitosan (FC) crosslinked casting films

Although glutaraldehyde (GLU) has been frequently preferred to improve some characteristics of bio-degradable food packages, it is regarded as a hazardous chemical. Therefore, in this study, the possibility of replacing GLU with citric acid (CA) a non-toxic compound was questioned in a film formation. Different ratios of GLU and CA on faba bean flour, chitosan and curcumin film were examined.

3.3.1 Physical properties of FC films

The main aim of the crosslinking in biopolymer films was to decrease solubility and swelling to improve water resistance and applicability. The solubility of the FC films was significantly lower than the films with similar compositions (Table 3.9). For example, the solubility of lentil flour (Aydogdu, Kirtil, et al., 2018), pea flour (Yildiz, Bayram, et al., 2021) and rice flour (Vargas et al., 2017) based films were between 25% and 42%. The main reason for this result might be the bond formation between the hydroxyl group of starch, amino groups of chitosan. This might decrease the water affinity, which resulted in even a further decrease in water solubility of the FC films without any cross linker (Bajer et al., 2020). While the amide group of chitosan might function as a proton acceptor, the hydroxyl group of starch might behave as a weak proton donor. Therefore, the formation of hydrogen bonding became more favorable (Sudhakar et al., 2012). Furthermore, the presence of curcumin might have a decreasing effect on water solubility due to its hydrophobic nature (Roy & Rhim, 2020d).

The addition of both crosslinking agents caused a decreasing trend in water solubility (Table 3.9). The hydrophobic ester bond formation between CA and polysaccharides lowered the number of available hydrophilic hydroxyl groups and, in turn, decreased the solubility of the films (Wu et al., 2019b). Similarly, the less available amino group of chitosan caused less soluble films. However, only CF-1.5C films had

significantly lower solubility than the control films. The main reason for that might be the higher crosslinking density of the CF-1.5C films.

Although chitosan is a polysaccharide, unlike many other biopolymers, it is insoluble in water. It dissolves in weakly acidic solutions and forms hydrogels. Since the hydrogels can absorb a high amount of water, this feature makes application chitosan-based films practically useless (Murray & Dutcher, 2006). Therefore, to prevent such an outcome, crosslinking of chitosan films becomes more critical. The main idea behind the crosslinking is to reduce the free volume by increasing the number of junctions and thereby restrict the possible hydrogen bond formation between chitosan and water molecules (Wu et al., 2019b).

The swelling degree of all the films decreased drastically with increasing the ratio of the crosslinking agents (Table 3.9). GLU has three hydroxyl groups, while CA has 3 carboxyls and 1 hydroxyl group in the structure. This means that CA has a higher chance to make covalent bonds as compared to glutaraldehyde. Therefore, the lowest amount of CA reduced swelling degree more than the highest amount of glutaraldehyde (Yoon, Chough, & Park, 2006).

Moisture content was expected to decrease in the crosslinked films; however, it had an increasing trend with the addition of the crosslinkers. Although GLU and CA reduced the starch and chitosan hydrophilic sides, both crosslinking agents might have unreacted hydroxyl or carbonyl groups. Since all the crosslinked molecules were bulky, steric hindrance might be the restrictive factor and the reason for unreacted groups. Therefore, water molecules might have attached to these available groups through hydrogen bonding and increased the moisture content of the crosslinked resulting films.

Table 3.9 WS, SD, MC and WVP of faba bean–chitosan curcumin cross-linked films

	WS (%)	SD (%)	MC(%)	WVP (10^{-11}) (g m^{-1} s^{-1} Pa^{-1})
FC-C	22.98±0.39[a]	136.58±3.83[a]	9.52±0.56[d]	42.55±9.01[a]
FC-0.5C	21.16±1.04[ab]	69.74±4.84[c]	10.37±0.38[cd]	0.34±0.02[c]
FC-1C	21.93±0.23[ab]	46.77±2.10[d]	12.25±0.24[bc]	0.47±0.02[b]
FC-1.5C	17.35±1.20[b]	33.63±4.37[d]	12.20±0.68[bc]	0.29±0.00[c]
FC-30GLU	22.40±1.14[ab]	126.11±3.56[ab]	15.52±0.40[a]	27.44±0.72[a]
FC-60GLU	20.51±2.20[ab]	128.47±1.36[ab]	12.21±1.02[bc]	0.32±0.02[c]
FC-120GLU	18.42±2.022[ab]	117.05±3.44[b]	12.99±0.92[b]	0.30±0.00[c]

Columns having different letters are significantly different (p ≤ 0.05).

3.3.2 Water Vapor Permeability (WVP)

WVP of the films were shown in Table 3.9. WVP of FC films was dependent on many factors such as crystalline-amorphous ratio, hydrophilic-hydrophobic ratio, the integrity of the film, polymer chain mobility (Balasubramanian et al., 2018), solubility in water and moisture content. Therefore, the permeability was shaped under multiple effects, not based on a single parameter. For example, moisture affected the intermolecular forces between polymer chains by increasing free volume and enhancing chain mobility (Yeamsuksawat & Liang, 2019). Thus, films with higher moisture content were expected to have higher permeability. Since molecule alignments were more compact and regular in the crystalline region compared to the

amorphous part, transferring rate of water molecules from one side to the other became relatively slow (Uygun et al., 2020).

As seen in Table 3.9, the addition of crosslinking agents to the films decreased WVP. However, WVP of FC-30GLU was not significantly different than that of FC-C. At that point, it should be noted that FC-30GLU achieved the highest moisture content, and this might be effective on their WVP. It might be concluded that during WVP measurement, exposing films to 100% RH might lead to the modification of film matrix and thereby increased the permeability. Although the solubility values of FC-1C were not different than control films (Table 3.9), it had relatively low swelling degrees. Under these effects, WVP of FC-1C received the highest permeability after FC-C and FC-30GLU. Finally, as expected crosslinking agents formed a more compact network by the increasing compatibility. This resulted in not only a reduction in the polarity of all components, but also a decrease in permeability.

3.3.3   Mechanical properties

Enhancement in TS was generally expected with introduction of cross-linking agents due to increasing and tightening molecular interactions. As shown in Table 3.10, although GLU addition resulted in increasing TS of the film, incorporation of CA decreased TS. Increasing TS might be interpreted as more resistance to mechanical stress. On the other hand, increasing EAB was the indicator of higher stretchability and more deformable films. High TS and low EAB were the indicators of brittle materials as in the example of GLU incorporated films. This showed that the motion of FC film matrices was more restricted after the incorporation of GLU. Similar findings were also reported in the study of gelatin films cross-linked with GLU (Martucci et al., 2012).

On the other hand, FC-1C and FC-1.5C films showed a yield-like deformation similar to the thermoplastic films with lower TS and high EAB. Although in this study, CA was preferred as a crosslinking agent, some studies also reported

plasticizer character of unreacted CA at high ratios by reducing the interaction between components (Wu et al., 2019b).

The present research showed that both effects might coexist, although these impacts seemed to be inconsistent with each other. TS of FC-1C and FC-1.5C films tended to decrease more than 30% compared to FC-C. EAB of FC-1C (4.23 ± 0.66 %) and FC-1.5C (12.93 ± 1.06 %) films were also significantly different than the FC-C (1.67 ± 0.30 %). Therefore, it might be concluded that CA played a role as a plasticizer for the mechanical properties of the films. On the other hand, especially for the FC-1.5C films, WS, SD, and WVP significantly decreased, reflecting the behavior of the crosslinking agent. Similar outcomes were also reported in the study of Azeredo et al., (2015) and Sebti, Delves-Broughton, & Coma, (2003).

These controversial outcomes were also explained by the higher heterogeneity of the spacing between cross-links (Sebti et al., 2003). This heterogeneity might distribute the stress on the chains, which were not stabilized by H-bonding. After non H-bonding chains had been broken, they transferred the stress to the other chains by forcing them to either break or slip to release the stress.

Although high TS was desirable for the packaging films, stretchability was another important characteristics for the film application. Therefore, GLU incorporated films with high TS, but low elongation and rigid structure restrict their application as a packaging material. On the other hand, lower TS and higher EAB of CA cross-linked films were more feasible in practice

91

Table 3.10 Mechanical and thermal properties of faba bean chitosan crosslinked films

	TS (MPa)	EAB (%)
FC-C	12.67± 0.08[c]	1.67±0.30[c]
FC-0.5C	9.04±1.01[d]	1.25±0.57[c]
FC-1C	8.62±0.21[d]	4.23±0.66[b]
FC-1.5C	7.15±0.30[d]	12.93±1.06[a]
FC-30GLU	14.61±0.31[c]	2.61±0.48[bc]
FC-60GLU	21.96±0.73[a]	2.43±0.17[bc]
FC-120GLU	19.28±0.06[b]	1.71±0.11[c]

Columns having different letters are significantly different ($p \leq 0.05$).

3.3.4 Thermal analysis (TGA &DSC) of FC films

The weight loss versus temperature curve of films, chitosan, faba bean flour and curcumin was shown in Figure 3.13. In general, the thermal decomposition of FC films followed multistep decomposition. The first step centered at 100°C was due to the evaporation of water and other volatile compounds. The second stage of degradation appeared around 200°C because of evaporation of glycerol (Bagheri et al., 2019). Furthermore, for CA cross-linked films, evaporation of CA derivatives also overlapped at these values (190- 200 °C) (Qiao et al., 2021) This was followed by a decomposition process which was the highest weight loss observed for all samples. This step corresponded to the depolymerization and decomposition of acetylated and deacetylated units of the polymer (Wu et al., 2019b), in other words, cleavage of covalent bonds formed during crosslinking between starch, protein and chitosan (Sharma et al., 2018). Although the peak temperature of this stage generally was positioned around 300°C, this stage shifted gradually to higher temperatures (nearly 315°C) with the increasing CA ratio in films which was the indicator of the strong intermolecular interactions between components. However, the degradation

92

temperature of GLU incorporated films had a similar decomposition peak temperature to FC-C, which was located approximately at 290°C.
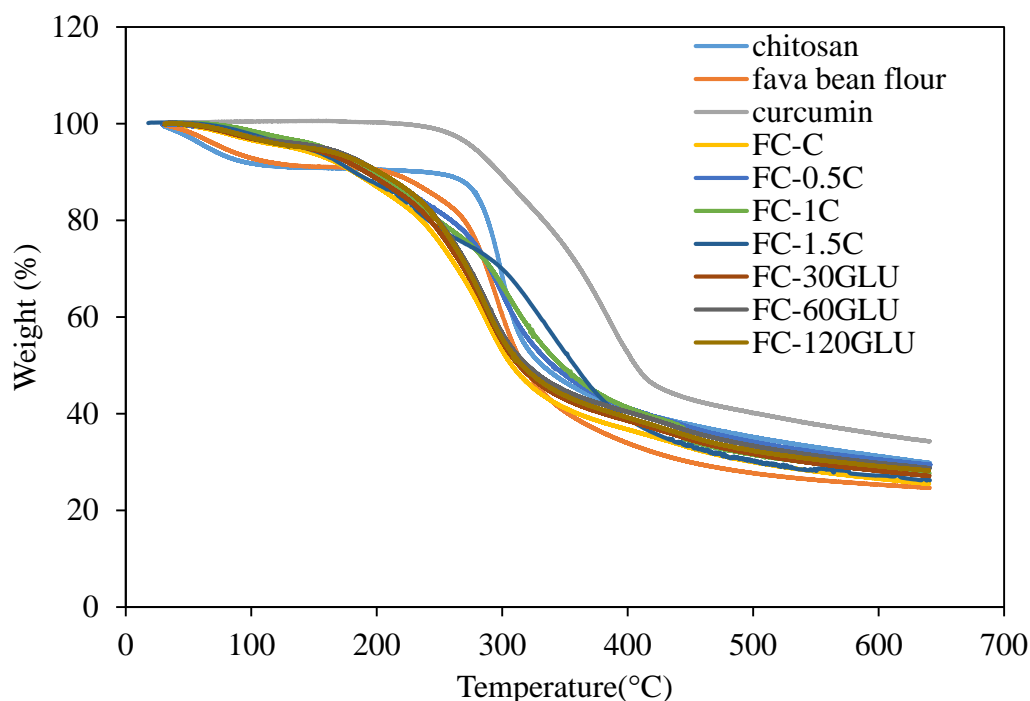
Figure 3.13. TGA curves of FC films

DSC results of all films were shown in Table 3.11. All films exhibited an endothermic peak between 170°C and 180°C. XRD analysis showed that crosslinking agents had a decreasing impact on the crystallinity of the films (Table 12). Therefore, it was expected a reduction in T_m and melting enthalpy (ΔHm) (Jose & Al-Harthi, 2017). On the other hand, it was reported that introducing cross linker slightly increased melting temperature by stabilizing bonds between all components (L. Sharma et al., 2018). In addition to that, crosslinking agents increased the molecular weight of the polymeric matrix through intermolecular interactions (L. Sharma et al., 2018). Therefore, under two counteracting effects, reduction of crystallinity and stabilizing bond strength, T_m did not change significantly. Although the melting enthalpy of GLU cross-linked films was nearly the same as FC-C, CA introduced films exhibited a noticeable increase in the melting enthalpy with an increasing CA ratio. In addition to bond stabilizing effect, melting of CA in the films

might also have an effect on increasing enthalpy because the melting temperature of CA (~190°C) overlapped the Tm of the films (Shafie et al., 2019).

Table 3.11 Thermal properties of faba bean chitosan crosslinked films

	Melting Onset (°C)	Melting Peak (°C)	Melting End (°C)	Melting Elthalpy (J/g)
FC-C	169.46±0.77[a]	173.67±1.58[a]	187.43±1.23[bc]	104.43±2.05[c]
FC-0.5C	173.56±1.0[a]	177.81±1.40[a]	191.64±0.69[b]	112.71±1.28[b]
FC-1C	171.22±1.6[a]	176.23±1.79[a]	193.54±1.03[b]	167.10±1.52[a]
FC-1.5C	173.05±1.46[a]	178.92±1.54[a]	200.10±2.65[a]	201.87±1.69[a]
FC-30GLU	169.1±0.42[a]	172.83±1.2[a]	185.17±1.20[c]	102.81±1.34[c]
FC-60GLU	173.22±1.66[a]	178.05±2.83[a]	193.24±1.72[b]	92.87±2.19[d]
FC-120GLU	174.95±2.87[a]	179.23±1.14[a]	192.26±1.76[b]	102.54±1.97[c]

Columns having different letters are significantly different (p ≤ 0.05).

3.3.5   XRD

The relative degree of crystallinity (RDC) was measured by the ratio between area of crystallinity and total area under the XRD diffraction pattern (Liu et al., 2019). RDC and XRD pattern of all films were shown in Table 3.12, and Figure 15. There might be two main reasons behind the crystallinity of the FC films. The first one was the retrogradation of starch (Seligra et al., 2016) and the second one was the presence of NH_2 (amine) group in chitosan which promotes the formation of hydrogen bonds between polymer chains (Pavoni et al., 2021). Introducing crosslinking agent showed a decreasing tendency on the crystallinity of the films because the carboxyl group of CA and GLU reacted with the hydroxyl and amine groups. Therefore, this interaction restricted the formation of crystal structure in starch and chitosan molecules. As seen, CA added samples had a significantly lower degree of crystallinity compared to FC-

C. As mentioned before, CA has more sides to make crosslinking than GLU. Therefore, CA might limit the chain segment movements and thereby interfere with crystallization (Ren et al., 2017).

The characteristic peaks of chitosan were observed around 10º, and 20 º (2θ). The first peak was the indicator of hydrated crystalline structure because of water molecules attached to the crystal lattice. The peak around 20º (2θ) was attributed to the amorphous part of chitosan (Giannakas et al., 2014). The diffraction peaks around 15.42º, 17º and 20º (2θ) corresponded to the B-type starch diffraction pattern in faba bean flour (H. Liu et al., 2013). As seen diffraction pattern of FC films, the intensity of peaks decreased and even some disappeared (15.42º), which was supported by the degree of crystallinity. This result showed that interaction between components (starch- chitosan and crosslinking agents) restrained the intramolecular interactions. However, the peak at 17.54º was observed in FC films for all formulations. This peak indicates the formation of a double helical B- type crystalline structure and is most sensitive to hydration (Zhong et al., 2011). These results were consistent with the previous research findings related to the amylose and amylopectin films (Myllärinen et al., 2002). It should be noted that although cross-linking decreased the solubility or water sensitivity of the films, the main components of these films were very hydrophilic (chitosan and faba bean). Therefore, a little amount of water interaction or water present in these films (MC) might have an ongoing impact on their structures.
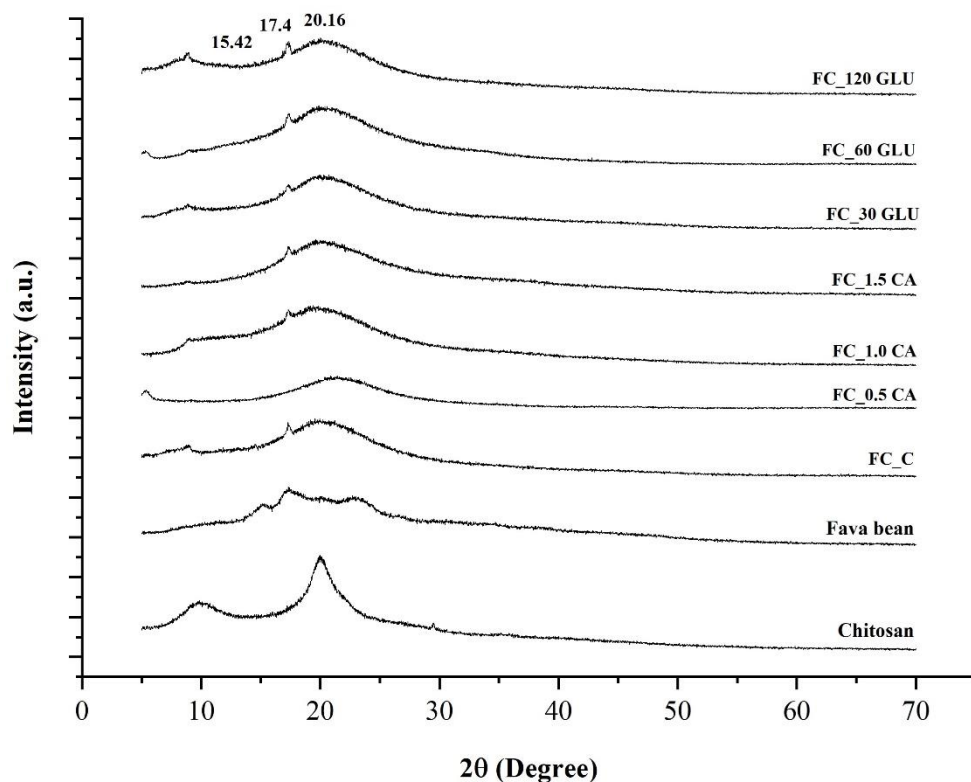
Figure 3.14. X-ray diffraction patterns of the FC films

3.3.6 Antioxidant Activity (DPPH& ABTS)

FC-C films showed the highest DPPH and ABTS activity because of curcumin and the active antioxidant biopolymer, chitosan. The hydroxyl and amino groups of chitosan interacted with free radicals and exhibited radical scavenging activity (Roy et al., 2021). In addition to this, antioxidant activity of curcumin originated from phenolic hydroxyl group and methylene group of β-diketone moiety (Priyadarsini et al., 2003)

As can be seen in Table 12, the addition of cross-linking agent decreased the antioxidant activity of the films by nearly 50%. Firstly, the cross-linking reaction might be responsible for this result. Carboxyl group of CA and GLU might have reacted with the hydroxyl and amino group of chitosan and active sides of curcumin during cross-linking reaction causing a decrease in the number of active sides

96

required for the antioxidant activity. In addition to that, releasing of the active agent, curcumin was inversely correlated with the cross-linking degree. Since the release rate was expected to be lower in the cross-linked polymer matrix, cross-linked films achieved relatively lower antioxidant activity (Valizadeh et al., 2019).

In parallel with this finding, releasing of active components was also linked to the swelling degree of polymer matrix (López de Dicastillo et al., 2016). As shown in Table 12, the highest swelling degree was observed for FC-C, as well as the highest DPPH and ABTS activity.

Although CA incorporated films achieved a relatively lower swelling degree, they showed higher antioxidant activity than GLU. This result was probably due to the antioxidant activity contribution of CA (Priyadarshi et al., 2018).

Table 3.12 DPPH and ABTS activity (%) and RDC of faba bean-chitosan crosslinked films

	RDC	DPPH activity (% scavenging activity)	ABTS activity (% scavenging activity)
FC-C	11.83 ± 1.49^a	20.74 ± 1.27^a	86.54 ± 1.15^a
FC-0.5C	5.15 ± 0.28^b	9.40 ± 1.82^c	33.01 ± 0.38^c
FC-1C	5.85 ± 0.74^b	15.20 ± 0.91^b	60.80 ± 3.55^b
FC-1.5C	4.96 ± 0.51^b	11.73 ± 0.01^{bc}	34.57 ± 0.28^c
FC-30GLU	13.31 ± 0.41^a	10.89 ± 0.16^c	27.66 ± 2.87^c
FC-60GLU	6.38 ± 0.62^b	8.56 ± 0.25^c	25.86 ± 1.01^c
FC-120GLU	10.38 ± 0.98^a	10.29 ± 1.18^c	28.20 ± 3.64^c

Columns having different letters are significantly different ($p \leq 0.05$).

3.3.7 Antimicrobial activity of FC films

Antimicrobial effects of FC-1.5C films on *E.coli* and *S.aureus* were shown in Figure 15. The inhibition zone of FC-1.5C films for *E.coli* and *S.aureus* was very similar and measured as 1.40 ± 0.27 cm^2 and 1.39 ± 0.22 cm^2, respectively. The antimicrobial effect of films was due to the presence of CA, curcumin and chitosan. CA, an organic carboxylic acid, has a local pH reduction effect which might disturb the cell pH and change the permeability of cell membrane by altering its substrate transport (Su et al., 2014). Furthermore, it has an also ability to bind the metal ions necessary for microbial growth. The effect of CA on growth of G (+) and G (-) might be different. This difference was attributed to the outer lipopolysaccharides membrane of G (-) which have a highly chelating charge surface compared to G (+) having peptidoglycan layer. Therefore, CA might be more effective on G (-) than G(+) bacteria (Ounkaew et al., 2018). In addition, the possible antimicrobial effect of chitosan is explained by two mechanisms. Firstly, chitosan might surround the cell and form a polymeric membrane which significantly hinders the entrance of nutrients to cell. Secondly, chitosan might enter or diffuse through the cell, adsorb the negatively charged substances, form an aggregate and finally terminate intracellular activity. The dominant antibacterial activity was reported as the first one for G (+) (*S.aureus*) whereas the second one was mostly valid for G(-) (*E.coli*). All these activities were displayed by SEM images (Zheng & Zhu, 2003). Although curcumin loaded chickpea flour/PEO nanofibers showed antimicrobial effects on only *E.coli,* the presence of other agents namely chitosan and citric acid increased antimicrobial effects and inhibited the growth of both microorganisms.
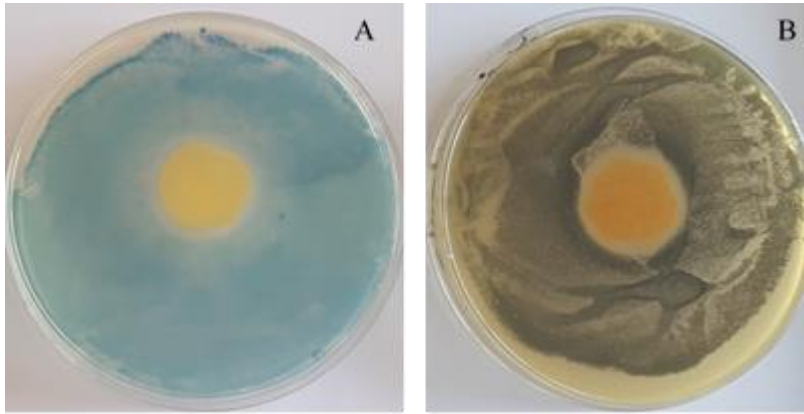
Figure 3.15. Antimicrobial activity of FC-1.5C against *E.coli* (A) and *S. auresus* (B)

3.4 Fabrication of citric acid cross-linked curcumin/chickpea flour/chitosan (CF/CS)

Up on previous research, citric acid crosslinked films had better performances than gluteraldehyde added ones. Therefore, in this study, the effect of citric acid (CA) on chickpea flour(CF), chitosan(CS) and curcumin(CUR) film were examined.

3.4.1 Physical properties of CF/CS films

The main aim of the chemical crosslinking with CA was to improve the physical properties of the biopolymer composite films. The thickness, MC, WS, SD and opacity of the CUR/CF/CS films were shown in Table 3.13.

MC values decreased significantly with the addition of CA to the films. The reason for the reduction could be a decrease in free hydrophilic groups in the film due to crosslinking. However, 0.5-CUR/CF/CS possessed the lowest moisture content ($9.74\pm0.12\%$) compared to 1-CUR/CF/CS ($12.25\pm0.15\%$) and 1.5/CUR/CF/CS ($11.66\pm0.07\%$) which was associated with hydrophilic carboxyl groups of excess CA in the film matrix. Similar findings were also reported in the study of CA cross-linked mung bean starch films (Yao et al., 2022).

Although the expected result was the reduction of WS of the active films, WS of CA cross-linked films was higher than that of the control sample CUR/CF/CS. Other researchers studied with CA cross-linked biopolymers also revealed similar findings and explained this phenomenon by free residual CA behaving like a plasticizing agent (Das et al., 2019) (Wu et al., 2019) However, the solubility of any CUR/CF/CS films was still lower than guar gum/orange oil/sodium trimetaphosphate cross-linked film (32.01 ± 1.53%) (Aydogdu et al., 2020) and carboxymethyl CS/polyvinyl alcohol CA cross-linked film (~40-80%) (Wen et al., 2021). CS is soluble in a weakly acidic solution and forms hydrogels that can absorb high amounts of water by swelling. To impede this behavior, it is necessary to limit possible hydrogen bond formation between CS and water molecules. CA has three carboxyl groups and one hydroxyl group per monomer. These carboxyl groups can react with either amino group of CS by forming amide linkages (Guerrero et al., 2019) or facilitate covalent di-ester linkages with hydroxyl groups of polysaccharides (Wu et al., 2019b). SD of CUR/CF/CS films was compared in Table 3.13. Control film (0- CUR/CF/CS) showed SD of 133.60±11.84% while incorporating CA markedly reduced that of cross-linked films up to 30.72±0.62% (1.5-CUR/CF/CS). SD decreased by increasing CA amount due to an increment in reactive carboxyl and hydroxyl groups and thereby, the crosslinking density of the films.

Table 3.13 MC WS, SD of chickpea flour–chitosan curcumin cross-linked films

	MC(%)	WS (%)	SD (%)
0- CUR/CF/CS	16.68 ± 0.56^a	19.58 ± 0.01^b	133.60 ± 11.84^a
0.5- CUR/CF/CS	9.74 ± 0.12^c	22.24 ± 0.25^a	66.78 ± 1.97^b
1- CUR/CF/CS	12.25 ± 0.15^b	24.01 ± 1.22^a	41.29 ± 7.07^{bc}
1.5- CUR/CF/CS	11.66 ± 0.07^b	22.38 ± 0.14^a	30.72 ± 0.62^c

Different letters in the same column show the significant difference between samples by Tukey's test ($p \leq 0.05$)

3.4.2 Water Vapor Permeability (WVP)

For practical applications, the WVP value of the developed packaging materials should be as low as possible. As seen in Table 3.14, WVP of the control sample (0-CUR/CF/CS) was $9.11\pm0.34 \times10^{-12}$ $gm^{-1}s^{-1}Pa^{-1}$ while WVP values of CA cross-linked films were between $5.70\pm0.13\times10^{-12}$ $gm^{-1}s^{-1}Pa^{-1}$ and $7.23\pm0.003\times10^{-12}$ $gm^{-1}s^{-1}Pa^{-1}$. However, the films with similar compositions had higher permeabilities than the ones stated in the literature. For example, WVP of CA cross-linked cassava starch films was found to be between $1.8\pm0.2\times10^{-10}$ $gm^{-1}s^{-1}Pa^{-1}$ and $2.9\pm0.2\times10^{-10}$ $gm^{-1}s^{-1}Pa^{-1}$ (Seligra et al., 2016), that of CA cross-linked potato starch/CS films ranged from 2.05×10^{-10} $gm^{-1}s^{-1}Pa^{-1}$ to $2.81\times10^{-10}gm^{-1}s^{-1}Pa^{-1}$. The following reasons might explain this result: (i) the hydrophobic nature of CUR: (Roy & Rhim, 2020a) and high-temperature treatment of (80°C, 45 min) CF leading to an increase in hydrophobic interactions (Aydogdu, Kirtil, et al., 2018). Overall, it was concluded that using CUR/CF/CS films was more advantageous in controlling the moisture transfer within the film matrix.

As mentioned before, the incorporation of CA caused a reduction in MC and SD which could be interpreted as a declining interaction between water molecules and film structure. As a result of this consequence, increasing CA concentration in formulation caused a gradual reduction in WVP of the films such that 1.5-CUR/CF/CS was 62.6% more resistant to the permeability of water vapor than 0-CUR/CF/CS. Therefore, CA addition significantly reduced WVP values and confirmed the cross-linked network formation in the film structure. This reduction might be attributed to the hydrophobic ester bond formation between starch in CF and CA, which decreased the number of available hydroxyl groups (Yildiz et al., 2021). Furthermore, crosslinking caused a reduction in polymer chain mobility which might be another factor impeding the diffusion of water vapor molecules (Azeredo et al., 2015).

Table 3.14 WVP and mechanical properties of the films

	WVP (10^{-12}) ($gm^{-1}s^{-1}Pa^{-1}$)	TS (MPa)	EAB (%)
0- CUR/CF/CS	9.11 ± 0.34^a	7.83 ± 0.08^a	1.64 ± 0.13^b
0.5- CUR/CF/CS	7.23 ± 0.003^b	7.16 ± 0.74^a	2.35 ± 0.37^b
1- CUR/CF/CS	7.04 ± 0.50^b	4.37 ± 0.63^b	8.88 ± 1.06^a
1.5- CUR/CF/CS	5.70 ± 0.13^c	3.58 ± 0.20^b	11.1 ± 1.21^a

Different letters in the same column show the significant difference between samples by Tukey's test ($p \leq 0.05$).

3.4.3 Mechanical properties (TS, EAB)

Food packaging material should have good mechanical properties to provide mechanical protection and structural integrity to foods during shipping, handling, and storage. Poor mechanical properties restrict the commercial application of biopolymer-based films, so the characterization of the mechanical properties of films is crucial. The most common parameters used to describe the mechanical properties of films are TS and EAB, which were given in Table 3.14. TS is the maximum stress that material can resist during stretching before breakage. EAB is the percent elongation of the film relative to its initial length (Aydogdu et al., 2020). While CA addition decreased TS of films, it significantly increased EAB of films. In general, an improvement in TS of films with crosslinking was expected due to higher inter-molecular interactions between molecules. However, in this study, CA addition at a concentration of more than 0.5% (w/v) reduced TS and increased EAB. It is known that the crosslinking agents and the plasticizers show opposite effects on the tensile properties.

Unlike crosslinking agents, plasticizers lower TS and increase EAB values. CA having one hydroxyl and three carboxyl groups in its chemical structure offer different functionalities by acting both as cross-linkers and plasticizers (Guerrero et al , 2019). Especially at high concentrations of CA, it decreases the interactions between the macromolecules and enhances the film flexibility (Wu et al., 2019). In

this study, although the crosslinking effect of CA addition was shown in other characterization experiments, the plasticizing effect of CA became clear when CA was added to the film solution at a concentration of more than 0.5% (w/v). In a similar study, CA addition of up to 10% increased the tensile strength of starch-based films, but CA concentration of more than 15% decreased TS due to the governing plasticizing effect (Ghanbarzadeh et al., 2011). In the study of Reddy and Yang, (2010), after CA concentration of 6%, lower TS was observed due to excess crosslinking that limited the mobility of the starch molecules.

Although it was aimed to produce films with mechanical properties close to commercial food packages with the help of crosslinking, the desired results could not be obtained. Increasing CA concentration in film formulation caused a reduction in TS from 7.83±0.08 MPa to 3.58±0.20 MPa as explained before. However, the tensile strength of commercial food packages like low-density polyethylene (LDPE), high-density polyethylene and (HDPE) and polylactic acid (PLA) was reported as 9.92 MPa (Thakore et al., 2001), 27 MPa (Sarkhel et al., 2006) and 32 MPa (J. Ahmed & Varshney, 2011), respectively. EAB values of CUR/CF/CS were between 1.64±0.13 % and 11.1±1.21 % whereas that of LDPE, PLA was 92.5% (Thakore et al., 2001) and 5% (Ahmed & Varshney, 2011). Although EAB of CUR/CF/CS films was comparable to PLA, LDPE showed much better flexibility under stress.

3.4.4 Thermal analysis (TGA &DSC) of CF/CS films

Active films exhibited mixed decomposition characteristics of film-forming components (Figure 3.16) with a different number of degradation stages. The film without CA (0- CUR/CF/CS) showed two stages of degradation (I: between 50-100 °C; II between 250- 450 °C), whereas the addition of CA increased the number of degradation stages. Sample 0.5-CUR/CF/CS (I: between 50-160°C, II: between 227-289°C, III: between 295-420°C) exhibited three degradation steps. However, 1-CUR/CF/CS and 1.5-CUR/CF/CS (I: between 65-150, II between 160-230°C, III between 232-298°C, and IV between 300-532 °C) had four stages of degradation

(Figure 3B). For all films, the first degradation step belonged to the removal of moisture (Istiqomah et al., 2022). Loss of moisture was observed at higher temperatures for CA cross-linked films, indicating more thermally stable hydrogen bonding between water molecules and film-forming components. The gradual increase of onset degradation temperatures ($T_{5\%}$) of the films at which 5% weight loss occurred (Sánchez-Safont et al., 2021) supported this idea. $T_{5\%}$ of 0-CUR/CF/CS, 0.5-CUR/CF/CS, 1-CUR/CF/CS and 1.5-CUR/CF/CS were 101.34°C, 133.5°C, 155.7°C and 151.67°C, respectively.

CA has two decomposition temperatures located around 170°C and 260°C (Sadik et al., 2018), and glycerol decomposes between 160–225 °C (Zhang et al., 2019). Therefore, the second step changes in 0.5-CUR/CF/CS were attributed to the presence of glycerol. However, the second and the third step changes of 1-CUR/CF/CS and 1.5-CUR/CF/CS were ascribed to the presence of CA and glycerol. The distinct CA curves were not observed in 0.5-CUR/CF/CS since nearly all the CA was used up for cross-linking.

The main degradation steps of the films which were the last degradation stages (between 340°C and 380°C) corresponded to both CS and CF decompositions. The degradation and decomposition of CS could be attributed to the depolymerization and degradation of CS D-Glucosamine and N-Acetyl-d-glucosamine units (Tavares et al., 2020). This stage was also associated with the decomposition of backbone protein and carbohydrate components (Díaz, et al., 2019).
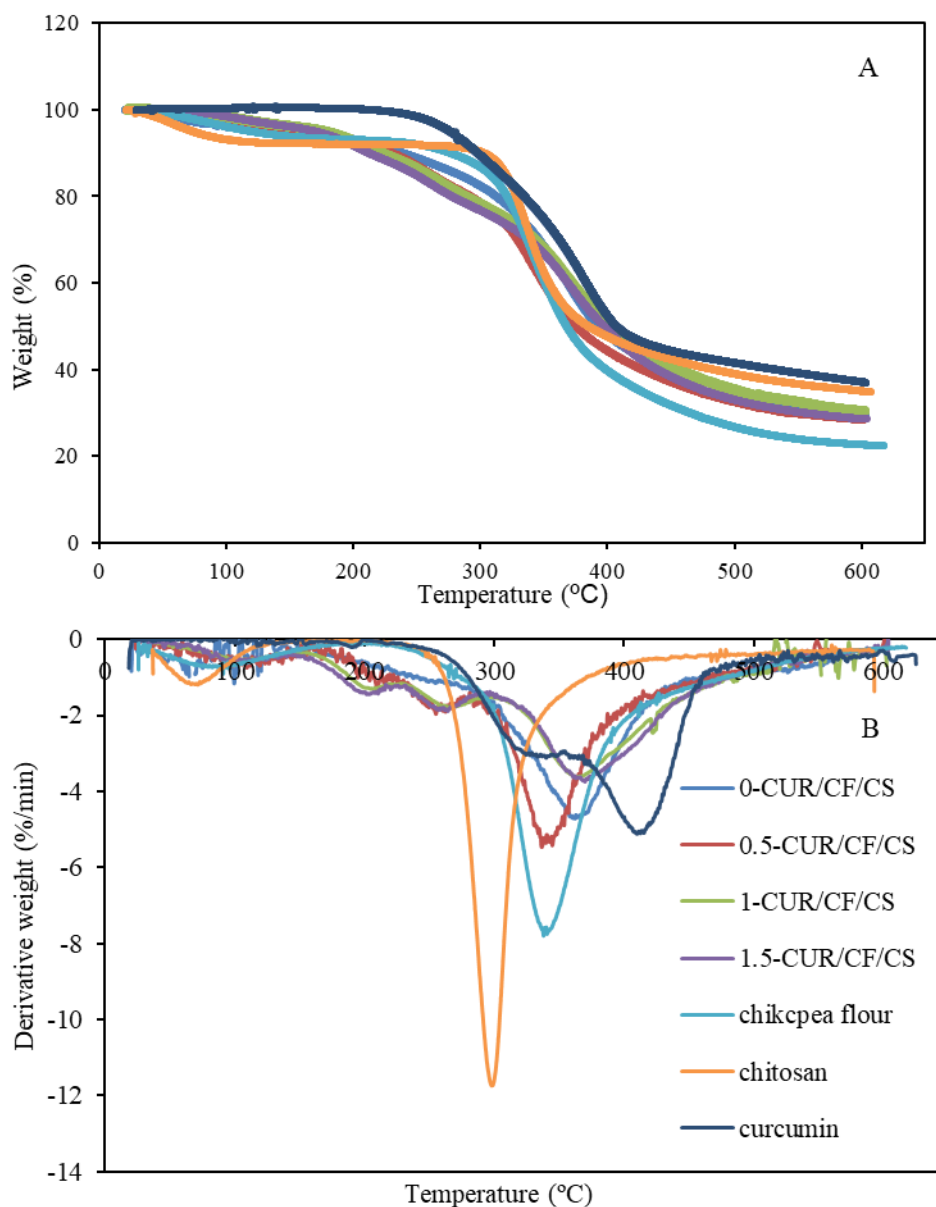
Figure 3.16. TGA and (B) DTG curves of pure components and films.

Table 3.15 shows the melting temperature end enthalpies of the films. In all of the films, melting onset, peak, and end temperatures showed no significant changes. In contrast, the enthalpy of the films showed an increasing trend with the addition of CA. Especially, enthalpy values of 1.0-CUR/CF/CS and 1.5-CUR/CF/CS films had markedly higher than that of 0.5-CUR/CF/CS and 0-CUR/CF/CS. Although higher

melting enthalpy was attributed to a higher degree of crystallinity (Majzoobi et al., 2014), XRD analysis showed the mostly amorphous structure of the films. However, increasing CA resulted in a higher crosslinking degree with more stable bond strength which required higher energy to break (Sholichah et al., 2017).

Table 3.15 DSC results of the films

	melting onset temperature (°C)	melting peak temperature (°C)	melting end temperature (°C)	melting enthalpy ΔH (J/g)
0-CUR/CF/CS	166.91 ± 2.03^a	170.25 ± 1.78^a	181.06 ± 0.41^a	81.17 ± 5.77^b
0.5-CUR/CF/CS	165.69 ± 1.93^a	176.30 ± 1.90^a	176.30 ± 1.71^a	99.98 ± 6.97^b
1-CUR/CF/CS	166.92 ± 4.32^a	179.58 ± 3.98^a	179.58 ± 2.23^a	144.32 ± 6.06^a
1.5-CUR/CF/CS	165.27 ± 6.97^a	178.44 ± 6.48^a	178.44 ± 4.08^a	149.17 ± 1.54^a

Different letters in the same column show the significant difference between samples by Tukey's test ($p \leq 0.05$).

3.4.5   XRD

The diffraction pattern of CF showed a more amorphous character rather than crystalline (Figure 3.18). This is different from other flours studied in literature such as faba bean flour (Yildiz et al., 2021)**,** plantain flour (Gutiérrez et al., 2016), cassava starch (Medina Jaramillo, et al., 2016). The crystallinity of the starch-based films was related more to amylose content (almost linear structure) than amylopectin content (almost branched structure) (Gutiérrez et al., 2016). Therefore, the amylopectin content of CF might be higher than the amylose content, which could hinder the intensity of possible crystalline peaks.

The CS has characteristic crystalline peaks around 10° and 20° due to the presence of NH_2 (amine) and –OH (hydroxyl) groups (Javaid et al., 2018).

The disappearance of the first peak and the transformation of the second peak to the broad halo form in active films corresponded to the change in CS structure from crystalline to amorphous form (Marín-Silva et al., 2019). Further, the films did not exhibit any characteristic peaks of any components, which was a strong evidence of good interaction and compatibility between components (Figure 3.17). Another reason for the lack of sharp diffraction peaks in films might be the slower water evaporation from the film matrix, which prevents re-crystallization (Soo & Sarbon, 2018). As a crosslinking agent, CA prevents the possible inter and intra-hydrogen bonds, thereby repackaging CS and starch (Ávila-Martín et al., 2020).

Further, CUR has a highly crystal structure, and many sharp diffraction peaks are observed in XRD spectra. However, any of CUR/CF/CS exhibited these characteristic patterns. Dissolving CUR in ethanol and incorporation into the film-forming solution promoted the hydrogen bonding between them, thereby causing the modification of the state of CUR from crystalline to amorphous.
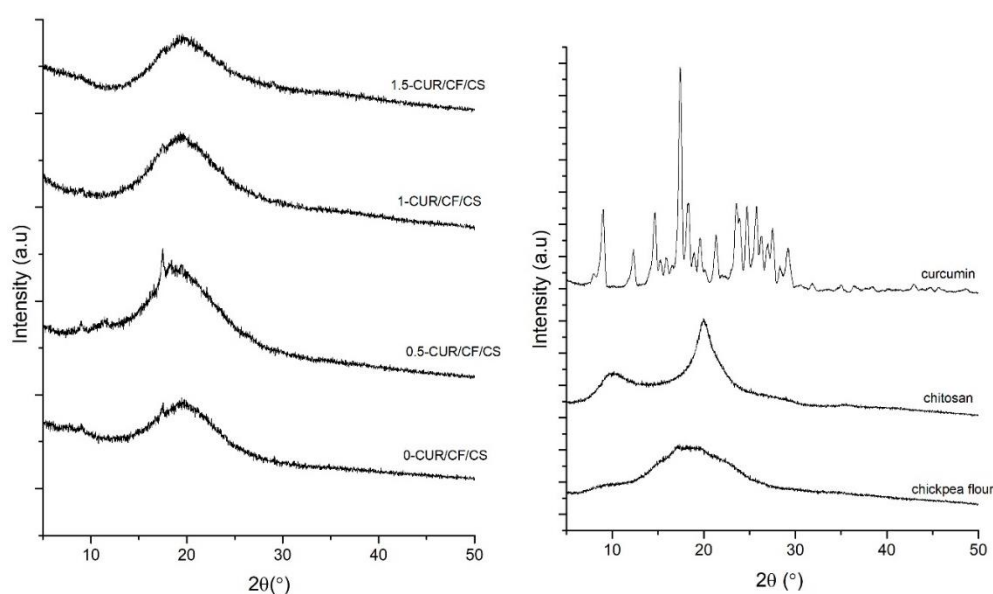
Figure 3.17. X-ray diffraction patterns of the CF/CS films

3.4.6 Antioxidant Activity (DPPH& ABTS)

The antioxidant activity values of films determined by DPPH and ABTS methods were represented in Table 3.16. In both methods, when the antioxidant radicals react with DPPH and ABTS reagents, discoloration occurs, and it is expressed as % scavenging activity. Antioxidant activity of the film was mainly attributed to the presence of CUR, CS, and CA. Antioxidant activity of the CUR has been extensively studied. The phenolic hydroxyl group and methylene group of β-diketone moiety in CUR structure are responsible for this activity (Yildiz et al., 2021). Further, the free amino groups in CS react with free radicals so CS exhibits radical scavenging activity (Wu et al., 2019). Among the films, 0.5-CUR/CF/CS showed the highest antioxidant activity. The potential antioxidant activity of CA was indicated in the study of Priyadarshi et al., (2018) and CA addition increased the antioxidant activity of CS films from 12.4% to 29.8%. However, in this study, contrary to expectation, the increase in CA amount in films did not contribute to the antioxidant activity of films. In other words, increasing CA concentration caused a reduction in antioxidant activity (Table 3.16). This result was due to the increased number of hydrogen bonds between CA and CS with increasing CA concentration. As the availability of free amino and hydroxyl groups decreases, the radical scavenging activity decreases as well (Zhang et al., 2022).

Table 3.16 DPPH and ABTS activity (%) of chickpea flour-chitosan crosslinked films

	DPPH (% scavenging activity)	ABTS (% scavenging activity)
0- CUR/CF/CS	32.65 ± 1.70^{b}	33.00 ± 3.40^{b}
0.5- CUR/CF/CS	52.12 ± 1.00^{a}	42.84 ± 0.90^{a}

Table 3.16 (Cont'd)

1- CUR/CF/CS	23.09±3.00[c]	5.38±0.80[c]
1.5- CUR/CF/CS	19.05±0.30[c]	3.68±0.200[c]

Different letters in the same column show the significant difference between samples by Tukey's test ($p \leq 0.05$).

3.4.7 Antimicrobial activity of CF/CS films

Figure 3.18 shows the antimicrobial activity and inhibition zones of CUR/CF/CS composite films against Gram-positive (*S. aureus*) and G-negative (*E. coli*) bacteria. The antimicrobial activity of CUR is based mainly on the inhibition of bacterial growth due to disruption of membrane and DNA damage (Tambawala et al., 2022). On the other hand, the chelating ability by binding essential metals and nutrients for the growth and polycationic structure eases interaction with the negatively charged cell surface and brings CS to antimicrobial ability (Hu et al., 2020). Although it is well-known that all film-forming components, except CF, have antimicrobial activity, 0-CUR/CF/CS and 0.5-CUR/CF/CS films did not exhibit any inhibition zone for either *E.coli* or *S.aureus*. The hydrophobic nature of CUR and insolubility in a hydrophilic environment might limit its efficiency. Similarly, due to the tight film structure, an insoluble form of CS might restrain its antimicrobial activity by limiting diffusion through the agar and inhibitory effect (Hafsa et al., 2016). As discussed before, CA had improved various physical properties of films. Its effect is not only on the physical properties of films but also on functional properties. Increasing CA concentration seemed to boost the antimicrobial effect of other components and also contributed to microbial inhibition by acidulation capability. In this sense, the injuries in the cellular membrane and damage to intracellular enzymes occur when the cell is exposed to an acidic environment. Moreover, due to the chelating effect, CA could interact with essential metal ions for growth (Ounkaew et al., 2018). Although 1-CUR/CF/CS film was effective on only *E.coli* (inhibition zone

109

area 3.89±0.91 cm^2), 1.5-CUR/CF/CS film showed an inhibitory effect on both *E.coli* (inhibition zone area 5.88±0.49 cm^2) cm and *S. aureus* (inhibition zone area 1.59±0.27 cm^2). The different efficiencies on different bacteria were attributed to the outer lipopolysaccharides membrane of G (-) which has a highly chelating charge surface compared to G (+) having peptidoglycan layer (Ounkaew et al., 2018).
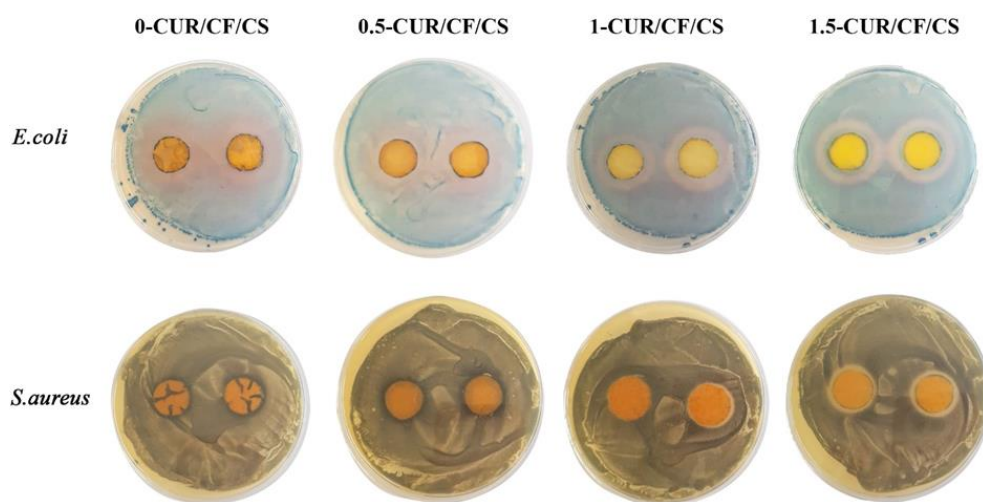
Figure 3.18. The inhibition zone of CUR/CF/CS films on *E.coli* and *S.aureus*

Compared to the CA crosslinked FC films, CA crosslinked CF/CS films had better antimicrobial activity on both tested microorganisms. Therefore, the activity of CF/CS films was tested on chicken breast packaging during the storage period.

3.4.8   Packaging application of active films on chicken breast

Chicken breast meat is a suitable substrate for promoting the growth of microorganisms due to its high moisture and protein content. To control spoilage and to maintain the microbial quality of susceptible products, antibacterial packaging films might be an excellent solution. Since 1.5-CUR/CF/CS film had an antimicrobial effect on Gram (+) and Gram (-) bacteria, it seemed to be the most promising food package. Therefore, the antimicrobial activity of 1.5-CUR/CF/CS films on chicken breast meat was tested at refrigeration temperature (4°C). Since 0-

CUR/CF/CS did not have antimicrobial activity on tested microorganisms, it was selected as a control package. Figure 3.19 showed the total bacterial count (TBC) of chicken breast meat in two different packages during 9 days of storage. The initial bacterial load of the sample was approximately 2 log CFU/g, yet it increased for all samples throughout the storage period. According to Turkish Standard (TS 24019:2014) and European legislation (EC Regulation 1441/2007, 2007) (Kilic et al., 2022), the acceptable threshold value of TBC was determined to be 6.7 log cfu/g. TBC of the sample packed with 0-CUR/CF/CS was recorded as 5.57$\pm$0.08 log cfu/g and 7.18$\pm$0.02 log cfu/g at the end of day 5 and 7, respectively. Therefore, the sample exceeded the limit approximately at end of the day 6. However, TBC of 1.5-CUR/CF/CS samples was still lower than this threshold (7.73$\pm$0.11 log cfu/g). Thus, 1.5-CUR/CF/CS caused a substantial reduction in the growth of microorganisms and extended the shelf life of chicken breast meat.
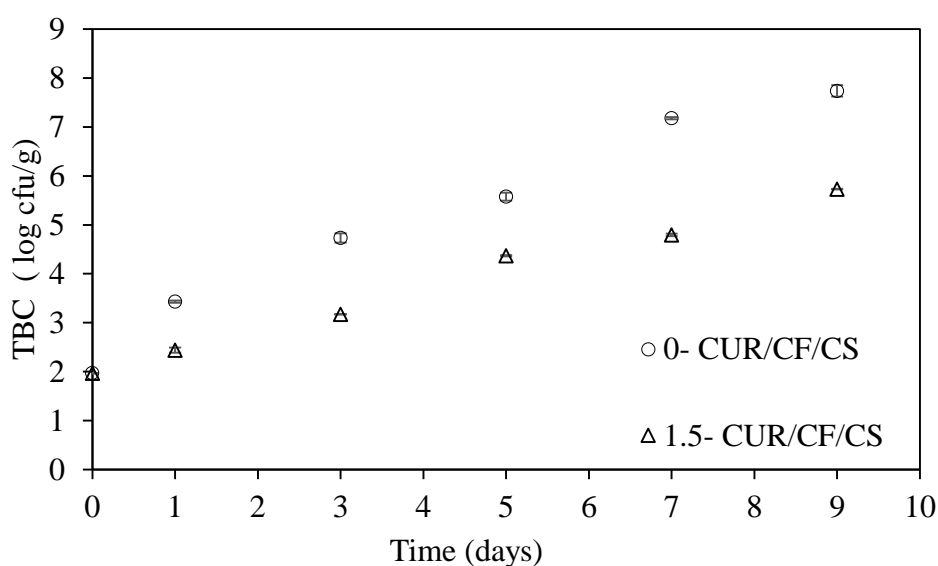
Figure 3.19. Total bacterial count (TBC) of chicken breast packaged with 0-CUR/CF/CS and 1.5- CUR/CF/CS during 9 days storage at 4 °C.

CHAPTER 4

CONCLUSION

In this study, it is aimed to produce intelligent and active food packages by taking the advantage of curcumin with electrospinning and casting methods. Since there has been an increasing interest in natural, non-toxic, and biodegradable food packages instead of plastic ones, as a film forming matrix, biodegredable polymers (chitosan, PEO) and flours (faba bean flour and chickpea flour) were utilized. In the electrospining method, solution properties had a great impact on nanofiber formation. For that purpose, rheological properties and conductivities of the electrospun solution were measured. Encapsulation of curcumin into PEO/chitosan matrix was successfully carried out for the purpose of intelligent film production. Results revealed that increasing chitosan amount in nanofibers decreased the diameter of the fibers. Color changes of curcumin loaded chitosan/PEO nanofiber film were evaluated on chicken breast package at 4 °C. The color of nanofiber film changed from bright yellow to reddish color which provided an opportunity to detect color changes by even the naked eyes of the consumer. As a result, curcumin loaded nanofiber allowed visualizing the real time monitoring of chicken spoilage and can be suggested as an intelligent food packaging. Curcumin was also encapsulated into the chickpea flour/PEO matrix to investigate its efficiency in active food package. Further, the effects of heating methods (conventional and microwave) on solution and film properties were also investigated. SEM images showed that the fiber morphology of the microwave-treated samples was as smooth as those of conventionally-treated ones. Neither the addition of curcumin nor the different heat treatments had any significant impact on the water vapor permeability of the samples. Both the DPPH and ABTS scavenging activities of the curcumin-containing and microwave-treated (CUR/MW) samples were higher than those of the conventionally-treated (CUR/CON) samples. Moreover, CUR/MW film had an

antimicrobial effect on *E.coli*. To eliminate the potential drawbacks of the bio-degradable food packages, different crosslinking agent performances were compared to faba bean flour–chitosan-curcumin films. The films with the highest citric acid concentration showed better swelling degree and permeability characteristics than the rest of the films. Although citric acid added samples had less mechanical strength and high elongation, the films containing gluteraldehyde exhibited high tensile strength and low elongation. In addition, the film with the highest citric acid content had a very similar antimicrobial effect on *E.coli*, and *S.aureus*. Therefore, citric acid can be suggested as a crosslinking agent instead of gluteraldehyde. Finally, citric acid was utilized as a crosslinker for the films produced by chitosan, chickpea flour, and active agent curcumin by a solvent casting technique. Chicken breast packed with the mentioned films remained below unacceptable microbial threshold limits even at the end of the 9th-day of storage compared to samples packaged with the film with no antibacterial activity. Chickpea flour and faba bean flour based films produced by casting methods had comparable moisture content, swelling degree and water solubility. Compared to citric acid crosslinked faba bean flour–chitosan-curcumin films, citric acid crosslinked chickpea flour-chitosan-curcumin films had better water vapor permeability and antimicrobial activity. Therefore, citric acid crosslinked chickpea flour/chitosan active film can be suggested for all other microbiologically susceptible perishable foods such as beef, fish and turkey.

For future studies, the improvement of mechanical properties and water sensitivity of electrospun film by crosslinlinking should be considered. The releasing behavior of the curcumin from the film matrix might also be analyzed and the antioxidant activity of the films might also be tested on lipid oxidation. Since production rate of single nozzle electrospinning is low, other methods like multi nozzle or centrifugal spinning can be suggested as an alternative nano/microfiber production methods. Since solubility and mechanical properties of nanofiber films did not satisfy with the expectations, nanofiber film can be utilzed by layer by layer technique to improve these properties.

REFERENCES

Abdollahi, M., Rezaei, M. & Farzi, G. (2012). Improvement of active chitosan film properties with rosemary essential oil for food packaging. *International Journal of Food Science and Technology*, *47*(4), 847–853. https://doi.org/10.1111/j.1365-2621.2011.02917.x

Adamczak, A., Ożarowski, M. & Karpiński, T. M. (2020). Curcumin, a natural antimicrobial agent with strain-specific activity. *Pharmaceuticals*, *13*(7), 1–12. https://doi.org/10.3390/ph13070153

Aghaei, Z., Ghorani, B., Emadzadeh, B., Kadkhodaee, R. & Tucker, N. (2020). Protein-based halochromic electrospun nanosensor for monitoring trout fish freshness. *Food Control*, *111*(December 2019), 107065. https://doi.org/10.1016/j.foodcont.2019.107065

Ahmed, A., Xu, L., Yin, J., Wang, M., Khan, F. & Ali, M. (2020). High-throughput Fabrication of Chitosan/Poly(ethylene oxide) Nanofibers by Modified Free Surface Electrospinning. *Fibers and Polymers*, *21*(9), 1945–1955. https://doi.org/10.1007/s12221-020-1109-9

Ahmed, J. & Varshney, S. K. (2011). Polylactides-chemistry, properties and green packaging technology: A review. *International Journal of Food Properties*, *14*(1), 37–58. https://doi.org/10.1080/10942910903125284

Akhtar, M. J., Jacquot, M., Jasniewski, J., Jacquot, C., Imran, M., Jamshidian, M., Paris, C. & Desobry, S. (2012). Antioxidant capacity and light-aging study of HPMC films functionalized with natural plant extract. *Carbohydrate Polymers*, *89*(4), 1150–1158. https://doi.org/10.1016/j.carbpol.2012.03.088

Alehosseini, A., Gómez-Mascaraque, L. G., Martínez-Sanz, M. & López-Rubio, A. (2019). Electrospun curcumin-loaded protein nanofiber mats as active/bioactive coatings for food packaging applications. *Food Hydrocolloids*, *87*(August 2018), 758–771. https://doi.org/10.1016/j.foodhyd.2018.08.056

115

Aliabbasi, N., Fathi, M. & Emam-Djomeh, Z. (2021). Curcumin: A promising bioactive agent for application in food packaging systems. *Journal of Environmental Chemical Engineering*, *9*(4), 105520. https://doi.org/10.1016/j.jece.2021.105520

Alven, S., Nqoro, X. & Aderibigbe, B. A. (2020). Polymer-based materials loaded with curcumin for wound healing applications. *Polymers*, *12*(10), 1–25. https://doi.org/10.3390/polym12102286

Alzagameem, A., Klein, S. E., Bergs, M., Do, X. T., Korte, I., Dohlen, S., Hüwe, C., Kreyenschmidt, J., Kamm, B., Larkins, M. & Schulze, M. (2019). Antimicrobial activity of lignin and lignin-derived cellulose and chitosan composites against selected pathogenic and spoilage microorganisms. *Polymers*, *11*(4). https://doi.org/10.3390/polym11040670

Ardiyansyah, Apriliyanti, M. W., Wahyono, A., Fatoni, M., Poerwanto, B. & Suryaningsih, W. (2018). The Potency of betacyanins extract from a peel of dragon fruits as a source of colourimetric indicator to develop intelligent packaging for fish freshness monitoring. *IOP Conference Series: Earth and Environmental Science*, *207*(1). https://doi.org/10.1088/1755-1315/207/1/012038

Ávila-Martín, L., Beltrán-Osuna, Á. A. & Perilla, J. E. (2020). Effect of the Addition of Citric Acid and Whey Protein Isolate in Canna indica L. Starch Films Obtained by Solvent Casting. *Journal of Polymers and the Environment*, *28*(3), 871–883. https://doi.org/10.1007/s10924-019-01648-z

Avossa, J., Paolesse, R., Di Natale, C., Zampetti, E., Bertoni, G., De Cesare, F., Scarascia-Mugnozza, G. & Macagnano, A. (2019). Electrospinning of polystyrene/polyhydroxybutyrate nanofibers doped with porphyrin and graphene for chemiresistor gas sensors. *Nanomaterials*, *9*(2). https://doi.org/10.3390/nano9020280

Aydogdu, A., Kirtil, E., Sumnu, G., Oztop, M. H. & Aydogdu, Y. (2018). Utilization of lentil flour as a biopolymer source for the development of edible

films. *Journal of Applied Polymer Science*, *135*(23), 1–10. https://doi.org/10.1002/app.46356

Aydogdu, A., Radke, C. J., Bezci, S. & Kirtil, E. (2020). Characterization of curcumin incorporated guar gum/orange oil antimicrobial emulsion films. *International Journal of Biological Macromolecules*, *148*, 110–120. https://doi.org/10.1016/j.ijbiomac.2019.12.255

Aydogdu, A., Sumnu, G. & Sahin, S. (2018). A novel electrospun hydroxypropyl methylcellulose/polyethylene oxide blend nanofibers: Morphology and physicochemical properties. *Carbohydrate Polymers*, *181*(October 2017), 234–246. https://doi.org/10.1016/j.carbpol.2017.10.071

Aydogdu, A., Sumnu, G. & Sahin, S. (2019). Fabrication of gallic acid loaded Hydroxypropyl methylcellulose nanofibers by electrospinning technique as active packaging material. *Carbohydrate Polymers*, *208*(December 2018), 241–250. https://doi.org/10.1016/j.carbpol.2018.12.065

Aydogdu, A., Yildiz, E., Aydogdu, Y., Sumnu, G., Sahin, S. & Ayhan, Z. (2019a). Enhancing oxidative stability of walnuts by using gallic acid loaded lentil flour based electrospun nanofibers as active packaging material. *Food Hydrocolloids*, *95*, 245–255. https://doi.org/10.1016/j.foodhyd.2019.04.020

Aydogdu, A., Yildiz, E., Aydogdu, Y., Sumnu, G., Sahin, S. & Ayhan, Z. (2019b). Enhancing oxidative stability of walnuts by using gallic acid loaded lentil flour based electrospun nanofibers as active packaging material. *Food Hydrocolloids*, *95*(April), 245–255. https://doi.org/10.1016/j.foodhyd.2019.04.020

Aydogdu, A., Yildiz, E., Ayhan, Z., Aydogdu, Y., Sumnu, G. & Sahin, S. (2019a). Nanostructured poly(lactic acid)/soy protein/HPMC films by electrospinning for potential applications in food industry. *European Polymer Journal*, *112*, 477–486. https://doi.org/10.1016/j.eurpolymj.2019.01.006

Aydogdu, A., Yildiz, E., Ayhan, Z., Aydogdu, Y., Sumnu, G. & Sahin, S. (2019b). Nanostructured poly(lactic acid)/soy protein/HPMC films by electrospinning

for potential applications in food industry. *European Polymer Journal*, *112*(December 2018), 477–486. https://doi.org/10.1016/j.eurpolymj.2019.01.006

Aydogdu Emir, A., Yildiz, E., Aydogdu, Y., Sumnu, G. & Sahin, S. (2021). Gallic acid encapsulated pea flour-based nanofibers produced by electrospinning as a potential active food packaging material. *Legume Science*, *February*, 1–10. https://doi.org/10.1002/leg3.90

Azeredo, H. M. C., Kontou-Vrettou, C., Moates, G. K., Wellner, N., Cross, K., Pereira, P. H. F. & Waldron, K. W. (2015). Wheat straw hemicellulose films as affected by citric acid. *Food Hydrocolloids*, *50*, 1–6. https://doi.org/10.1016/j.foodhyd.2015.04.005

Bagheri, F., Radi, M. & Amiri, S. (2019). Drying conditions highly influence the characteristics of glycerol-plasticized alginate films. *Food Hydrocolloids*, *90*(November 2018), 162–171. https://doi.org/10.1016/j.foodhyd.2018.12.001

Bailén, G., Guillén, F., Castillo, S., Serrano, M., Valero, D. & Martínez-Romero, D. (2006). Use of activated carbon inside modified atmosphere packages to maintain tomato fruit quality during cold storage. *Journal of Agricultural and Food Chemistry*, *54*(6), 2229–2235. https://doi.org/10.1021/jf0528761

Bajer, D., Janczak, K. & Bajer, K. (2020). Novel Starch/Chitosan/Aloe Vera Composites as Promising Biopackaging Materials. *Journal of Polymers and the Environment*, *28*(3), 1021–1039. https://doi.org/10.1007/s10924-020-01661-7

Balamatsia, C. C., Patsias, A., Kontominas, M. G. & Savvaidis, I. N. (2007). Possible role of volatile amines as quality-indicating metabolites in modified atmosphere-packaged chicken fillets: Correlation with microbiological and sensory attributes. *Food Chemistry*, *104*(4), 1622–1628. https://doi.org/10.1016/j.foodchem.2007.03.013

Balasubramanian, R., Kim, S. S. & Lee, J. (2018). Novel synergistic transparent k-Carrageenan/Xanthan gum/Gellan gum hydrogel film: Mechanical, thermal

and water barrier properties. *International Journal of Biological Macromolecules*, *118*, 561–568. https://doi.org/10.1016/j.ijbiomac.2018.06.110

Balbinot-Alfaro, E., Craveiro, D. V., Lima, K. O., Costa, H. L. G., Lopes, D. R. & Prentice, C. (2019). Intelligent Packaging with pH Indicator Potential. *Food Engineering Reviews*, 1–10. https://doi.org/10.1007/s12393-019-09198-9

Becerril, R., Nerín, C. & Silva, F. (2021). Bring some colour to your package: Freshness indicators based on anthocyanin extracts. *Trends in Food Science and Technology*, *111*(August 2020), 495–505. https://doi.org/10.1016/j.tifs.2021.02.042

Bhawana, Basniwal, R. K., Buttar, H. S., Jain, V. K. & Jain, N. (2011). Curcumin nanoparticles: Preparation, characterization, and antimicrobial study. *Journal of Agricultural and Food Chemistry*, *59*(5), 2056–2061. https://doi.org/10.1021/jf104402t

Bi, F., Qin, Y., Chen, D., Kan, J. & Liu, J. (2021). International Journal of Development of active packaging fi lms based on chitosan and nano-encapsulated luteolin. *International Journal of Biological Macromolecules*, *182*, 545–553. https://doi.org/10.1016/j.ijbiomac.2021.04.063

Bianco, A., Calderone, M. & Cacciotti, I. (2013). Electrospun PHBV/PEO co-solution blends: Microstructure, thermal and mechanical properties. *Materials Science and Engineering C*, *33*(3), 1067–1077. https://doi.org/10.1016/j.msec.2012.11.030

Biji, K. B., Ravishankar, C. N., Mohan, C. O. & Srinivasa Gopal, T. K. (2015). Smart packaging systems for food applications: a review. *Journal of Food Science and Technology*, *52*(10), 6125–6135. https://doi.org/10.1007/s13197-015-1766-7

Camerlo, A., Vebert-Nardin, C., Rossi, R. M. & Popa, A. M. (2013). Fragrance encapsulation in polymeric matrices by emulsion electrospinning. *European Polymer Journal*, *49*(12), 3806–3813.

https://doi.org/10.1016/j.eurpolymj.2013.08.028

Cao, L., Sun, G., Zhang, C., Liu, W., Li, J. & Wang, L. (2019). An Intelligent Film Based on Cassia Gum Containing Bromothymol Blue-Anchored Cellulose Fibers for Real-Time Detection of Meat Freshness. *Journal of Agricultural and Food Chemistry*, *67*(7), 2066–2074. https://doi.org/10.1021/acs.jafc.8b06493

Castro Coelho, S., Nogueiro Estevinho, B. & Rocha, F. (2021). Encapsulation in food industry with emerging electrohydrodynamic techniques: Electrospinning and electrospraying – A review. *Food Chemistry*, *339*(December 2019), 127850. https://doi.org/10.1016/j.foodchem.2020.127850

Celebioglu, A. & Uyar, T. (2020). Fast-dissolving antioxidant curcumin/cyclodextrin inclusion complex electrospun nanofibrous webs. *Food Chemistry*, *317*(October 2019), 126397. https://doi.org/10.1016/j.foodchem.2020.126397

Chatterjee, N. S., Panda, S. K., Navitha, M., Asha, K. K., Anandan, R. & Mathew, S. (2015). Vanillic acid and coumaric acid grafted chitosan derivatives: improved grafting ratio and potential application in functional food. *Journal of Food Science and Technology*, *52*(11), 7153–7162. https://doi.org/10.1007/s13197-015-1874-4

Chavoshizadeh, S., Pirsa, S. & Mohtarami, F. (2020). Sesame Oil Oxidation Control by Active and Smart Packaging System Using Wheat Gluten/Chlorophyll Film to Increase Shelf Life and Detecting Expiration Date. *European Journal of Lipid Science and Technology*, *122*(3), 1–12. https://doi.org/10.1002/ejlt.201900385

Chen, F. & Chi, C. (2021). Development of pullulan/carboxylated cellulose nanocrystal/tea polyphenol bionanocomposite films for active food packaging. *International Journal of Biological Macromolecules*, *186*(July), 405–413. https://doi.org/10.1016/j.ijbiomac.2021.07.025

Chen, H. zhi, Zhang, M., Bhandari, B. & Yang, C. hui. (2020). Novel pH-sensitive films containing curcumin and anthocyanins to monitor fish freshness. *Food Hydrocolloids*, *100*(October 2019), 105438. https://doi.org/10.1016/j.foodhyd.2019.105438

Choi, I., Lee, J. Y., Lacroix, M. & Han, J. (2017). Intelligent pH indicator film composed of agar/potato starch and anthocyanin extracts from purple sweet potato. *Food Chemistry*, *218*, 122–128. https://doi.org/10.1016/j.foodchem.2016.09.050

Chuang, W. Y., Young, T. H., Yao, C. H. & Chiu, W. Y. (1999). Properties of the poly(vinyl alcohol)/chitosan blend and its effect on the culture of fibroblast in vitro. *Biomaterials*, *20*(16), 1479–1487. https://doi.org/10.1016/S0142-9612(99)00054-X

Confederat, L. G., Tuchilus, C. G., Dragan, M., Sha'at, M. & Dragostin, O. M. (2021). Preparation and Antimicrobial Activity of Chitosan and Its Derivatives: A Concise Review. *Molecules (Basel, Switzerland)*, *26*(12). https://doi.org/10.3390/molecules26123694

Cui, S., Yao, B., Sun, X., Hu, J., Zhou, Y. & Liu, Y. (2016). Reducing the content of carrier polymer in pectin nanofibers by electrospinning at low loading followed with selective washing. *Materials Science and Engineering C*, *59*, 885–893. https://doi.org/10.1016/j.msec.2015.10.086

Das, A., Uppaluri, R. & Das, C. (2019). Feasibility of poly-vinyl alcohol/starch/glycerol/citric acid composite films for wound dressing applications. *International Journal of Biological Macromolecules*, *131*, 998–1007. https://doi.org/10.1016/j.ijbiomac.2019.03.160

De Vrieze, S., Van Camp, T., Nelvig, A., Hagström, B., Westbroek, P. & De Clerck, K. (2009). The effect of temperature and humidity on electrospinning. *Journal of Materials Science*, *44*(5), 1357–1362. https://doi.org/10.1007/s10853-008-3010-6

Demirkesen, I., Campanella, O. H., Sumnu, G., Sahin, S. & Hamaker, B. R. (2014).

A Study on Staling Characteristics of Gluten-Free Breads Prepared with Chestnut and Rice Flours. *Food and Bioprocess Technology*, *7*(3), 806–820. https://doi.org/10.1007/s11947-013-1099-3

Deng, L., Kang, X., Liu, Y., Feng, F. & Zhang, H. (2018). Characterization of gelatin/zein films fabricated by electrospinning vs solvent casting. *Food Hydrocolloids*, *74*, 324–332. https://doi.org/10.1016/j.foodhyd.2017.08.023

Deng, L., Taxipalati, M., Zhang, A., Que, F., Wei, H., Feng, F. & Zhang, H. (2018). Electrospun Chitosan/Poly(ethylene oxide)/Lauric Arginate Nanofibrous Film with Enhanced Antimicrobial Activity. *Journal of Agricultural and Food Chemistry*, *66*(24), 6219–6226. https://doi.org/10.1021/acs.jafc.8b01493

Díaz-Galindo, E. P., Nesic, A., Cabrera-Barjas, G., Mardones, C., Von Baer, D., Bautista-Baños, S. & Garcia, O. D. (2020). Physical-chemical evaluation of active food packaging material based on thermoplastic starch loaded with grape cane extract. *Molecules*, *25*(6). https://doi.org/10.3390/molecules25061306

Díaz, O., Ferreiro, T., Rodríguez-Otero, J. L. & Cobos, Á. (2019). Characterization of chickpea (Cicer arietinum L.) flour films: Effects of pH and plasticizer concentration. *International Journal of Molecular Sciences*, *20*(5). https://doi.org/10.3390/ijms20051246

Dilamian, M., Montazer, M. & Masoumi, J. (2013). Antimicrobial electrospun membranes of chitosan/poly(ethylene oxide) incorporating poly(hexamethylene biguanide) hydrochloride. *Carbohydrate Polymers*, *94*(1), 364–371. https://doi.org/10.1016/j.carbpol.2013.01.059

Ding, L., Li, X., Hu, L., Zhang, Y., Jiang, Y., Mao, Z., Xu, H., Wang, B., Feng, X. & Sui, X. (2020). A naked-eye detection polyvinyl alcohol/cellulose-based pH sensor for intelligent packaging. *Carbohydrate Polymers*, *233*(January), 115859. https://doi.org/10.1016/j.carbpol.2020.115859

Dong, X., Dong, M., Lu, Y., Turley, A., Jin, T. & Wu, C. (2011). Antimicrobial

and antioxidant activities of lignin from residue of corn stover to ethanol production. *Industrial Crops and Products*, *34*(3), 1629–1634. https://doi.org/10.1016/j.indcrop.2011.06.002

Drago, E., Campardelli, R., Pettinato, M. & Perego, P. (2020). Innovations in smart packaging concepts for food: An extensive review. *Foods*, *9*(11). https://doi.org/10.3390/foods9111628

Duvoix, A., Blasius, R., Delhalle, S., Schnekenburger, M., Morceau, F., Henry, E., Dicato, M. & Diederich, M. (2005). Chemopreventive and therapeutic effects of curcumin. *Cancer Letters*, *223*(2), 181–190. https://doi.org/10.1016/j.canlet.2004.09.041

Echegaray, N., Guzel, N., Kumar, M., Guzel, M., Hassoun, A. & Manuel Lorenzo, J. (2022). Recent advancements in natural colorants and their application as coloring in food and in intelligent food packaging. *Food Chemistry*, *404*(PA), 134453. https://doi.org/10.1016/j.foodchem.2022.134453

Erdem, R. & Akalın, M. (2015). Characterization and evaluation of antimicrobial properties of electrospun chitosan/polyethylene oxide based nanofibrous scaffolds (with/without nanosilver). *Journal of Industrial Textiles*, *44*(4), 553–571. https://doi.org/10.1177/1528083713503000

Ezati, P. & Rhim, J. W. (2020). pH-responsive pectin-based multifunctional films incorporated with curcumin and sulfur nanoparticles. *Carbohydrate Polymers*, *230*(October 2019), 115638. https://doi.org/10.1016/j.carbpol.2019.115638

Ezati, P., Tajik, H., Moradi, M. & Molaei, R. (2019). Intelligent pH-sensitive indicator based on starch-cellulose and alizarin dye to track freshness of rainbow trout fillet. *International Journal of Biological Macromolecules*, *132*, 157–165. https://doi.org/10.1016/j.ijbiomac.2019.03.173

Farhan, A. & Hani, N. M. (2020). Active edible films based on semi-refined κ-carrageenan: Antioxidant and color properties and application in chicken breast packaging. *Food Packaging and Shelf Life*, *24*(November 2019), 100476. https://doi.org/10.1016/j.fpsl.2020.100476

Fazel, R., Torabi, S. F., Naseri-Nosar, P., Ghasempur, S., Ranaei-Siadat, S. O. & Khajeh, K. (2016). Electrospun polyvinyl alcohol/bovine serum albumin biocomposite membranes for horseradish peroxidase immobilization. *Enzyme and Microbial Technology*, *93–94*, 1–10. https://doi.org/10.1016/j.enzmictec.2016.07.002

Fernandes, J. C., Tavaria, F. K., Soares, J. C., Ramos, Ó. S., João Monteiro, M., Pintado, M. E. & Xavier Malcata, F. (2008). Antimicrobial effects of chitosans and chitooligosaccharides, upon Staphylococcus aureus and Escherichia coli, in food model systems. *Food Microbiology*, *25*(7), 922–928. https://doi.org/10.1016/j.fm.2008.05.003

Fernández-Bedmar, Z. & Alonso-Moraga, A. (2016). In vivo and in vitro evaluation for nutraceutical purposes of capsaicin, capsanthin, lutein and four pepper varieties. *Food and Chemical Toxicology*, *98*, 89–99. https://doi.org/10.1016/j.fct.2016.10.011

Fonseca, L. M., Cruxen, C. E. dos S., Bruni, G. P., Fiorentini, Â. M., Zavareze, E. da R., Lim, L. T. & Dias, A. R. G. (2019). Development of antimicrobial and antioxidant electrospun soluble potato starch nanofibers loaded with carvacrol. *International Journal of Biological Macromolecules*, *139*, 1182–1190. https://doi.org/10.1016/j.ijbiomac.2019.08.096

Ghanbarzadeh, B., Almasi, H. & Entezami, A. A. (2011). Improving the barrier and mechanical properties of corn starch-based edible films: Effect of citric acid and carboxymethyl cellulose. *Industrial Crops and Products*, *33*(1), 229–235. https://doi.org/10.1016/j.indcrop.2010.10.016

Giannakas, A., Grigoriadi, K., Leontiou, A., Barkoula, N. M. & Ladavos, A. (2014). Preparation, characterization, mechanical and barrier properties investigation of chitosan-clay nanocomposites. *Carbohydrate Polymers*, *108*(1), 103–111. https://doi.org/10.1016/j.carbpol.2014.03.019

Gómez-Estaca, J., Balaguer, M. P., López-Carballo, G., Gavara, R. & Hernández-Muñoz, P. (2017). Improving antioxidant and antimicrobial properties of

curcumin by means of encapsulation in gelatin through electrohydrodynamic atomization. *Food Hydrocolloids*, *70*, 313–320. https://doi.org/10.1016/j.foodhyd.2017.04.019

Gonenc, I. & Us, F. (2019). Effect of Glutaraldehyde Crosslinking on Degree of Substitution, Thermal, Structural, and Physicochemical Properties of Corn Starch. *Starch/Staerke*, *71*(3–4), 1–10. https://doi.org/10.1002/star.201800046

Grande, C. D., Mangadlao, J., Fan, J., De Leon, A., Delgado-Ospina, J., Rojas, J. G., Rodrigues, D. F. & Advincula, R. (2017). Chitosan Cross-Linked Graphene Oxide Nanocomposite Films with Antimicrobial Activity for Application in Food Industry. *Macromolecular Symposia*, *374*(1), 1–8. https://doi.org/10.1002/masy.201600114

Grkovic, M., Stojanovic, D. B., Pavlovic, V. B., Rajilic-Stojanovic, M., Bjelovic, M. & Uskokovic, P. S. (2017). Improvement of mechanical properties and antibacterial activity of crosslinked electrospun chitosan/poly (ethylene oxide) nanofibers. *Composites Part B: Engineering*, *121*, 58–67. https://doi.org/10.1016/j.compositesb.2017.03.024

Guerrero, P., Muxika, A., Zarandona, I. & Caba, K. De. (2019). Crosslinking of chitosan fi lms processed by compression molding. *Carbohydrate Polymers*, *206*(August 2018), 820–826. https://doi.org/10.1016/j.carbpol.2018.11.064

Guerrero, P., Muxika, A., Zarandona, I. & de la Caba, K. (2019). Crosslinking of chitosan films processed by compression molding. *Carbohydrate Polymers*, *206*(November 2018), 820–826. https://doi.org/10.1016/j.carbpol.2018.11.064

Gülçin, I. (2010). Antioxidant properties of resveratrol: A structure-activity insight. *Innovative Food Science and Emerging Technologies*, *11*(1), 210–218. https://doi.org/10.1016/j.ifset.2009.07.002

Gutiérrez, T. J., Suniaga, J., Monsalve, A. & García, N. L. (2016). Influence of beet flour on the relationship surface-properties of edible and intelligent films made from native and modified plantain flour. *Food Hydrocolloids*, *54*, 234–244. https://doi.org/10.1016/j.foodhyd.2015.10.012

Hafsa, J., Smach, M. ali, Ben Khedher, M. R., Charfeddine, B., Limem, K., Majdoub, H. & Rouatbi, S. (2016). Physical, antioxidant and antimicrobial properties of chitosan films containing Eucalyptus globulus essential oil. *LWT - Food Science and Technology*, *68*, 356–364. https://doi.org/10.1016/j.lwt.2015.12.050

Hajikhani, M., Emam-Djomeh, Z. & Askari, G. (2020). Fabrication and Characterization of Gluten Film Reinforced by Lycopene-Loaded Electrospun Polylactic Acid Nano-fibers. *Food and Bioprocess Technology*, *13*(12), 2217–2227. https://doi.org/10.1007/s11947-020-02561-3

Halim, A. L. A., Kamari, A. & Phillip, E. (2018). Chitosan, gelatin and methylcellulose films incorporated with tannic acid for food packaging. *International Journal of Biological Macromolecules*, *120*, 1119–1126. https://doi.org/10.1016/j.ijbiomac.2018.08.169

Han, J. W., Ruiz-Garcia, L., Qian, J. P. & Yang, X. T. (2018). Food Packaging: A Comprehensive Review and Future Trends. *Comprehensive Reviews in Food Science and Food Safety*, *17*(4), 860–877. https://doi.org/10.1111/1541-4337.12343

Hassouna, F., Morlat-Thérias, S., Mailhot, G. & Gardette, J. L. (2007). Influence of water on the photodegradation of poly(ethylene oxide). *Polymer Degradation and Stability*, *92*(11), 2042–2050. https://doi.org/10.1016/j.polymdegradstab.2007.07.016

Heleno, S. A., Martins, A., Queiroz, M. J. R. P. & Ferreira, I. C. F. R. (2015). Bioactivity of phenolic acids: Metabolites versus parent compounds: A review. *Food Chemistry*, *173*, 501–513. https://doi.org/10.1016/j.foodchem.2014.10.057

Hu, H., Yao, X., Qin, Y., Yong, H. & Liu, J. (2020). Development of multifunctional food packaging by incorporating betalains from vegetable amaranth (Amaranthus tricolor L.) into quaternary ammonium chitosan/fish gelatin blend films. *International Journal of Biological Macromolecules*, *159*,

675–684. https://doi.org/10.1016/j.ijbiomac.2020.05.103

Hu, J., Zhou, F., Lin, Y., Zhou, A., Tan, B. K., Zeng, S., Hamzah, S. S. & Lin, S. (2019). The effects of photodynamically activated curcumin on the preservation of low alum treated ready-to-eat jellyfish. *Lwt*, *115*(June). https://doi.org/10.1016/j.lwt.2019.108443

Huang, X., Ji, Y., Guo, L., Xu, Q., Jin, L., Fu, Y. & Wang, Y. (2022). Incorporating tannin onto regenerated cellulose film towards sustainable active packaging. *Industrial Crops and Products*, *180*(February), 114710. https://doi.org/10.1016/j.indcrop.2022.114710

Huang, X. W., Zou, X. B., Shi, J. Y., Guo, Y., Zhao, J. W., Zhang, J. & Hao, L. (2014). Determination of pork spoilage by colorimetric gas sensor array based on natural pigments. *Food Chemistry*, *145*, 549–554. https://doi.org/10.1016/j.foodchem.2013.08.101

Hurley, B. R. A., Ouzts, A., Fischer, J. & Gomes, T. (2013a). A Multi-functional Biofilm Used as an Active Insert in Modified Atmosphere Packaging for Fresh Produce By. *Packaging and Technology and Science*, *29*(January), 399–412. https://doi.org/10.1002/pts

Hurley, B. R. A., Ouzts, A., Fischer, J. & Gomes, T. (2013b). Reducing Oxidation of Foods Through Antioxidant Active Packaging Based on Ethyl Vinyl Alcohol and Natural Flavonoids. *Packaging and Technology and Science*, *29*(January), 399–412. https://doi.org/10.1002/pts

Hurley, B. R. A., Ouzts, A., Fischer, J. & Gomes, T. (2014). A Novel On-Package Sticker Sensor Based on Methyl Red for Real-Time Monitoring of Broiler Chicken Cut Freshness. *Packaging and Technology and Science*, *27*, 399–412. https://doi.org/10.1002/pts

Islam, Md Shahidul & Karim, M. R. (2010). Fabrication and characterization of poly(vinyl alcohol)/alginate blend nanofibers by electrospinning method. *Colloids and Surfaces A: Physicochemical and Engineering Aspects*, *366*(1–3), 135–140. https://doi.org/10.1016/j.colsurfa.2010.05.038

Islam, Md Shariful, Ang, B. C., Andriyana, A. & Afifi, A. M. (2019). A review on fabrication of nanofibers via electrospinning and their applications. *SN Applied Sciences*, *1*(10), 1–16. https://doi.org/10.1007/s42452-019-1288-4

Istiqomah, A., Utami, M. R., Firdaus, M., Suryanti, V. & Kusumaningsih, T. (2022). Antibacterial chitosan-Dioscorea alata starch film enriched with essential oils optimally prepared by following response surface methodology. *Food Bioscience*, *46*(February), 101603. https://doi.org/10.1016/j.fbio.2022.101603

Janani, N., Zare, E. N., Salimi, F. & Makvandi, P. (2020). Antibacterial tragacanth gum-based nanocomposite films carrying ascorbic acid antioxidant for bioactive food packaging. *Carbohydrate Polymers*, *247*(June), 116678. https://doi.org/10.1016/j.carbpol.2020.116678

Javaid, M. A., Rizwan, M., Khera, R. A., Zia, K. M., Saito, K., Zuber, M., Iqbal, J. & Langer, P. (2018). Thermal degradation behavior and X-ray diffraction studies of chitosan based polyurethane bio-nanocomposites using different diisocyanates. *International Journal of Biological Macromolecules*, *117*, 762–772. https://doi.org/10.1016/j.ijbiomac.2018.05.209

Ji, Y., Xu, Q., Jin, L. & Fu, Y. (2020). Cellulosic paper with high antioxidative and barrier properties obtained through incorporation of tannin into kraft pulp fibers. *International Journal of Biological Macromolecules*, *162*, 678–684. https://doi.org/10.1016/j.ijbiomac.2020.06.101

Jose, J. & Al-Harthi, M. A. (2017). Citric acid crosslinking of poly(vinyl alcohol)/starch/graphene nanocomposites for superior properties. *Iranian Polymer Journal (English Edition)*, *26*(8), 579–587. https://doi.org/10.1007/s13726-017-0542-0

Jridi, M., Boughriba, S., Abdelhedi, O., Nciri, H., Nasri, R., Kchaou, H., Kaya, M., Sebai, H., Zouari, N. & Nasri, M. (2019). Investigation of physicochemical and antioxidant properties of gelatin edible film mixed with blood orange (Citrus sinensis) peel extract. *Food Packaging and Shelf Life*, *21*(September

2018), 100342. https://doi.org/10.1016/j.fpsl.2019.100342

Kalaycıoğlu, Z., Torlak, E., Akın-Evingür, G., Özen, İ. & Erim, F. B. (2017). Antimicrobial and physical properties of chitosan films incorporated with turmeric extract. *International Journal of Biological Macromolecules*, *101*, 882–888. https://doi.org/10.1016/j.ijbiomac.2017.03.174

Kalpana, S., Priyadarshini, S. R., Maria Leena, M., Moses, J. A. & Anandharamakrishnan, C. (2019). Intelligent packaging: Trends and applications in food systems. *Trends in Food Science and Technology*, *93*(October 2018), 145–157. https://doi.org/10.1016/j.tifs.2019.09.008

Kanatt, S. R. (2020). Development of active/intelligent food packaging film containing Amaranthus leaf extract for shelf life extension of chicken/fish during chilled storage. *Food Packaging and Shelf Life*, *24*(December 2019), 100506. https://doi.org/10.1016/j.fpsl.2020.100506

Kaya, E., Kahyaoglu, L. N. & Sumnu, G. (2022). Development of curcumin incorporated composite films based on chitin and glucan complexes extracted from Agaricus bisporus for active packaging of chicken breast meat. *International Journal of Biological Macromolecules*, *221*(September), 536–546. https://doi.org/10.1016/j.ijbiomac.2022.09.025

Kilic, B., Dogan, V., Kilic, V. & Kahyaoglu, L. N. (2022). Colorimetric food spoilage monitoring with carbon dot and UV light reinforced fish gelatin films using a smartphone application. *International Journal of Biological Macromolecules*, *209*(PA), 1562–1572. https://doi.org/10.1016/j.ijbiomac.2022.04.119

Kim, D., Lee, S., Lee, K., Baek, S. & Seo, J. (2017). Development of a pH indicator composed of high moisture-absorbing materials for real-time monitoring of chicken breast freshness. *Food Science and Biotechnology*, *26*(1), 37–42. https://doi.org/10.1007/s10068-017-0005-6

Kim, S., Baek, S. K. & Song, K. Bin. (2018). Physical and antioxidant properties of alginate films prepared from Sargassum fulvellum with black chokeberry

extract. *Food Packaging and Shelf Life*, *18*(November), 157–163. https://doi.org/10.1016/j.fpsl.2018.11.008

Kocakulak, S., Sumnu, G. & Sahin, S. (2019). Chickpea flour-based biofilms containing gallic acid to be used as active edible films. *Journal of Applied Polymer Science*, *136*(26), 1–9. https://doi.org/10.1002/app.47704

Kong, F. & Singh, R. P. (2011). Advances in instrumental methods to determine food quality deterioration. In *Food and Beverage Stability and Shelf Life*. Woodhead Publishing Limited. https://doi.org/10.1533/9780857092540.2.381

Kong, L. & Ziegler, G. R. (2014). Fabrication of pure starch fibers by electrospinning. *Food Hydrocolloids*, *36*, 20–25. https://doi.org/10.1016/j.foodhyd.2013.08.021

Konuk Takma, D. & Korel, F. (2019). Active packaging films as a carrier of black cumin essential oil: Development and effect on quality and shelf-life of chicken breast meat. *Food Packaging and Shelf Life*, *19*(November 2018), 210–217. https://doi.org/10.1016/j.fpsl.2018.11.002

Koosha, M. & Mirzadeh, H. (2015). Electrospinning, mechanical properties, and cell behavior study of chitosan/PVA nanofibers. *Journal of Biomedical Materials Research - Part A*, *103*(9), 3081–3093. https://doi.org/10.1002/jbm.a.35443

Kriegel, C., Kit, K. M., McClements, D. J. & Weiss, J. (2009a). Influence of surfactant type and concentration on electrospinning of chitosan-poly(ethylene oxide) blend nanofibers. *Food Biophysics*, *4*(3), 213–228. https://doi.org/10.1007/s11483-009-9119-6

Kriegel, C., Kit, K. M., McClements, D. J. & Weiss, J. (2009b). Influence of surfactant type and concentration on electrospinning of chitosan-poly(ethylene oxide) blend nanofibers. *Food Biophysics*, *4*(3), 213–228. https://doi.org/10.1007/s11483-009-9119-6

Kuswandi, B., Asih, N. P. N., Pratoko, D. K., Kristiningrum, N. & Moradi, M.

(2020). Edible pH sensor based on immobilized red cabbage anthocyanins into bacterial cellulose membrane for intelligent food packaging. *Packaging Technology and Science*, *33*(8), 321–332. https://doi.org/10.1002/pts.2507

Kuswandi, B., Jayus, Larasati, T. S., Abdullah, A. & Heng, L. Y. (2012). Real-Time Monitoring of Shrimp Spoilage Using On-Package Sticker Sensor Based on Natural Dye of Curcumin. *Food Analytical Methods*, *5*(4), 881–889. https://doi.org/10.1007/s12161-011-9326-x

Kuswandi, B., Wicaksono, Y., Jayus, Abdullah, A., Heng, L. Y. & Ahmad, M. (2011). Smart packaging: Sensors for monitoring of food quality and safety. *Sensing and Instrumentation for Food Quality and Safety*, *5*(3–4), 137–146. https://doi.org/10.1007/s11694-011-9120-x

Kutzli, I., Gibis, M., Baier, S. K. & Weiss, J. (2019). Electrospinning of whey and soy protein mixed with maltodextrin – Influence of protein type and ratio on the production and morphology of fibers. *Food Hydrocolloids*, *93*(January), 206–214. https://doi.org/10.1016/j.foodhyd.2019.02.028

LakshmiBalasubramaniam, S. P., Howell, C., Tajvidi, M. & Skonberg, D. (2022). Characterization of novel cellulose nanofibril and phenolic acid-based active and hydrophobic packaging films. *Food Chemistry*, *374*(November 2021), 131773. https://doi.org/10.1016/j.foodchem.2021.131773

Lan, W., Liang, X., Lan, W., Ahmed, S., Liu, Y. & Qin, W. (2019). Electrospun polyvinyl alcohol/d-limonene fibers prepared by ultrasonic processing for antibacterial active packaging material. *Molecules*, *24*(4). https://doi.org/10.3390/molecules24040767

Lee, S. J., Kim, S. S. & Lee, Y. M. (2000). Interpenetrating polymer network hydrogels based on poly(ethylene glycol) macromer and chitosan. *Carbohydrate Polymers*, *41*(2), 197–205. https://doi.org/10.1016/S0144-8617(99)00088-0

Leite, L. S. F., Pham, C., Bilatto, S., Azeredo, H. M. C., Cranston, E. D., Moreira, F. K., Mattoso, L. H. C. & Bras, J. (2021). Effect of Tannic Acid and

Cellulose Nanocrystals on Antioxidant and Antimicrobial Properties of Gelatin Films. *ACS Sustainable Chemistry and Engineering*. https://doi.org/10.1021/acssuschemeng.1c01774

Li, B. & Yang, X. (2020). Rutin-loaded cellulose acetate/poly(ethylene oxide) fiber membrane fabricated by electrospinning: A bioactive material. *Materials Science and Engineering C*, *109*(December 2019), 110601. https://doi.org/10.1016/j.msec.2019.110601

Li, C., Wu, K., Su, Y., Riffat, S. B., Ni, X. & Jiang, F. (2019). Effect of drying temperature on structural and thermomechanical properties of konjac glucomannan-zein blend films. *International Journal of Biological Macromolecules*, *138*, 135–143. https://doi.org/10.1016/j.ijbiomac.2019.07.007

Li, H., Liu, C., Sun, J. & Lv, S. (2022). Bioactive Edible Sodium Alginate Films Incorporated with Tannic Acid as Antimicrobial and Antioxidative Food Packaging. *Foods*, *11*(19). https://doi.org/10.3390/foods11193044

Li, J., Zivanovic, S., Davidson, P. M. & Kit, K. (2010). Characterization and comparison of chitosan/PVP and chitosan/PEO blend films. *Carbohydrate Polymers*, *79*(3), 786–791. https://doi.org/10.1016/j.carbpol.2009.09.028

Li, L., Wang, H., Chen, M., Jiang, S., Jiang, S., Li, X. & Wang, Q. (2018). Butylated hydroxyanisole encapsulated in gelatin fiber mats: Volatile release kinetics, functional effectiveness and application to strawberry preservation. *Food Chemistry*, *269*(July), 142–149. https://doi.org/10.1016/j.foodchem.2018.06.150

Lin, J., Pan, D., Sun, Y., Ou, C., Wang, Y. & Cao, J. (2019). The modification of gelatin films: Based on various cross-linking mechanism of glutaraldehyde at acidic and alkaline conditions. *Food Science and Nutrition*, *7*(12), 4140–4146. https://doi.org/10.1002/fsn3.1282

Liu, H., Adhikari, R., Guo, Q. & Adhikari, B. (2013). Preparation and characterization of glycerol plasticized (high-amylose) starch-chitosan films.

Journal of Food Engineering, *116*(2), 588–597.
https://doi.org/10.1016/j.jfoodeng.2012.12.037

Liu, Jingrong, Wang, H., Guo, M., Li, L., Chen, M., Jiang, S., Li, X. & Jiang, S. (2019). Extract from Lycium ruthenicum Murr. Incorporating κ-carrageenan colorimetric film with a wide pH–sensing range for food freshness monitoring. *Food Hydrocolloids*, *94*(February), 1–10. https://doi.org/10.1016/j.foodhyd.2019.03.008

Liu, Jingrong, Wang, H., Wang, P., Guo, M., Jiang, S., Li, X. & Jiang, S. (2018). Films based on κ-carrageenan incorporated with curcumin for freshness monitoring. *Food Hydrocolloids*, *83*, 134–142. https://doi.org/10.1016/j.foodhyd.2018.05.012

Liu, Jun, Meng, C. guang, Liu, S., Kan, J. & Jin, C. hai. (2017). Preparation and characterization of protocatechuic acid grafted chitosan films with antioxidant activity. *Food Hydrocolloids*, *63*, 457–466. https://doi.org/10.1016/j.foodhyd.2016.09.035

Liu, Y., Cai, Z., Sheng, L., Ma, M., Xu, Q. & Jin, Y. (2019). Structure-property of crosslinked chitosan/silica composite films modified by genipin and glutaraldehyde under alkaline conditions. *Carbohydrate Polymers*, *215*(March), 348–357. https://doi.org/10.1016/j.carbpol.2019.04.001

López de Dicastillo, C., Bustos, F., Guarda, A. & Galotto, M. J. (2016). Cross-linked methyl cellulose films with murta fruit extract for antioxidant and antimicrobial active food packaging. *Food Hydrocolloids*, *60*, 335–344. https://doi.org/10.1016/j.foodhyd.2016.03.020

Lu, J. W., Zhu, Y. L., Guo, Z. X., Hu, P. & Yu, J. (2006). Electrospinning of sodium alginate with poly(ethylene oxide). *Polymer*, *47*(23), 8026–8031. https://doi.org/10.1016/j.polymer.2006.09.027

Luchese, C. L., Pavoni, J. M. F., dos Santos, N. Z., Quines, L. K., Pollo, L. D., Spada, J. C. & Tessaro, I. C. (2018). Effect of chitosan addition on the properties of films prepared with corn and cassava starches. *Journal of Food*

Science and Technology, *55*(8), 2963–2973. https://doi.org/10.1007/s13197-018-3214-y

Luo, N., Varaprasad, K., Reddy, G. V. S., Rajulu, A. V. & Zhang, J. (2012). Preparation and characterization of cellulose/curcumin composite films. *RSC Advances*, *2*(22), 8483–8488. https://doi.org/10.1039/c2ra21465b

Luo, X. & Lim, L.-T. (2020). Curcumin-loaded electrospun nonwoven as a colorimetric indicator for volatile amines. *Lwt*, *128*(January), 109493. https://doi.org/10.1016/j.lwt.2020.109493

Luo, X., Zaitoon, A. & Lim, L. T. (2022). A review on colorimetric indicators for monitoring product freshness in intelligent food packaging: Indicator dyes, preparation methods, and applications. *Comprehensive Reviews in Food Science and Food Safety*, *21*(3), 2489–2519. https://doi.org/10.1111/1541-4337.12942

Ma, L., Deng, L. & Chen, J. (2014). Applications of poly(ethylene oxide) in controlled release tablet systems: A review. *Drug Development and Industrial Pharmacy*, *40*(7), 845–851. https://doi.org/10.3109/03639045.2013.831438

Ma, Q., Du, L. & Wang, L. (2017). Tara gum/polyvinyl alcohol-based colorimetric NH3 indicator films incorporating curcumin for intelligent packaging. *Sensors and Actuators, B: Chemical*, *244*, 759–766. https://doi.org/10.1016/j.snb.2017.01.035

Ma, Q., Ren, Y. & Wang, L. (2017). Investigation of antioxidant activity and release kinetics of curcumin from tara gum/ polyvinyl alcohol active film. *Food Hydrocolloids*, *70*, 286–292. https://doi.org/10.1016/j.foodhyd.2017.04.018

Ma, X., Chen, Y., Huang, J., Lv, P., Hussain, T. & Wei, Q. (2020). In situ formed active and intelligent bacterial cellulose/cotton fiber composite containing curcumin. *Cellulose*, *27*(16), 9371–9382. https://doi.org/10.1007/s10570-020-03413-1

Maftoonazad, N. & Ramaswamy, H. (2019). Design and testing of an electrospun nanofiber mat as a pH biosensor and monitor the pH associated quality in fresh date fruit (Rutab). *Polymer Testing*, *75*(December 2018), 76–84. https://doi.org/10.1016/j.polymertesting.2019.01.011

Mahajan, P. V., Rodrigues, F. A. S., Motel, A. & Leonhard, A. (2008). Development of a moisture absorber for packaging of fresh mushrooms (Agaricus bisporous). *Postharvest Biology and Technology*, *48*(3), 408–414. https://doi.org/10.1016/j.postharvbio.2007.11.007

Majzoobi, M., Beparva, P., Farahnaky, A. & Badii, F. (2014). Effects of malic acid and citric acid on the functional properties of native and cross-linked wheat starches. *Starch/Staerke*, *66*(5–6), 491–495. https://doi.org/10.1002/star.201300188

Malafaya, P. B., Silva, G. A. & Reis, R. L. (2007). Natural-origin polymers as carriers and scaffolds for biomolecules and cell delivery in tissue engineering applications. *Advanced Drug Delivery Reviews*, *59*(4–5), 207–233. https://doi.org/10.1016/j.addr.2007.03.012

Manzanarez-López, F., Soto-Valdez, H., Auras, R. & Peralta, E. (2011). Release of α-Tocopherol from Poly(lactic acid) films, and its effect on the oxidative stability of soybean oil. *Journal of Food Engineering*, *104*(4), 508–517. https://doi.org/10.1016/j.jfoodeng.2010.12.029

Marín-Silva, D. A., Rivero, S. & Pinotti, A. (2019). Chitosan-based nanocomposite matrices: Development and characterization. *International Journal of Biological Macromolecules*, *123*, 189–200. https://doi.org/10.1016/j.ijbiomac.2018.11.035

Martucci, J. F., Accareddu, A. E. M. & Ruseckaite, R. A. (2012). Preparation and characterization of plasticized gelatin films cross-linked with low concentrations of Glutaraldehyde. *Journal of Materials Science*, *47*(7), 3282–3292. https://doi.org/10.1007/s10853-011-6167-3

Medina Jaramillo, C., Gutiérrez, T. J., Goyanes, S., Bernal, C. & Famá, L. (2016).

Biodegradability and plasticizing effect of yerba mate extract on cassava starch edible films. *Carbohydrate Polymers*, *151*, 150–159. https://doi.org/10.1016/j.carbpol.2016.05.025

Merz, B., Capello, C., Leandro, G. C., Moritz, D. E., Monteiro, A. R. & Valencia, G. A. (2020). A novel colorimetric indicator film based on chitosan, polyvinyl alcohol and anthocyanins from jambolan (Syzygium cumini) fruit for monitoring shrimp freshness. *International Journal of Biological Macromolecules*, *153*, 625–632. https://doi.org/10.1016/j.ijbiomac.2020.03.048

Millar, K. A., Gallagher, E., Burke, R., McCarthy, S. & Barry-Ryan, C. (2019). Proximate composition and anti-nutritional factors of fava-bean (Vicia faba), green-pea and yellow-pea (Pisum sativum) flour. *Journal of Food Composition and Analysis*, *82*(July 2018), 103233. https://doi.org/10.1016/j.jfca.2019.103233

Moazami Goodarzi, M., Moradi, M., Tajik, H., Forough, M., Ezati, P. & Kuswandi, B. (2020). Development of an easy-to-use colorimetric pH label with starch and carrot anthocyanins for milk shelf life assessment. *International Journal of Biological Macromolecules*, *153*, 240–247. https://doi.org/10.1016/j.ijbiomac.2020.03.014

Mohamad, N., Mazlan, M. M., Tawakkal, I. S. M. A., Talib, R. A., Kian, L. K., Fouad, H. & Jawaid, M. (2020). Development of active agents filled polylactic acid films for food packaging application. *International Journal of Biological Macromolecules*, *163*, 1451–1457. https://doi.org/10.1016/j.ijbiomac.2020.07.209

Mohamed, S. A. A., El-Sakhawy, M. & El-Sakhawy, M. A. M. (2020). Polysaccharides, Protein and Lipid -Based Natural Edible Films in Food Packaging: A Review. *Carbohydrate Polymers*, *238*(March), 116178. https://doi.org/10.1016/j.carbpol.2020.116178

Mohammadalinejhad, S., Almasi, H. & Moradi, M. (2020). Immobilization of

Echium amoenum anthocyanins into bacterial cellulose film: A novel colorimetric pH indicator for freshness/spoilage monitoring of shrimp. *Food Control*, *113*(January), 107169. https://doi.org/10.1016/j.foodcont.2020.107169

Mohammadian, E., Alizadeh-Sani, M. & Jafari, S. M. (2020). Smart monitoring of gas/temperature changes within food packaging based on natural colorants. *Comprehensive Reviews in Food Science and Food Safety*, *19*(6), 2885–2931. https://doi.org/10.1111/1541-4337.12635

Moradi, M., Tajik, H., Almasi, H., Forough, M. & Ezati, P. (2019). A novel pH-sensing indicator based on bacterial cellulose nanofibers and black carrot anthocyanins for monitoring fish freshness. *Carbohydrate Polymers*, *222*(March), 115030. https://doi.org/10.1016/j.carbpol.2019.115030

Mücke, N., da Silva, T. B. V., de Oliveira, A., Moreira, T. F. M., Venancio, C. D. S., Marques, L. L. M., Valderrama, P., Gonçalves, O. H., da Silva-Buzanello, R. A., Yamashita, F., Shirai, M. A., Genena, A. K. & Leimann, F. V. (2021). Use of Water-Soluble Curcumin in TPS/PBAT Packaging Material: Interference on Reactive Extrusion and Oxidative Stability of Chia Oil. *Food and Bioprocess Technology*, *14*(3), 471–482. https://doi.org/10.1007/s11947-021-02584-4

Müller, P. & Schmid, M. (2019). Intelligent packaging in the food sector: A brief overview. *Foods*, *8*(1). https://doi.org/10.3390/foods8010016

Multari, S., Stewart, D. & Russell, W. R. (2015). Potential of Fava Bean as Future Protein Supply to Partially Replace Meat Intake in the Human Diet. *Comprehensive Reviews in Food Science and Food Safety*, *14*(5), 511–522. https://doi.org/10.1111/1541-4337.12146

Murray, C. A. & Dutcher, J. R. (2006). Effect of changes in relative and temperature on ultrathin chitosan films. *Biomacromolecules*, *7*(12), 3460–3465. https://doi.org/10.1021/bm060416q

Musialik, M., Kuzmicz, R., Pawlowski, T. S. & Litwinienko, G. (2009). Acidity of

hydroxyl groups: An overlooked influence on antiradical properties of flavonoids. *Journal of Organic Chemistry*, *74*(7), 2699–2709. https://doi.org/10.1021/jo802716v

Musso, Y. S., Salgado, P. R. & Mauri, A. N. (2017). Smart edible films based on gelatin and curcumin. *Food Hydrocolloids*, *66*, 8–15. https://doi.org/10.1016/j.foodhyd.2016.11.007

Mutlu, G., Calamak, S., Ulubayram, K. & Guven, E. (2018). Curcumin-loaded electrospun PHBV nanofibers as potential wound-dressing material. *Journal of Drug Delivery Science and Technology*, *43*, 185–193. https://doi.org/10.1016/j.jddst.2017.09.017

Myllärinen, P., Buleon, A., Lahtinen, R. & Forssell, P. (2002). The crystallinity of amylose and amylopectin films. *Carbohydrate Polymers*, *48*(1), 41–48. https://doi.org/10.1016/S0144-8617(01)00208-9

Naghdi, S., Rezaei, M. & Abdollahi, M. (2021). A starch-based pH-sensing and ammonia detector film containing betacyanin of paperflower for application in intelligent packaging of fish. *International Journal of Biological Macromolecules*, *191*(August), 161–170. https://doi.org/10.1016/j.ijbiomac.2021.09.045

Nascimento da Silva, M., de Matos Fonseca, J., Feldhaus, H. K., Soares, L. S., Valencia, G. A., Maduro de Campos, C. E., Di Luccio, M. & Monteiro, A. R. (2019). Physical and morphological properties of hydroxypropyl methylcellulose films with curcumin polymorphs. *Food Hydrocolloids*, *97*(March), 105217. https://doi.org/10.1016/j.foodhyd.2019.105217

Nataraj, D., Sakkara, S., Meghwal, M. & Reddy, N. (2018). Crosslinked chitosan films with controllable properties for commercial applications. *International Journal of Biological Macromolecules*, *120*, 1256–1264. https://doi.org/10.1016/j.ijbiomac.2018.08.187

Nguyen, T. T., Thi Dao, U. T., Thi Bui, Q. P., Bach, G. L., Ha Thuc, C. N. & Ha Thuc, H. (2020). Enhanced antimicrobial activities and physiochemical

properties of edible film based on chitosan incorporated with Sonneratia caseolaris (L.) Engl. leaf extract. *Progress in Organic Coatings*, *140*(November 2019), 105487. https://doi.org/10.1016/j.porgcoat.2019.105487

Nogueira, G. F., Fakhouri, F. M., Velasco, J. I. & de Oliveira, R. A. (2019). Active edible films based on arrowroot starch with microparticles of blackberry pulp obtained by freeze-drying for food packaging. *Polymers*, *11*(9). https://doi.org/10.3390/polym11091382

Nokhasteh, S., Molavi, A. M., Khorsand-Ghayeni, M. & Sadeghi-Avalshahr, A. (2019). Preparation of PVA/Chitosan samples by electrospinning and film casting methods and evaluating the effect of surface morphology on their antibacterial behavior. *Materials Research Express*, *7*(1). https://doi.org/10.1088/2053-1591/ab572c

Ochoa-Yepes, O., Di Giogio, L., Goyanes, S., Mauri, A. & Famá, L. (2019). Influence of process (extrusion/thermo-compression, casting) and lentil protein content on physicochemical properties of starch films. *Carbohydrate Polymers*, *208*(December 2018), 221–231. https://doi.org/10.1016/j.carbpol.2018.12.030

Oladzadabbasabadi, N., Mohammadi Nafchi, A., Ariffin, F., Wijekoon, M. M. J. O., Al-Hassan, A. A., Dheyab, M. A. & Ghasemlou, M. (2022). Recent advances in extraction, modification, and application of chitosan in packaging industry. *Carbohydrate Polymers*, *277*(September 2021), 118876. https://doi.org/10.1016/j.carbpol.2021.118876

Olga, D., Ferreiro, T., Rodr, L. & Cobos, Á. (2019). Characterization of Chickpea (Cicer arietinum L .) Flour Films : Effects of pH and Plasticizer Concentration. *International Journal of Molecular Sciences*, *20*(5), 3–16. https://doi.org/10.3390/ijms20051246

Ounkaew, A., Kasemsiri, P., Kamwilaisak, K., Saengprachatanarug, K., Mongkolthanaruk, W., Souvanh, M., Pongsa, U. & Chindaprasirt, P. (2018).

Polyvinyl Alcohol (PVA)/Starch Bioactive Packaging Film Enriched with Antioxidants from Spent Coffee Ground and Citric Acid. *Journal of Polymers and the Environment*, *26*(9), 3762–3772. https://doi.org/10.1007/s10924-018-1254-z

Pakravan, M., Heuzey, M. C. & Ajji, A. (2011). A fundamental study of chitosan/PEO electrospinning. *Polymer*, *52*(21), 4813–4824. https://doi.org/10.1016/j.polymer.2011.08.034

Park, J. S. (2010). Electrospinning and its applications. *Advances in Natural Sciences: Nanoscience and Nanotechnology*, *1*(4). https://doi.org/10.1088/2043-6262/1/4/043002

Pavoni, J. M. F., dos Santos, N. Z., May, I. C., Pollo, L. D. & Tessaro, I. C. (2021). Impact of acid type and glutaraldehyde crosslinking in the physicochemical and mechanical properties and biodegradability of chitosan films. *Polymer Bulletin*, *78*(2), 981–1000. https://doi.org/10.1007/s00289-020-03140-4

Pereda, M., Ponce, A. G., Marcovich, N. E., Ruseckaite, R. A. & Martucci, J. F. (2011). Chitosan-gelatin composites and bi-layer films with potential antimicrobial activity. *Food Hydrocolloids*, *25*(5), 1372–1381. https://doi.org/10.1016/j.foodhyd.2011.01.001

Pereira, V. A., de Arruda, I. N. Q. & Stefani, R. (2015). Active chitosan/PVA films with anthocyanins from Brassica oleraceae (Red Cabbage) as Time-Temperature Indicators for application in intelligent food packaging. *Food Hydrocolloids*, *43*, 180–188. https://doi.org/10.1016/j.foodhyd.2014.05.014

Powell, H. M., Supp, D. M. & Boyce, S. T. (2008). Influence of electrospun collagen on wound contraction of engineered skin substitutes. *Biomaterials*, *29*(7), 834–843. https://doi.org/10.1016/j.biomaterials.2007.10.036

Prietto, L., Mirapalhete, T. C., Pinto, V. Z., Hoffmann, J. F., Vanier, N. L., Lim, L. T., Guerra Dias, A. R. & da Rosa Zavareze, E. (2017). pH-sensitive films containing anthocyanins extracted from black bean seed coat and red cabbage. *Lwt*, *80*, 492–500. https://doi.org/10.1016/j.lwt.2017.03.006

Prietto, L., Pinto, V. Z., El Halal, S. L. M., de Morais, M. G., Costa, J. A. V., Lim, L. T., Dias, A. R. G. & Zavareze, E. da R. (2018). Ultrafine fibers of zein and anthocyanins as natural pH indicator. *Journal of the Science of Food and Agriculture*, *98*(7), 2735–2741. https://doi.org/10.1002/jsfa.8769

Priyadarshi, R., Sauraj, Kumar, B. & Negi, Y. S. (2018). Chitosan film incorporated with citric acid and glycerol as an active packaging material for extension of green chilli shelf life. *Carbohydrate Polymers*, *195*(December 2017), 329–338. https://doi.org/10.1016/j.carbpol.2018.04.089

Priyadarsini, K. I., Maity, D. K., Naik, G. H., Kumar, M. S., Unnikrishnan, M. K., Satav, J. G. & Mohan, H. (2003). Role of phenolic O-H and methylene hydrogen on the free radical reactions and antioxidant activity of curcumin. *Free Radical Biology and Medicine*, *35*(5), 475–484. https://doi.org/10.1016/S0891-5849(03)00325-3

Qiao, C., Ma, X., Wang, X. & Liu, L. (2021). Structure and properties of chitosan films: Effect of the type of solvent acid. *Lwt*, *135*(August 2020), 109984. https://doi.org/10.1016/j.lwt.2020.109984

Qin, Y., Liu, Y., Zhang, X. & Liu, J. (2020). Development of active and intelligent packaging by incorporating betalains from red pitaya (Hylocereus polyrhizus) peel into starch/polyvinyl alcohol films. *Food Hydrocolloids*, *100*(August 2019), 105410. https://doi.org/10.1016/j.foodhyd.2019.105410

Qin, Z. yu, Jia, X. W., Liu, Q., Kong, B. hua & Wang, H. (2019). Fast dissolving oral films for drug delivery prepared from chitosan/pullulan electrospinning nanofibers. *International Journal of Biological Macromolecules*, *137*, 224–231. https://doi.org/10.1016/j.ijbiomac.2019.06.224

Rahmati, M., Mills, D. K., Urbanska, A. M., Saeb, M. R., Venugopal, J. R., Ramakrishna, S. & Mozafari, M. (2021). Electrospinning for tissue engineering applications. *Progress in Materials Science*, *117*(July 2020), 100721. https://doi.org/10.1016/j.pmatsci.2020.100721

Rajeswari, A., Christy, E. J. S., Swathi, E. & Pius, A. (2020). Fabrication of

improved cellulose acetate-based biodegradable films for food packaging applications. *Environmental Chemistry and Ecotoxicology*, *2*, 107–114. https://doi.org/10.1016/j.enceco.2020.07.003

Rao, M. S., Kanatt, S. R., Chawla, S. P. & Sharma, A. (2010). Chitosan and guar gum composite films: Preparation, physical, mechanical and antimicrobial properties. *Carbohydrate Polymers*, *82*(4), 1243–1247. https://doi.org/10.1016/j.carbpol.2010.06.058

Reddy, N. & Yang, Y. (2010). Citric acid cross-linking of starch films. *Food Chemistry*, *118*(3), 702–711. https://doi.org/10.1016/j.foodchem.2009.05.050

Reesha, K. V., Satyen Kumar, P., Bindu, J. & Varghese, T. O. (2015). Development and characterization of an LDPE/chitosan composite antimicrobial film for chilled fish storage. *International Journal of Biological Macromolecules*, *79*, 934–942. https://doi.org/10.1016/j.ijbiomac.2015.06.016

Remanan, M. K. & Zhu, F. (2021). Encapsulation of rutin using quinoa and maize starch nanoparticles. *Food Chemistry*, *353*(July 2020), 128534. https://doi.org/10.1016/j.foodchem.2020.128534

Ren, L., Yan, X., Zhou, J., Tong, J. & Su, X. (2017). Influence of chitosan concentration on mechanical and barrier properties of corn starch/chitosan films. *International Journal of Biological Macromolecules*, *105*, 1636–1643. https://doi.org/10.1016/j.ijbiomac.2017.02.008

Ribeiro, A. M., Estevinho, B. N. & Rocha, F. (2021). Preparation and Incorporation of Functional Ingredients in Edible Films and Coatings. *Food and Bioprocess Technology*, *14*(2), 209–231. https://doi.org/10.1007/s11947-020-02528-4

Riveros, C. G., Martin, M. P., Aguirre, A. & Grosso, N. R. (2018). Film preparation with high protein defatted peanut flour: characterisation and potential use as food packaging. *International Journal of Food Science and Technology*, *53*(4), 969–975. https://doi.org/10.1111/ijfs.13670

Rodriguez-Garcia, I., Cruz-Valenzuela, M. R., Silva-Espinoza, B. A., Gonzalez-Aguilar, G. A., Moctezuma, E., Gutierrez-Pacheco, M. M., Tapia-Rodriguez, M. R., Ortega-Ramirez, L. A. & Ayala-Zavala, J. F. (2016). Oregano (Lippia graveolens) essential oil added within pectin edible coatings prevents fungal decay and increases the antioxidant capacity of treated tomatoes. *Journal of the Science of Food and Agriculture*, *96*(11), 3772–3778. https://doi.org/10.1002/jsfa.7568

Rosa-Sibakov, N., Heiniö, R. L., Cassan, D., Holopainen-Mantila, U., Micard, V., Lantto, R. & Sozer, N. (2016). Effect of bioprocessing and fractionation on the structural, textural and sensory properties of gluten-free faba bean pasta. *LWT - Food Science and Technology*, *67*, 27–36. https://doi.org/10.1016/j.lwt.2015.11.032

Rošic, R., Pelipenko, J., Kocbek, P., Baumgartner, S., Bešter-Rogač, M. & Kristl, J. (2012). The role of rheology of polymer solutions in predicting nanofiber formation by electrospinning. *European Polymer Journal*, *48*(8), 1374–1384. https://doi.org/10.1016/j.eurpolymj.2012.05.001

Rostamabadi, H., Assadpour, E., Tabarestani, H. S., Falsafi, S. R. & Jafari, S. M. (2020). Electrospinning approach for nanoencapsulation of bioactive compounds; recent advances and innovations. *Trends in Food Science and Technology*, *100*(January), 190–209. https://doi.org/10.1016/j.tifs.2020.04.012

Roy, S., Priyadarshi, R., Ezati, P. & Rhim, J. W. (2022). Curcumin and its uses in active and smart food packaging applications - a comprehensive review. *Food Chemistry*, *375*(August 2021), 131885. https://doi.org/10.1016/j.foodchem.2021.131885

Roy, S. & Rhim, J. W. (2020a). Carboxymethyl cellulose-based antioxidant and antimicrobial active packaging film incorporated with curcumin and zinc oxide. *International Journal of Biological Macromolecules*, *148*, 666–676. https://doi.org/10.1016/j.ijbiomac.2020.01.204

Roy, S. & Rhim, J. W. (2020b). Preparation of antimicrobial and antioxidant

gelatin/curcumin composite films for active food packaging application. *Colloids and Surfaces B: Biointerfaces*, *188*(December 2019), 110761. https://doi.org/10.1016/j.colsurfb.2019.110761

Roy, S. & Rhim, J. W. (2020c). Preparation of bioactive functional poly(lactic acid)/curcumin composite film for food packaging application. *International Journal of Biological Macromolecules*, *162*, 1780–1789. https://doi.org/10.1016/j.ijbiomac.2020.08.094

Roy, S. & Rhim, J. W. (2020d). Preparation of carbohydrate-based functional composite films incorporated with curcumin. *Food Hydrocolloids*, *98*(August 2019), 105302. https://doi.org/10.1016/j.foodhyd.2019.105302

Roy, S. & Rhim, J. W. (2021). Effect of chitosan modified halloysite on the physical and functional properties of pullulan/chitosan biofilm integrated with rutin. *Applied Clay Science*, *211*(July), 106205. https://doi.org/10.1016/j.clay.2021.106205

Roy, S., Zhai, L., Kim, Ch. H., Pham, H. D., Alrobei, H. & Kim, J. (2021). Tannic-Acid-Cross-Linked and TiO 2 -Nanoparticle-Reinforced Chitosan-Based Nanocomposite Film. *Polymers*, *13*, 2–18.

Rukchon, C., Nopwinyuwong, A., Trevanich, S., Jinkarn, T. & Suppakul, P. (2014). Development of a food spoilage indicator for monitoring freshness of skinless chicken breast. *Talanta*, *130*, 547–554. https://doi.org/10.1016/j.talanta.2014.07.048

Sabaghi, M., Maghsoudlou, Y. & Habibi, P. (2015). Enhancing structural properties and antioxidant activity of kefiran films by chitosan addition. *Food Structure*, *5*, 66–71. https://doi.org/10.1016/j.foostr.2015.06.003

Sadik, T., Pillon, C., Carrot, C. & Reglero Ruiz, J. A. (2018). Dsc studies on the decomposition of chemical blowing agents based on citric acid and sodium bicarbonate. *Thermochimica Acta*, *659*(November 2017), 74–81. https://doi.org/10.1016/j.tca.2017.11.007

Sánchez-Safont, E. L., Aldureid, A., Lagarón, J. M., Gamez-Perez, J. & Cabedo, L. (2021). Effect of the Purification Treatment on the Valorization of Natural Cellulosic Residues as Fillers in PHB-Based Composites for Short Shelf Life Applications. *Waste and Biomass Valorization*, *12*(5), 2541–2556. https://doi.org/10.1007/s12649-020-01192-1

Sarkhel, G., Banerjee, A. & Bhattacharya, P. (2006). Rheological and mechanical properties of LDPE/HDPE blends. *Polymer - Plastics Technology and Engineering*, *45*(6), 713–718. https://doi.org/10.1080/03602550600609663

Sebti, I., Delves-Broughton, J. & Coma, V. (2003). Physicochemical Properties and Bioactivity of Nisin-Containing Cross-Linked Hydroxypropylmethylcellulose Films. *Journal of Agricultural and Food Chemistry*, *51*(22), 6468–6474. https://doi.org/10.1021/jf0302613

Seligra, P. G., Medina Jaramillo, C., Famá, L. & Goyanes, S. (2016). Biodegradable and non-retrogradable eco-films based on starch-glycerol with citric acid as crosslinking agent. *Carbohydrate Polymers*, *138*, 66–74. https://doi.org/10.1016/j.carbpol.2015.11.041

Shafie, M. H., Yusof, R. & Gan, C. Y. (2019). Synthesis of citric acid monohydrate-choline chloride based deep eutectic solvents (DES) and characterization of their physicochemical properties. *Journal of Molecular Liquids*, *288*. https://doi.org/10.1016/j.molliq.2019.111081

Shahidi, F. & Ambigaipalan, P. (2015). Phenolics and polyphenolics in foods, beverages and spices: Antioxidant activity and health effects - A review. *Journal of Functional Foods*, *18*, 820–897. https://doi.org/10.1016/j.jff.2015.06.018

Shariful, M. I., Sepehr, T., Mehrali, M., Ang, B. C. & Amalina, M. A. (2018). Adsorption capability of heavy metals by chitosan/poly(ethylene oxide)/activated carbon electrospun nanofibrous membrane. *Journal of Applied Polymer Science*, *135*(7), 1–14. https://doi.org/10.1002/app.45851

Sharma, L., Sharma, H. K. & Saini, C. S. (2018). Edible films developed from

carboxylic acid cross-linked sesame protein isolate: barrier, mechanical, thermal, crystalline and morphological properties. *Journal of Food Science and Technology*, *55*(2), 532–539. https://doi.org/10.1007/s13197-017-2962-4

Sharma, R. A., Gescher, A. J. & Steward, W. P. (2005). Curcumin: The story so far. *European Journal of Cancer*, *41*(13), 1955–1968. https://doi.org/10.1016/j.ejca.2005.05.009

Sholichah, E., Purwono, B. & Nugroho, P. (2017). Improving Properties of Arrowroot Starch (Maranta arundinacea)/PVA Blend Films by Using Citric Acid as Cross-linking Agent. *IOP Conference Series: Earth and Environmental Science*, *101*(1). https://doi.org/10.1088/1755-1315/101/1/012018

Silva-Weiss, A., Bifani, V., Ihl, M., Sobral, P. J. A. & Gómez-Guillén, M. C. (2013). Structural properties of films and rheology of film-forming solutions based on chitosan and chitosan-starch blend enriched with murta leaf extract. *Food Hydrocolloids*, *31*(2), 458–466. https://doi.org/10.1016/j.foodhyd.2012.11.028

Silva, C. K. da, Mastrantonio, D. J. da S., Costa, J. A. V. & de Morais, M. G. (2019). Innovative pH sensors developed from ultrafine fibers containing açaí (Euterpe oleracea) extract. *Food Chemistry*, *294*(April), 397–404. https://doi.org/10.1016/j.foodchem.2019.05.059

Siriamornpun, S., Tangkhawanit, E. & Kaewseejan, N. (2016). Reducing retrogradation and lipid oxidation of normal and glutinous rice flours by adding mango peel powder. *Food Chemistry*, *201*, 160–167. https://doi.org/10.1016/j.foodchem.2016.01.094

Siripatrawan, U. & Harte, B. R. (2010). Physical properties and antioxidant activity of an active film from chitosan incorporated with green tea extract. *Food Hydrocolloids*, *24*(8), 770–775. https://doi.org/10.1016/j.foodhyd.2010.04.003

Solaberrieta, I., Jiménez, A., Cacciotti, I. & Garrigós, M. C. (2020). Encapsulation of bioactive compounds from aloe vera agrowastes in electrospun poly

(ethylene oxide) nanofibers. *Polymers*, *12*(6).
https://doi.org/10.3390/polym12061323

Soo, P. Y. & Sarbon, N. M. (2018). Preparation and characterization of edible
chicken skin gelatin film incorporated with rice flour. *Food Packaging and
Shelf Life*, *15*(January), 1–8. https://doi.org/10.1016/j.fpsl.2017.12.009

Soto-Cantú, C. D., Graciano-Verdugo, A. Z., Peralta, E., Islas-Rubio, A. R.,
González-Córdova, A., González-León, A. & Soto-Valdez, H. (2008). Release
of butylated hydroxytoluene from an active film packaging to asadero cheese
and its effect on oxidation and odor stability. *Journal of Dairy Science*, *91*(1),
11–19. https://doi.org/10.3168/jds.2007-0464

Soysal, Ç., Bozkurt, H., Dirican, E., Güçlü, M., Bozhüyük, E. D., Uslu, A. E. &
Kaya, S. (2015). Effect of antimicrobial packaging on physicochemical and
microbial quality of chicken drumsticks. *Food Control*, *54*, 294–299.
https://doi.org/10.1016/j.foodcont.2015.02.009

Sozer, N., Melama, L., Silbir, S., Rizzello, C. G., Flander, L. & Poutanen, K.
(2019). Lactic acid fermentation as a pre-treatment process for faba bean flour
and its effect on textural, structural and nutritional properties of protein-
enriched gluten-free faba bean breads. *Foods*, *8*(10).
https://doi.org/10.3390/foods8100431

Sreerama, Y. N., Sashikala, V. B. & Pratape, V. M. (2010). Variability in the
distribution of phenolic compounds in milled fractions of chickpea and horse
gram: Evaluation of their antioxidant properties. *Journal of Agricultural and
Food Chemistry*, *58*(14), 8322–8330. https://doi.org/10.1021/jf101335r

Stoll, L., Costa, T. M. H., Jablonski, A., Flôres, S. H. & de Oliveira Rios, A.
(2016). Microencapsulation of Anthocyanins with Different Wall Materials
and Its Application in Active Biodegradable Films. *Food and Bioprocess
Technology*, *9*(1), 172–181. https://doi.org/10.1007/s11947-015-1610-0

Su, L. C., Xie, Z., Zhang, Y., Nguyen, K. T. & Yang, J. (2014). Study on the
antimicrobial properties of citrate-based biodegradable polymers. *Frontiers in*

Bioengineering and Biotechnology, *2*(JUL), 1–9.
https://doi.org/10.3389/fbioe.2014.00023

Subtaweesin, C., Woraharn, W., Taokaew, S., Chiaoprakobkij, N., Sereemaspun, A. & Phisalaphong, M. (2018). Characteristics of curcumin-loaded bacterial cellulose films and anticancer properties against malignant melanoma skin cancer cells. *Applied Sciences*, *8*(7), 1–15.
https://doi.org/10.3390/app8071188

Sudhakar, Y. N., Sowmya, Selvakumar, M. & Bhat, D. K. (2012). Miscibility studies of chitosan and starch blends in buffer solution. *Journal of Macromolecular Science, Part A: Pure and Applied Chemistry*, *49*(12), 1099–1105. https://doi.org/10.1080/10601325.2012.728492

Sun, W., Liu, Y., Jia, L., Saldaña, M. D. A., Dong, T., Jin, Y. & Sun, W. (2021). A smart nanofibre sensor based on anthocyanin/poly-l-lactic acid for mutton freshness monitoring. *International Journal of Food Science and Technology*, *56*(1), 342–351. https://doi.org/10.1111/ijfs.14648

Suppakul, P., Miltz, J., Sonneveld, K. & Bigger, S. W. (2003). Antimicrobial properties of basil and its possible application in food packaging. *Journal of Agricultural and Food Chemistry*, *51*(11), 3197–3207.
https://doi.org/10.1021/jf021038t

Surendhiran, D., Li, C., Cui, H. & Lin, L. (2020). Fabrication of high stability active nanofibers encapsulated with pomegranate peel extract using chitosan/PEO for meat preservation. *Food Packaging and Shelf Life*, *23*(November 2019), 100439. https://doi.org/10.1016/j.fpsl.2019.100439

Suriyatem, R., Auras, R. A., Rachtanapun, C. & Rachtanapun, P. (2018). Biodegradable rice starch/carboxymethyl chitosan films with added propolis extract for potential use as active food packaging. *Polymers*, *10*(9).
https://doi.org/10.3390/polym10090954

Taghavi Kevij, H., Salami, M., Mohammadian, M. & Khodadadi, M. (2020). Fabrication and investigation of physicochemical, food simulant release, and

antioxidant properties of whey protein isolate-based films activated by loading with curcumin through the pH-driven method. *Food Hydrocolloids*, *108*(March), 106026. https://doi.org/10.1016/j.foodhyd.2020.106026

Tambawala, H., Batra, S., Shirapure, Y. & More, A. P. (2022). Curcumin- A Bio-based Precursor for Smart and Active Food Packaging Systems: A Review. In *Journal of Polymers and the Environment* (Vol. 30, Issue 6). Springer US. https://doi.org/10.1007/s10924-022-02372-x

Tanwar, R., Gupta, V., Kumar, P., Kumar, A., Singh, S. & Gaikwad, K. K. (2021). Development and characterization of PVA-starch incorporated with coconut shell extract and sepiolite clay as an antioxidant film for active food packaging applications. *International Journal of Biological Macromolecules*, *185*(May), 451–461. https://doi.org/10.1016/j.ijbiomac.2021.06.179

Tapia-Blácido, D., Sobral, P. J. & Menegalli, F. C. (2005). Development and characterization of biofilms based on Amaranth flour (Amaranthus caudatus). *Journal of Food Engineering*, *67*(1–2), 215–223. https://doi.org/10.1016/j.jfoodeng.2004.05.054

Tavares, L., Esparza Flores, E. E., Rodrigues, R. C., Hertz, P. F. & Noreña, C. P. Z. (2020). Effect of deacetylation degree of chitosan on rheological properties and physical chemical characteristics of genipin-crosslinked chitosan beads. *Food Hydrocolloids*, *106*(February). https://doi.org/10.1016/j.foodhyd.2020.105876

Thakore, I. M., Desai, S., Sarawade, B. D. & Devi, S. (2001). Studies on biodegradability, morphology and thermo-mechanical properties of LDPE/modified starch blends. *European Polymer Journal*, *37*(1), 151–160. https://doi.org/10.1016/S0014-3057(00)00086-0

Thakur, R., Pristijono, P., Scarlett, C. J., Bowyer, M., Singh, S. P. & Vuong, Q. V. (2019). Starch-based films: Major factors affecting their properties. *International Journal of Biological Macromolecules*, *132*, 1079–1089. https://doi.org/10.1016/j.ijbiomac.2019.03.190

Thavasi, V., Singh, G. & Ramakrishna, S. (2008). Electrospun nanofibers in energy and environmental applications. *Energy and Environmental Science*, *1*(2), 205–221. https://doi.org/10.1039/b809074m

Torres-Arreola, W., Soto-Valdez, H., Peralta, E., Cárdenas-López, J. L. & Ezquerra-Brauer, J. M. (2007). Effect of a low-density polyethylene film containing butylated hydroxytoluene on lipid oxidation and protein quality of sierra fish (Scomberomorus sierra) muscle during frozen storage. *Journal of Agricultural and Food Chemistry*, *55*(15), 6140–6146. https://doi.org/10.1021/jf070418h

Tsai, R. Y., Kuo, T. Y., Hung, S. C., Lin, C. M., Hsien, T. Y., Wang, D. M. & Hsieh, H. J. (2015). Use of gum arabic to improve the fabrication of chitosan-gelatin-based nanofibers for tissue engineering. *Carbohydrate Polymers*, *115*, 525–532. https://doi.org/10.1016/j.carbpol.2014.08.108

Ünalan, I. U., Korel, F. & Yemenicioğlu, A. (2011). Active packaging of ground beef patties by edible zein films incorporated with partially purified lysozyme and Na 2EDTA. *International Journal of Food Science and Technology*, *46*(6), 1289–1295. https://doi.org/10.1111/j.1365-2621.2011.02625.x

Uygun, E., Yildiz, E., Sumnu, G. & Sahin, S. (2020). Microwave Pretreatment for the Improvement of Physicochemical Properties of Carob Flour and Rice Starch–Based Electrospun Nanofilms. *Food and Bioprocess Technology*, *13*(5), 838–850. https://doi.org/10.1007/s11947-020-02440-x

Valderrama Solano, A. C. & Rojas de Gante, C. (2014). Development of biodegradable films based on blue corn flour with potential applications in food packaging. Effects of plasticizers on mechanical, thermal, and microstructural properties of flour films. *Journal of Cereal Science*, *60*(1), 60–66. https://doi.org/10.1016/j.jcs.2014.01.015

Valizadeh, S., Naseri, M., Babaei, S., Hosseini, S. M. H. & Imani, A. (2019). Development of bioactive composite films from chitosan and carboxymethyl cellulose using glutaraldehyde, cinnamon essential oil and oleic acid.

International Journal of Biological Macromolecules, *134*, 604–612.
https://doi.org/10.1016/j.ijbiomac.2019.05.071

Vargas, C. G., Costa, T. M. H., Rios, A. de O. & Flôres, S. H. (2017). Comparative study on the properties of films based on red rice (Oryza glaberrima) flour and starch. *Food Hydrocolloids*, *65*, 96–106.
https://doi.org/10.1016/j.foodhyd.2016.11.006

Vasconcelos, L. A., Reis, L. C. B., Dias, Ê. R., Camilloto, G. P. & Branco, A. (2021). Characterization of a flavonol-rich antioxidant fraction from Spondias purpurea L. pulp and the effect of its incorporation on cellulose acetate-based film. *Journal of the Science of Food and Agriculture*, *101*(8), 3270–3279.
https://doi.org/10.1002/jsfa.10956

Vega-Lugo, A. C. & Lim, L. T. (2012). Effects of poly(ethylene oxide) and pH on the electrospinning of whey protein isolate. *Journal of Polymer Science, Part B: Polymer Physics*, *50*(16), 1188–1197. https://doi.org/10.1002/polb.23106

Wang, H., Hao, L., Wang, P., Chen, M., Jiang, S. & Jiang, S. (2017). Release kinetics and antibacterial activity of curcumin loaded zein fibers. *Food Hydrocolloids*, *63*, 437–446. https://doi.org/10.1016/j.foodhyd.2016.09.028

Wang, J. & Jiang, Z. (2022). Synthesis, characterisation, antioxidant and antibacterial properties of p-hydroxybenzoic acid-grafted chitosan conjugates. *International Journal of Food Science and Technology*, *57*(2), 1283–1290.
https://doi.org/10.1111/ijfs.15518

Wang, L., Mu, R. J., Li, Y., Lin, L., Lin, Z. & Pang, J. (2019a). Characterization and antibacterial activity evaluation of curcumin loaded konjac glucomannan and zein nanofibril films. *LWT*, *113*(May), 108293.
https://doi.org/10.1016/j.lwt.2019.108293

Wang, L., Mu, R. J., Li, Y., Lin, L., Lin, Z. & Pang, J. (2019b). Characterization and antibacterial activity evaluation of curcumin loaded konjac glucomannan and zein nanofibril films. *Lwt*, *113*(February), 108293.
https://doi.org/10.1016/j.lwt.2019.108293

Wang, P., Li, Y., Zhang, C., Que, F., Weiss, J. & Zhang, H. (2020). Characterization and antioxidant activity of trilayer gelatin/dextran-propyl gallate/gelatin films: Electrospinning versus solvent casting. *Lwt*, *128*(March), 109536. https://doi.org/10.1016/j.lwt.2020.109536

Wen, L., Liang, Y., Lin, Z., Xie, D., Zheng, Z., Xu, C. & Lin, B. (2021). Design of multifunctional food packaging films based on carboxymethyl chitosan/polyvinyl alcohol crosslinked network by using citric acid as crosslinker. *Polymer*, *230*(July), 124048. https://doi.org/10.1016/j.polymer.2021.124048

Wilhelm, S. & Wolfbeis, O. S. (2011). Irreversible sensing of oxygen ingress. *Sensors and Actuators, B: Chemical*, *153*(1), 199–204. https://doi.org/10.1016/j.snb.2010.10.037

Wu, C., Sun, J., Chen, M., Ge, Y., Ma, J., Hu, Y., Pang, J. & Yan, Z. (2019). Effect of oxidized chitin nanocrystals and curcumin into chitosan films for seafood freshness monitoring. *Food Hydrocolloids*, *95*(December 2018), 308–317. https://doi.org/10.1016/j.foodhyd.2019.04.047

Wu, H., Lei, Y., Lu, J., Zhu, R., Xiao, D., Jiao, C., Xia, R., Zhang, Z., Shen, G., Liu, Y., Li, S. & Li, M. (2019a). Effect of citric acid induced crosslinking on the structure and properties of potato starch/chitosan composite films. *Food Hydrocolloids*, *97*(July), 105208. https://doi.org/10.1016/j.foodhyd.2019.105208

Wu, H., Lei, Y., Lu, J., Zhu, R., Xiao, D., Jiao, C., Xia, R., Zhang, Z., Shen, G., Liu, Y., Li, S. & Li, M. (2019b). Effect of citric acid induced crosslinking on the structure and properties of potato starch/chitosan composite films. *Food Hydrocolloids*, *97*(March), 105208. https://doi.org/10.1016/j.foodhyd.2019.105208

Wu, J., Sun, X., Guo, X., Ji, M., Wang, J. & Cheng, C. (2021). Physicochemical , Antioxidant , In Vitro Release , and Heat Sealing Properties of Fish Gelatin Films Incorporated with β -Cyclodextrin / Curcumin Complexes for Apple

Juice Preservation. *Food and Bioprocess Technology*, *11*(2018), 447–461.

Wu, L. T., Tsai, I. L., Ho, Y. C., Hang, Y. H., Lin, C., Tsai, M. L. & Mi, F. L. (2021). Active and intelligent gellan gum-based packaging films for controlling anthocyanins release and monitoring food freshness. *Carbohydrate Polymers*, *254*(October 2020), 117410. https://doi.org/10.1016/j.carbpol.2020.117410

Wu, S., Qin, X. & Li, M. (2014). The structure and properties of cellulose acetate materials: A comparative study on electrospun membranes and casted films. *Journal of Industrial Textiles*, *44*(1), 85–98. https://doi.org/10.1177/1528083713477443

Xie, J. & Wang, C. H. (2006). Electrospun micro- and nanofibers for sustained delivery of paclitaxel to treat C6 glioma in vitro. *Pharmaceutical Research*, *23*(8), 1817–1826. https://doi.org/10.1007/s11095-006-9036-z

Xie, Y., Yan, M., Yuan, S., Sun, S. & Huo, Q. (2013). Effect of microwave treatment on the physicochemical properties of potato starch granules. *Chemistry Central Journal*, *7*(1), 2–7. https://doi.org/10.1186/1752-153X-7-113

Xu, Y., Liu, X., Jiang, Q., Yu, D., Xu, Y., Wang, B. & Xia, W. (2021). Development and properties of bacterial cellulose, curcumin, and chitosan composite biodegradable films for active packaging materials. *Carbohydrate Polymers*, *260*(November 2020), 117778. https://doi.org/10.1016/j.carbpol.2021.117778

Yang, Y., Shi, Y., Cao, X., Liu, Q., Wang, H. & Kong, B. (2021). Preparation and functional properties of poly(vinyl alcohol)/ethyl cellulose/tea polyphenol electrospun nanofibrous films for active packaging material. *Food Control*, *130*(May), 108331. https://doi.org/10.1016/j.foodcont.2021.108331

Yang, Z., Peng, H., Wang, W. & Liu, T. (2008). Water Vapor Absorption and Permeability of Films Based on Chitosan and Sodium Caseinate. *Journal of Applied Polymer Science*, *111*(5), 2777–2784. https://doi.org/10.1002/app

Yang, Z., Peng, H., Wang, W. & Liu, T. (2010). Crystallization behavior of poly(ε-caprolactone)/layered double hydroxide nanocomposites. *Journal of Applied Polymer Science*, *116*(5), 2658–2667. https://doi.org/10.1002/app

Yao, F., Gao, Y., Chen, F. & Du, Y. (2022). Preparation and properties of electrospun peanut protein isolate/poly-L-lactic acid nanofibers. *Lwt*, *153*(August 2021), 112418. https://doi.org/10.1016/j.lwt.2021.112418

Yao, S., Wang, B.-J. & Weng, Y.-M. (2022). Preparation and characterization of mung bean starch edible films using citric acid as cross-linking agent. *Food Packaging and Shelf Life*, *32*(March), 100845. https://doi.org/10.1016/j.fpsl.2022.100845

Yao, X., Qin, Y., Zhang, M., Zhang, J., Qian, C. & Liu, J. (2021). Development of active and smart packaging films based on starch, polyvinyl alcohol and betacyanins from different plant sources. *International Journal of Biological Macromolecules*, *183*, 358–368. https://doi.org/10.1016/j.ijbiomac.2021.04.152

Yeamsuksawat, T. & Liang, J. (2019). Characterization and release kinetic of crosslinked chitosan film incorporated with α-tocopherol. *Food Packaging and Shelf Life*, *22*(August), 100415. https://doi.org/10.1016/j.fpsl.2019.100415

Yildirim, S., Röcker, B., Pettersen, M. K., Nilsen-Nygaard, J., Ayhan, Z., Rutkaite, R., Radusin, T., Suminska, P., Marcos, B. & Coma, V. (2018). Active Packaging Applications for Food. *Comprehensive Reviews in Food Science and Food Safety*, *17*(1), 165–199. https://doi.org/10.1111/1541-4337.12322

Yildiz, E., Bayram, I., Sumnu, G., Sahin, S. & Ibis, O. I. (2021). Development of pea flour based active films produced through different homogenization methods and their effects on lipid oxidation. *Food Hydrocolloids*, *111*(August 2020), 106238. https://doi.org/10.1016/j.foodhyd.2020.106238

Yildiz, E., Ilhan, E., Kahyaoglu, L. N., Sumnu, G. & Oztop, M. H. (2021). The effects of crosslinking agents on faba bean flour–chitosan-curcumin films and

their characterization. *Legume Science*, *August*, 1–13. https://doi.org/10.1002/leg3.121

Yildiz, E., İlhan, E., Kahyaoglu, L. N., Sumnu, G. & Oztop, M. H. (2021). The effects of crosslinking agents on faba bean flour–chitosan- curcumin films and their characterization. *Legume Science*, 1–13.

Yong, H. & Liu, J. (2020). Recent advances in the preparation, physical and functional properties, and applications of anthocyanins-based active and intelligent packaging films. *Food Packaging and Shelf Life*, *26*(July), 100550. https://doi.org/10.1016/j.fpsl.2020.100550

Yoon, S. Do, Chough, S. H. & Park, H. R. (2006). Properties of starch-based blend films using citric acid as additive. II. *Journal of Applied Polymer Science*, *100*(3), 2554–2560. https://doi.org/10.1002/app.23783

Younes, I. & Rinaudo, M. (2015). Chitin and chitosan preparation from marine sources. Structure, properties and applications. *Marine Drugs*, *13*(3), 1133–1174. https://doi.org/10.3390/md13031133

Yun, D., Cai, H., Liu, Y., Xiao, L., Song, J. & Liu, J. (2019). Development of active and intelligent films based on cassava starch and Chinese bayberry (: Myrica rubra Sieb. et Zucc.) anthocyanins. *RSC Advances*, *9*(53), 30905–30916. https://doi.org/10.1039/c9ra06628d

Zadeh, E. M., O'Keefe, S. F. & Kim, Y. T. (2018). Utilization of Lignin in Biopolymeric Packaging Films. *ACS Omega*, *3*(7), 7388–7398. https://doi.org/10.1021/acsomega.7b01341

Zeng, P., Chen, X., Qin, Y. R., Zhang, Y. H., Wang, X. P., Wang, J. Y., Ning, Z. X., Ruan, Q. J. & Zhang, Y. S. (2019). Preparation and characterization of a novel colorimetric indicator film based on gelatin/polyvinyl alcohol incorporating mulberry anthocyanin extracts for monitoring fish freshness. *Food Research International*, *126*(August), 108604. https://doi.org/10.1016/j.foodres.2019.108604

Zhai, X., Wang, X., Zhang, J., Yang, Z., Sun, Y., Li, Z., Huang, X., Holmes, M., Gong, Y., Povey, M., Shi, J. & Zou, X. (2020). Extruded low density polyethylene-curcumin film : A hydrophobic ammonia sensor for intelligent food packaging. *Food Packaging and Shelf Life*, *26*(March), 100595. https://doi.org/10.1016/j.fpsl.2020.100595

Zhang, C., Li, Y., Wang, P. & Zhang, H. (2020). Electrospinning of nanofibers: Potentials and perspectives for active food packaging. *Comprehensive Reviews in Food Science and Food Safety*, *19*(2), 479–502. https://doi.org/10.1111/1541-4337.12536

Zhang, J., Huang, X., Zou, X., Shi, J., Zhai, X., Liu, L., Li, Z., Holmes, M., Gong, Y., Povey, M. & Xiao, J. (2021). A visual indicator based on curcumin with high stability for monitoring the freshness of freshwater shrimp, Macrobrachium rosenbergii. *Journal of Food Engineering*, *292*(May 2020), 110290. https://doi.org/10.1016/j.jfoodeng.2020.110290

Zhang, J., Zou, X., Zhai, X., Huang, X. W., Jiang, C. & Holmes, M. (2019). Preparation of an intelligent pH film based on biodegradable polymers and roselle anthocyanins for monitoring pork freshness. *Food Chemistry*, *272*(April 2018), 306–312. https://doi.org/10.1016/j.foodchem.2018.08.041

Zhang, L., Liu, Z., Wang, X., Dong, S., Sun, Y. & Zhao, Z. (2019). The properties of chitosan/zein blend film and effect of film on quality of mushroom (Agaricus bisporus). *Postharvest Biology and Technology*, *155*(November 2018), 47–56. https://doi.org/10.1016/j.postharvbio.2019.05.013

Zhang, Q., Wang, X., Fu, J., Liu, R., He, H., Ma, J., Yu, M., Ramakrishna, S. & Long, Y. (2018). Electrospinning of ultrafine conducting polymer composite nanofibers with diameter less than 70 nm as high sensitive gas sensor. *Materials*, *11*(9). https://doi.org/10.3390/ma11091744

Zhang, W., Jiang, Q., Shen, J., Gao, P., Yu, D. & Xu, Y. (2022). The role of organic acid structures in changes of physicochemical and antioxidant properties of crosslinked chitosan films. *Food Packaging and Shelf Life*,

31(October 2021), 100792. https://doi.org/10.1016/j.fpsl.2021.100792

Zhang, Xiahong, Lu, S. & Chen, X. (2014). A visual pH sensing film using natural dyes from Bauhinia blakeana Dunn. *Sensors and Actuators, B: Chemical*, *198*, 268–273. https://doi.org/10.1016/j.snb.2014.02.094

Zhang, Xin, Liu, Y., Yong, H., Qin, Y., Liu, J. & Liu, J. (2019). Development of multifunctional food packaging films based on chitosan, TiO 2 nanoparticles and anthocyanin-rich black plum peel extract. *Food Hydrocolloids*, *94*(February), 80–92. https://doi.org/10.1016/j.foodhyd.2019.03.009

Zhao, B., Sun, S., Lin, H., Chen, L., Qin, S., Wu, W., Zheng, B. & Guo, Z. (2019). Physicochemical properties and digestion of the lotus seed starch-green tea polyphenol complex under ultrasound-microwave synergistic interaction. *Ultrasonics Sonochemistry*, *52*(July 2018), 50–61. https://doi.org/10.1016/j.ultsonch.2018.11.001

Zheng, L. Y. & Zhu, J. F. (2003). Study on antimicrobial activity of chitosan with different molecular weights. *Carbohydrate Polymers*, *54*(4), 527–530. https://doi.org/10.1016/j.carbpol.2003.07.009

Zhong, Y., Song, X. & Li, Y. (2011). Antimicrobial, physical and mechanical properties of kudzu starch-chitosan composite films as a function of acid solvent types. *Carbohydrate Polymers*, *84*(1), 335–342. https://doi.org/10.1016/j.carbpol.2010.11.041

Zhou, C., Abdel-Samie, M. A., Li, C., Cui, H. & Lin, L. (2020). Active packaging based on swim bladder gelatin/galangal root oil nanofibers: Preparation, properties and antibacterial application. *Food Packaging and Shelf Life*, *26*(July), 100586. https://doi.org/10.1016/j.fpsl.2020.100586

Zhou, J., Zhang, J., Ma, Y. & Tong, J. (2008). Surface photo-crosslinking of corn starch sheets. *Carbohydrate Polymers*, *74*(3), 405–410. https://doi.org/10.1016/j.carbpol.2008.03.006

Zia, J., Paul, U. C., Heredia-Guerrero, J. A., Athanassiou, A. & Fragouli, D.

(2019). Low-density polyethylene/curcumin melt extruded composites with enhanced water vapor barrier and antioxidant properties for active food packaging. *Polymer*, *175*(May), 137–145. https://doi.org/10.1016/j.polymer.2019.05.012

APPENDICES

A. ANOVA TABLES

Table 3.1 One way Analysis of Variance (ANOVA) and Tukey's comparison test for conductivity values of chitosan/PEO solutions

Method

Null hypothesis	All means are equal
Alternative hypothesis	Not all means are equal
Significance level	$\alpha = 0{,}05$

Equal variances were assumed for the analysis.

Factor Information

Factor	Levels	Values
sample	3	1.5/8.5; 2.0/8.0; 2.5/7.5

Analysis of Variance

Source	DF	Adj SS	Adj MS	F-Value	P-Value
sample	2	1178,00	589,000	60,93	0,000
Error	6	58,00	9,667		
Total	8	1236,00			

Model Summary

S	R-sq	R-sq(adj)	R-sq(pred)
3,10913	95,31%	93,74%	89,44%

Means

sample	N	Mean	StDev	95% CI
1.5/8.5	3	283,00	2,65	(278,61; 287,39)
2.0/8.0	3	296,00	4,58	(291,61; 300,39)
2.5/7.5	3	311,000	1,000	(306,608; 315,392)

Pooled StDev = 3,10913

Tukey Pairwise Comparisons

Grouping Information Using the Tukey Method and 95% Confidence

sample	N	Mean	Grouping		
2.5/7.5	3	311,000	A		
2.0/8.0	3	296,00		B	
1.5/8.5	3	283,00			C

Means that do not share a letter are significantly different.

Table 3.1 One way Analysis of Variance (ANOVA) and Tukey's comparison test for consistency index values of chitosan/PEO solutions

Method

Null hypothesis	All means are equal
Alternative hypothesis	Not all means are equal
Significance level	$\alpha = 0{,}05$

Equal variances were assumed for the analysis.

Factor Information

Factor	Levels Values
samples	3 1.5-8.5; 2.0-8.0; 2.5-7.5

Analysis of Variance

Source	DF	Adj SS	Adj MS	F-Value	P-Value
samples	2	0,009248	0,004624	3,83	0,149
Error	3	0,003622	0,001207		
Total	5	0,012869			

Model Summary

S	R-sq	R-sq(adj)	R-sq(pred)
0,0347444	71,86%	53,10%	0,00%

Means

samples	N	Mean	StDev	95% CI
1.5-8.5	2	1,2656	0,0229	(1,1874; 1,3438)
2.0-8.0	2	1,1774	0,0363	(1,0992; 1,2556)
2.5-7.5	2	1,1883	0,0422	(1,1101; 1,2665)

Pooled StDev = 0,0347444

Tukey Pairwise Comparisons

Grouping Information Using the Tukey Method and 95% Confidence

samples	N	Mean	Grouping
1.5-8.5	2	1,2656	A
2.5-7.5	2	1,1883	A
2.0-8.0	2	1,1774	A

Means that do not share a letter are significantly different.

Table 3.1 One way Analysis of Variance (ANOVA) and Tukey's comparison test for flow behavior index values of chitosan/PEO solutions

Method

Null hypothesis	All means are equal
Alternative hypothesis	Not all means are equal
Significance level	$\alpha = 0{,}05$

Equal variances were assumed for the analysis.

Factor Information

Factor	Levels	Values
samples	3	1.5-8.5; 2.0-8.0; 2.5-7.5

Analysis of Variance

Source	DF	Adj SS	Adj MS	F-Value	P-Value
samples	2	0,000796	0,000398	0,59	0,608
Error	3	0,002025	0,000675		
Total	5	0,002821			

Model Summary

S	R-sq	R-sq(adj)	R-sq(pred)
0,0259782	28,22%	0,00%	0,00%

Means

samples	N	Mean	StDev	95% CI
1.5-8.5	2	0,8919	0,0392	(0,8334; 0,9504)
2.0-8.0	2	0,91850	0,00976	(0,86004; 0,97696)
2.5-7.5	2	0,9133	0,0199	(0,8549; 0,9718)

Pooled StDev = 0,0259782

Tukey Pairwise Comparisons

Grouping Information Using the Tukey Method and 95% Confidence

samples	N	Mean	Grouping
2.0-8.0	2	0,91850	A
2.5-7.5	2	0,9133	A
1.5-8.5	2	0,8919	A

Means that do not share a letter are significantly different.

Table 3.1 One way Analysis of Variance (ANOVA) and Tukey's comparison test for fiber sizes chitosan/PEO fibers

Method

Null hypothesis	All means are equal
Alternative hypothesis	Not all means are equal
Significance level	$\alpha = 0,05$

Equal variances were assumed for the analysis.

Factor Information

Factor	Levels	Values
samples	3	7.5-2.5; 8.0-2.0; 8.5-1.5

Analysis of Variance

Source	DF	Adj SS	Adj MS	F-Value	P-Value
samples	2	155123	77561,5	80,38	0,000
Error	295	284660	964,9		
Total	297	439783			

Model Summary

	S	R-sq	R-sq(adj)	R-sq(pred)
	31,0636	35,27%	34,83%	33,95%

Means

samples	N	Mean	StDev	95% CI
7.5-2.5	99	283,18	27,98	(277,04; 289,33)
8.0-2.0	100	304,44	28,90	(298,33; 310,55)
8.5-1.5	99	338,66	35,75	(332,51; 344,80)

Pooled StDev = 31,0636

Tukey Pairwise Comparisons

Grouping Information Using the Tukey Method and 95% Confidence

samples	N	Mean	Grouping		
8.5-1.5	99	338,66	A		
8.0-2.0	100	304,44		B	
7.5-2.5	99	283,18			C

Means that do not share a letter are significantly different.

Table 3.2 One way Analysis of Variance (ANOVA) and Tukey's comparison test for WVP of chitosan/PEO fibers

Method

Null hypothesis	All means are equal
Alternative hypothesis	Not all means are equal
Significance level	$\alpha = 0,05$

Equal variances were assumed for the analysis.

Factor Information

Factor	Levels	Values
samples	3	1.5-8.5; 2.0-8.0; 2.5-7.5

Analysis of Variance

Source	DF	Adj SS	Adj MS	F-Value	P-Value
samples	2	55,2519	27,6259	109,99	0,002
Error	3	0,7535	0,2512		
Total	5	56,0054			

Model Summary

	S	R-sq	R-sq(adj)	R-sq(pred)
	0,501166	98,65%	97,76%	94,62%

Means

samples	N	Mean	StDev	95% CI
1.5-8.5	2	14,280	0,581	(13,152; 15,408)
2.0-8.0	2	13,0326	0,1298	(11,9048; 14,1603)
2.5-7.5	2	7,310	0,632	(6,182; 8,438)

Pooled StDev = 0,501166

Tukey Pairwise Comparisons

Grouping Information Using the Tukey Method and 95% Confidence

samples	N	Mean	Grouping	
1.5-8.5	2	14,280	A	
2.0-8.0	2	13,0326	A	
2.5-7.5	2	7,310		B

Means that do not share a letter are significantly different.

Table 3.3 One way Analysis of Variance (ANOVA) and Tukey's comparison test for tensile strength of chitosan/PEO fibers

Method

Null hypothesis	All means are equal
Alternative hypothesis	Not all means are equal
Significance level	$\alpha = 0,05$

Equal variances were assumed for the analysis.

Factor Information

Factor	Levels	Values
samples	3	1.5-8.5; 2.0-8.0; 2.5-7.5

Analysis of Variance

Source	DF	Adj SS	Adj MS	F-Value	P-Value
samples	2	5,6297	2,81484	35,53	0,008
Error	3	0,2376	0,07921		
Total	5	5,8673			

Model Summary

S	R-sq	R-sq(adj)	R-sq(pred)
0,281451	95,95%	93,25%	83,80%

Means

samples	N	Mean	StDev	95% CI
1.5-8.5	2	2,426	0,480	(1,793; 3,059)
2.0-8.0	2	4,1658	0,0342	(3,5325; 4,7992)
2.5-7.5	2	4,6932	0,0804	(4,0598; 5,3265)

Pooled StDev = 0,281451

Tukey Pairwise Comparisons

Grouping Information Using the Tukey Method and 95% Confidence

samples	N	Mean	Grouping
2.5-7.5	2	4,6932	A
2.0-8.0	2	4,1658	A
1.5-8.5	2	2,426	B

Means that do not share a letter are significantly different.

Table 3.3 One way Analysis of Variance (ANOVA) and Tukey's comparison test for tensile strength of chitosan/PEO fibers

Method

Null hypothesis	All means are equal
Alternative hypothesis	Not all means are equal
Significance level	$\alpha = 0,05$

Equal variances were assumed for the analysis.

Factor Information

Factor	Levels	Values
samples	3	1.5-8.5; 2.0-8.0; 2.5-7.5

Analysis of Variance

Source	DF	Adj SS	Adj MS	F-Value	P-Value
samples	2	187,83	93,916	9,85	0,048
Error	3	28,60	9,533		
Total	5	216,43			

Model Summary

S	R-sq	R-sq(adj)	R-sq(pred)
3,08758	86,79%	77,98%	47,14%

Means

samples	N	Mean	StDev	95% CI
1.5-8.5	2	17,881	1,370	(10,933; 24,829)
2.0-8.0	2	27,95	5,07	(21,00; 34,90)
2.5-7.5	2	14,863	0,991	(7,915; 21,811)

Pooled StDev = 3,08758

Tukey Pairwise Comparisons

Grouping Information Using the Tukey Method and 95% Confidence

samples	N	Mean	Grouping	
2.0-8.0	2	27,95	A	
1.5-8.5	2	17,881	A	B
2.5-7.5	2	14,863		B

Means that do not share a letter are significantly different.

Table 3.5 One way Analysis of Variance (ANOVA) and Tukey's comparison test for consistency index values of chickpea flour/PEO solutions

Method

Null hypothesis	All means are equal
Alternative hypothesis	Not all means are equal
Significance level	$\alpha = 0,05$

Equal variances were assumed for the analysis.

Factor Information

Factor	Levels	Values
samples	4	C/CON; C/MW; CUR/CON; CUR/MW

Analysis of Variance

Source	DF	Adj SS	Adj MS	F-Value	P-Value
samples	3	0,214925	0,071642	139,86	0,000
Error	4	0,002049	0,000512		
Total	7	0,216974			

Model Summary

S	R-sq	R-sq(adj)	R-sq(pred)
0,0226329	99,06%	98,35%	96,22%

Means

samples	N	Mean	StDev	95% CI
C/CON	2	0,60000	0,00141	(0,55557; 0,64443)
C/MW	2	0,9100	0,0212	(0,8656; 0,9544)
CUR/CON	2	0,45750	0,00919	(0,41307; 0,50193)
CUR/MW	2	0,6325	0,0389	(0,5881; 0,6769)

Pooled StDev = 0,0226329

Grouping Information Using the Tukey Method and 95% Confidence

samples	N	Mean	Grouping		
C/MW	2	0,9100	A		
CUR/MW	2	0,6325		B	
C/CON	2	0,60000		B	
CUR/CON	2	0,45750			C

Means that do not share a letter are significantly different.

Table 3.5 One way Analysis of Variance (ANOVA) and Tukey's comparison test for flow behavior index values of chickpea flour/PEO solutions

Method

Null hypothesis	All means are equal
Alternative hypothesis	Not all means are equal
Significance level	$\alpha = 0,05$

Equal variances were assumed for the analysis.

Factor Information

Factor	Levels	Values
samples	4	C/CON; C/MW; CUR/CON; CUR/MW

Analysis of Variance

Source	DF	Adj SS	Adj MS	F-Value	P-Value
samples	3	0,004605	0,001535	6,37	0,053
Error	4	0,000964	0,000241		
Total	7	0,005570			

Model Summary

S	R-sq	R-sq(adj)	R-sq(pred)
0,0155265	82,69%	69,70%	30,75%

Means

samples	N	Mean	StDev	95% CI
C/CON	2	0,8943	0,0228	(0,8638; 0,9248)
C/MW	2	0,85775	0,00629	(0,82727; 0,88823)
CUR/CON	2	0,83690	0,01315	(0,80642; 0,86738)
CUR/MW	2	0,8916	0,0153	(0,8611; 0,9221)

Pooled StDev = 0,0155265

Tukey Pairwise Comparisons

Grouping Information Using the Tukey Method and 95% Confidence

samples	N	Mean	Grouping
C/CON	2	0,8943	A
CUR/MW	2	0,8916	A
C/MW	2	0,85775	A
CUR/CON	2	0,83690	A

Means that do not share a letter are significantly different.

Table 3.5 One way Analysis of Variance (ANOVA) and Tukey's comparison test for conductivity values of chickpea flour/PEO solutions

Method

Null hypothesis	All means are equal
Alternative hypothesis	Not all means are equal
Significance level	$\alpha = 0,05$

Equal variances were assumed for the analysis.

Factor Information

Factor	Levels	Values
samples	4	C/CON; CUR/CON; C/MW; CUR/MW

Analysis of Variance

Source	DF	Adj SS	Adj MS	F-Value	P-Value
samples	3	249547	83182,3	4211,76	0,000
Error	4	79	19,8		
Total	7	249626			

Model Summary

S	R-sq	R-sq(adj)	R-sq(pred)
4,44410	99,97%	99,94%	99,87%

Means

samples	N	Mean	StDev	95% CI
C/MW	2	636,00	2,83	(627,28; 644,72)
CUR/MW	2	294,50	3,54	(285,78; 303,22)
CUR/CON	2	323,50	6,36	(314,78; 332,22)
C/CON	2	684,00	4,24	(675,28; 692,72)

Pooled StDev = 4,44410

Tukey Pairwise Comparisons

Grouping Information Using the Tukey Method and 95% Confidence

samples	N	Mean	Grouping			
C/CON	2	684,00	A			
C/MW	2	636,00		B		
CUR/CON	2	323,50			C	
CUR/MW	2	294,50				D

Means that do not share a letter are significantly different.

Table 3.5 One way Analysis of Variance (ANOVA) and Tukey's comparison test for average fiber size of chickpea flour/PEO fibers

Method

Null hypothesis	All means are equal
Alternative hypothesis	Not all means are equal
Significance level	$\alpha = 0,05$
Rows unused	105

Equal variances were assumed for the analysis.

Factor Information

Factor	Levels	Values
sample	4	C/CON; CUR/CON; C/MW; CUR/MW

Analysis of Variance

Source	DF	Adj SS	Adj MS	F-Value	P-Value
sample	3	330297	110099	30,24	0,000
Error	421	1532674	3641		
Total	424	1862972			

Model Summary

S	R-sq	R-sq(adj)	R-sq(pred)
60,3370	17,73%	17,14%	16,16%

Means

sample	N	Mean	StDev	95% CI
C/CON	98	273,81	66,20	(261,83; 285,79)
CUR/CON	113	332,11	65,97	(320,95; 343,26)
C/MW	105	258,71	54,55	(247,14; 270,29)
CUR/MW	109	285,30	53,64	(273,94; 296,66)

Pooled StDev = 60,3370

Tukey Pairwise Comparisons

Grouping Information Using the Tukey Method and 95% Confidence

sample	N	Mean	Grouping		
CUR/CON	113	332,11	A		
CUR/MW	109	285,30		B	
C/CON	98	273,81		B	C
C/MW	105	258,71			C

Means that do not share a letter are significantly different.

Table 3.6 One way Analysis of Variance (ANOVA) and Tukey's comparison test for WVP of chickpea flour/PEO fibers

Method

Null hypothesis	All means are equal
Alternative hypothesis	Not all means are equal
Significance level	$\alpha = 0,05$

Equal variances were assumed for the analysis.

Factor Information

Factor	Levels	Values
samples	4	C/CON; C/MW; CUR/CON; CUR/MW

Analysis of Variance

Source	DF	Adj SS	Adj MS	F-Value	P-Value
samples	3	0,5939	0,19798	2,07	0,247
Error	4	0,3823	0,09558		
Total	7	0,9763			

Model Summary

S	R-sq	R-sq(adj)	R-sq(pred)
0,309162	60,84%	31,47%	0,00%

Means

samples	N	Mean	StDev	95% CI
C/CON	2	1,543	0,271	(0,936; 2,150)
C/MW	2	1,8959	0,0573	(1,2890; 2,5029)
CUR/CON	2	1,128	0,370	(0,521; 1,735)
CUR/MW	2	1,477	0,410	(0,870; 2,083)

Pooled StDev = 0,309162

Tukey Pairwise Comparisons

Grouping Information Using the Tukey Method and 95% Confidence

samples	N	Mean	Grouping
C/MW	2	1,8959	A
C/CON	2	1,543	A
CUR/MW	2	1,477	A
CUR/CON	2	1,128	A

Means that do not share a letter are significantly different.

Table 3.6 One way Analysis of Variance (ANOVA) and Tukey's comparison test for tensile strength of chickpea flour/PEO fibers

Factor Information

Factor	Levels	Values
sample	4	C/CON; C/MW; CUR/CON; CUR/MW

Analysis of Variance

Source	DF	Adj SS	Adj MS	F-Value	P-Value
sample	3	3,29258	1,09753	176,55	0,000
Error	4	0,02487	0,00622		
Total	7	3,31744			

Model Summary

S	R-sq	R-sq(adj)	R-sq(pred)
0,0788456	99,25%	98,69%	97,00%

Means

sample	N	Mean	StDev	95% CI
C/CON	2	0,8865	0,0870	(0,7317; 1,0413)
C/MW	2	2,0250	0,1061	(1,8702; 2,1798)
CUR/CON	2	0,38900	0,00141	(0,23421; 0,54379)
CUR/MW	2	0,5350	0,0778	(0,3802; 0,6898)

Pooled StDev = 0,0788456

Tukey Pairwise Comparisons

Grouping Information Using the Tukey Method and 95% Confidence

sample	N	Mean	Grouping		
C/MW	2	2,0250	A		
C/CON	2	0,8865		B	
CUR/MW	2	0,5350			C
CUR/CON	2	0,38900			C

Means that do not share a letter are significantly different.

Table 3.6 One way Analysis of Variance (ANOVA) and Tukey's comparison test for EAB values of chickpea flour/PEO fibers

Method

Null hypothesis	All means are equal
Alternative hypothesis	Not all means are equal
Significance level	$\alpha = 0,05$

Equal variances were assumed for the analysis.

Factor Information

Factor	Levels	Values
sample	4	C/CON; C/MW; CUR/CON; CUR/MW

Analysis of Variance

Source	DF	Adj SS	Adj MS	F-Value	P-Value
sample	3	256,30	85,434	8,57	0,032
Error	4	39,87	9,967		
Total	7	296,17			

Model Summary

S	R-sq	R-sq(adj)	R-sq(pred)
3,15706	86,54%	76,44%	46,16%

Means

sample	N	Mean	StDev	95% CI
C/CON	2	39,531	0,433	(33,333; 45,729)
C/MW	2	47,02	4,53	(40,83; 53,22)
CUR/CON	2	33,63	4,25	(27,43; 39,83)
CUR/MW	2	32,942	1,030	(26,743; 39,140)

Pooled StDev = 3,15706

Tukey Pairwise Comparisons

Grouping Information Using the Tukey Method and 95% Confidence

sample	N	Mean	Grouping	
C/MW	2	47,02	A	
C/CON	2	39,531	A	B
CUR/CON	2	33,63		B
CUR/MW	2	32,942		B

Means that do not share a letter are significantly different.

Table 3.7 One way Analysis of Variance (ANOVA) and Tukey's comparison test for Tm values of chickpea flour/PEO fibers

Method

Null hypothesis	All means are equal
Alternative hypothesis	Not all means are equal
Significance level	$\alpha = 0,05$

Equal variances were assumed for the analysis.

Factor Information

Factor	Levels	Values
samples	4	C/CON; C/MW; CUR/CON; CUR/MW

Analysis of Variance

Source	DF	Adj SS	Adj MS	F-Value	P-Value
samples	3	8,0332	2,6777	11,93	0,018
Error	4	0,8978	0,2244		
Total	7	8,9310			

Model Summary

S	R-sq	R-sq(adj)	R-sq(pred)
0,473748	89,95%	82,41%	59,79%

Means

samples	N	Mean	StDev	95% CI
C/CON	2	61,045	0,304	(60,115; 61,975)
C/MW	2	61,515	0,460	(60,585; 62,445)
CUR/CON	2	58,955	0,771	(58,025; 59,885)
CUR/MW	2	59,87	0,00	(58,94; 60,80)

Pooled StDev = 0,473748

Tukey Pairwise Comparisons

Grouping Information Using the Tukey Method and 95% Confidence

samples	N	Mean	Grouping	
C/MW	2	61,515	A	
C/CON	2	61,045	A	
CUR/MW	2	59,87	A	B
CUR/CON	2	58,955		B

Means that do not share a letter are significantly different.

Table 3.7 One way Analysis of Variance (ANOVA) and Tukey's comparison test for melting enthalpy values of chickpea flour/PEO fibers

Method

Null hypothesis	All means are equal
Alternative hypothesis	Not all means are equal
Significance level	$\alpha = 0,05$

Equal variances were assumed for the analysis.

Factor Information

Factor	Levels	Values
samples	4	C/CON; C/MW; CUR/CON; CUR/MW

Analysis of Variance

Source	DF	Adj SS	Adj MS	F-Value	P-Value
samples	3	183,624	61,208	28,49	0,004
Error	4	8,594	2,148		
Total	7	192,218			

Model Summary

S	R-sq	R-sq(adj)	R-sq(pred)
1,46574	95,53%	92,18%	82,12%

Means

samples	N	Mean	StDev	95% CI
C/CON	2	53,03	1,88	(50,15; 55,91)
C/MW	2	51,428	1,129	(48,550; 54,305)
CUR/CON	2	46,43	1,89	(43,56; 49,31)
CUR/MW	2	40,766	0,490	(37,888; 43,643)

Pooled StDev = 1,46574

173

Tukey Pairwise Comparisons

Grouping Information Using the Tukey Method and 95% Confidence

samples	N	Mean	Grouping		
C/CON	2	53,03	A		
C/MW	2	51,428	A	B	
CUR/CON	2	46,43		B	C
CUR/MW	2	40,766			C

Means that do not share a letter are significantly different.

Table 3.8 One way Analysis of Variance (ANOVA) and Tukey's comparison test for DPPH scavenging activity of chickpea flour/PEO fibers

Method

Null hypothesis	All means are equal
Alternative hypothesis	Not all means are equal
Significance level	α = 0,05

Equal variances were assumed for the analysis.

Factor Information

Factor	Levels	Values
samples	4	C/CON; C/MW; CUR/CON; CUR/MW

Analysis of Variance

Source	DF	Adj SS	Adj MS	F-Value	P-Value
samples	3	2294,94	764,980	939,15	0,000
Error	4	3,26	0,815		
Total	7	2298,20			

Model Summary

S	R-sq	R-sq(adj)	R-sq(pred)
0,902523	99,86%	99,75%	99,43%

Means

samples	N	Mean	StDev	95% CI
C/CON	2	2,442	0,157	(0,670; 4,214)
C/MW	2	5,938	0,392	(4,166; 7,710)
CUR/CON	2	20,089	0,785	(18,317; 21,861)
CUR/MW	2	45,50	1,57	(43,73; 47,28)

Pooled StDev = 0,902523

174

Tukey Pairwise Comparisons

Grouping Information Using the Tukey Method and 95% Confidence

samples	N	Mean	Grouping		
CUR/MW	2	45,50	A		
CUR/CON	2	20,089		B	
C/MW	2	5,938			C
C/CON	2	2,442			C

Means that do not share a letter are significantly different.

Table 3.8 One way Analysis of Variance (ANOVA) and Tukey's comparison test for ABTS scavenging activity of chickpea flour/PEO fibers

Factor Information

Factor	Levels	Values
samples	4	C/CON; C/MW; CUR/CON; CUR/MW

Analysis of Variance

Source	DF	Adj SS	Adj MS	F-Value	P-Value
samples	3	8842,89	2947,63	722,92	0,000
Error	4	16,31	4,08		
Total	7	8859,20			

Model Summary

S	R-sq	R-sq(adj)	R-sq(pred)
2,01925	99,82%	99,68%	99,26%

Means

samples	N	Mean	StDev	95% CI
C/CON	2	10,8531	0,0764	(6,8889; 14,8174)
C/MW	2	4,860	0,153	(0,895; 8,824)
CUR/CON	2	49,78	3,51	(45,82; 53,75)
CUR/MW	2	87,47	1,99	(83,51; 91,44)

Pooled StDev = 2,01925

Tukey Pairwise Comparisons

Grouping Information Using the Tukey Method and 95% Confidence

samples	N	Mean	Grouping		
CUR/MW	2	87,47	A		
CUR/CON	2	49,78		B	
C/CON	2	10,8531			C
C/MW	2	4,860			C

Means that do not share a letter are significantly different.

Table 3.8 One way Analysis of Variance (ANOVA) and Tukey's comparison test for XRD crystallinity of chickpea flour/PEO fibers

Method

Null hypothesis	All means are equal
Alternative hypothesis	Not all means are equal
Significance level	$\alpha = 0.05$

Equal variances were assumed for the analysis.

Factor Information

Factor	Levels	Values
C1	4	C/CON; C/MW; CUR/CON; CUR/MW

Analysis of Variance

Source	DF	Adj SS	Adj MS	F-Value	P-Value
C1	3	107.851	35.9503	227.26	0.000
Error	4	0.633	0.1582		
Total	7	108.484			

Model Summary

S	R-sq	R-sq(adj)	R-sq(pred)
0.397728	99.42%	98.98%	97.67%

Means

C1	N	Mean	StDev	95% CI
C/CON	2	9.920	0.523	(9.139; 10.701)
C/MW	2	7.615	0.205	(6.834; 8.396)
CUR/CON	2	16.695	0.474	(15.914; 17.476)
CUR/MW	2	14.945	0.304	(14.164; 15.726)

Pooled StDev = 0.397728

Tukey Pairwise Comparisons

Grouping Information Using the Tukey Method and 95% Confidence

C1	N	Mean	Grouping			
CUR/CON	2	16.695	A			
CUR/MW	2	14.945		B		
C/CON	2	9.920			C	
C/MW	2	7.615				D

Means that do not share a letter are significantly different.

Table 3.8 One way Analysis of Variance (ANOVA) and Tukey's comparison test for curcumin crystallinity contribution to RDC

Method

Null hypothesis	All means are equal
Alternative hypothesis	Not all means are equal
Significance level	$\alpha = 0.05$

Equal variances were assumed for the analysis.

Factor Information

Factor	Levels Values
C5	2 CUR/CON; CUR/MW

Analysis of Variance

Source	DF	Adj SS	Adj MS	F-Value	P-Value
C5	1	106.916	106.916	463.64	0.002
Error	2	0.461	0.231		
Total	3	107.377			

Model Summary

S	R-sq	R-sq(adj)	R-sq(pred)
0.480208	99.57%	99.36%	98.28%

Means

C5	N	Mean	StDev	95% CI
CUR/CON	2	54.790	0.580	(53.329; 56.251)
CUR/MW	2	44.450	0.354	(42.989; 45.911)

Pooled StDev = 0.480208

Tukey Pairwise Comparisons

Grouping Information Using the Tukey Method and 95% Confidence

C5	N	Mean	Grouping	
CUR/CON	2	54.790	A	
CUR/MW	2	44.450		B

Means that do not share a letter are significantly different.

Table 3.9 One way Analysis of Variance (ANOVA) and Tukey's comparison test
for MC of faba bean–chitosan curcumin cross-linked films

Method

Null hypothesis	All means are equal
Alternative hypothesis	Not all means are equal
Significance level	$\alpha = 0{,}05$

Equal variances were assumed for the analysis.

Factor Information

Factor	Levels	Values
samples	7	FC-0.5C; FC-1.5C; FC-120GLU; FC-1C; FC-30GLU; FC-60GLU; FC-C

Analysis of Variance

Source	DF	Adj SS	Adj MS	F-Value	P-Value
samples	6	47,244	7,8739	19,58	0,000
Error	8	3,217	0,4021		
Total	14	50,460			

Model Summary

S	R-sq	R-sq(adj)	R-sq(pred)
0,634114	93,63%	88,84%	75,51%

Means

samples	N	Mean	StDev	95% CI
FC-0.5C	3	10,378	0,382	(9,534; 11,222)
FC-1.5C	2	12,202	0,687	(11,168; 13,236)
FC-120GLU	2	12,997	0,926	(11,963; 14,031)
FC-1C	2	12,258	0,244	(11,224; 13,292)
FC-30GLU	2	15,524	0,405	(14,490; 16,558)
FC-60GLU	2	12,220	1,026	(11,186; 13,254)
FC-C	2	9,527	0,565	(8,493; 10,561)

Pooled StDev = 0,634114

Tukey Pairwise Comparisons

Grouping Information Using the Tukey Method and 95% Confidence

samples	N	Mean	Grouping		
FC-30GLU	2	15,524	A		
FC-120GLU	2	12,997	B		
FC-1C	2	12,258	B	C	
FC-60GLU	2	12,220	B	C	
FC-1.5C	2	12,202	B	C	
FC-0.5C	3	10,378		C	D
FC-C	2	9,527			D

Means that do not share a letter are significantly different.

Table 3.9 One way Analysis of Variance (ANOVA) and Tukey's comparison test for SD of faba bean–chitosan curcumin cross-linked films

Method

Null hypothesis	All means are equal
Alternative hypothesis	Not all means are equal
Significance level	$\alpha = 0,05$

Equal variances were assumed for the analysis.

Factor Information

Factor	Levels	Values
samples	7	FC-0.5C; FC-1.5C; FC-120GLU; FC-1C; FC-30GLU; FC-60GLU; FC-C

Analysis of Variance

Source	DF	Adj SS	Adj MS	F-Value	P-Value
samples	6	22607,6	3767,93	269,81	0,000
Error	8	111,7	13,96		
Total	14	22719,3			

Model Summary

S	R-sq	R-sq(adj)	R-sq(pred)
3,73697	99,51%	99,14%	98,40%

Means

samples	N	Mean	StDev	95% CI
FC-0.5C	3	69,75	4,85	(64,77; 74,72)
FC-1.5C	2	33,64	4,37	(27,54; 39,73)
FC-120GLU	2	117,06	3,44	(110,97; 123,15)
FC-1C	2	46,77	2,11	(40,68; 52,87)
FC-30GLU	2	126,12	3,57	(120,02; 132,21)
FC-60GLU	2	128,473	1,363	(122,380; 134,567)
FC-C	2	136,59	3,84	(130,50; 142,68)

Pooled StDev = 3,73697

Tukey Pairwise Comparisons

Grouping Information Using the Tukey Method and 95% Confidence

samples	N	Mean	Grouping		
FC-C	2	136,59	A		
FC-60GLU	2	128,473	A	B	
FC-30GLU	2	126,12	A	B	
FC-120GLU	2	117,06		B	
FC-0.5C	3	69,75			C
FC-1C	2	46,77			D
FC-1.5C	2	33,64			D

Means that do not share a letter are significantly different.

Table 3.9 One way Analysis of Variance (ANOVA) and Tukey's comparison test for WS of faba bean–chitosan curcumin cross-linked films

Method

Null hypothesis	All means are equal
Alternative hypothesis	Not all means are equal
Significance level	$\alpha = 0,05$

Equal variances were assumed for the analysis.

Factor Information

Factor	Levels	Values
samples	7	FC-0.5C; FC-1.5C; FC-120GLU; FC-1C; FC-30GLU; FC-60GLU; FC-C

Analysis of Variance

Source	DF	Adj SS	Adj MS	F-Value	P-Value
samples	6	52,77	8,794	4,98	0,021
Error	8	14,13	1,766		
Total	14	66,89			

Model Summary

S	R-sq	R-sq(adj)	R-sq(pred)
1,32887	78,88%	63,04%	21,24%

Means

samples	N	Mean	StDev	95% CI
FC-0.5C	3	21,168	1,045	(19,399; 22,937)
FC-1.5C	2	17,356	1,207	(15,189; 19,523)
FC-120GLU	2	18,43	2,02	(16,26; 20,59)
FC-1C	2	21,934	0,237	(19,768; 24,101)
FC-30GLU	2	22,409	1,149	(20,242; 24,575)
FC-60GLU	2	20,52	2,21	(18,35; 22,69)
FC-C	2	22,986	0,394	(20,820; 25,153)

Pooled StDev = 1,32887

Tukey Pairwise Comparisons

Grouping Information Using the Tukey Method and 95% Confidence

samples	N	Mean	Grouping	
FC-C	2	22,986	A	
FC-30GLU	2	22,409	A	B
FC-1C	2	21,934	A	B
FC-0.5C	3	21,168	A	B
FC-60GLU	2	20,52	A	B
FC-120GLU	2	18,43	A	B
FC-1.5C	2	17,356		B

Means that do not share a letter are significantly different.

Table 3.10 One way Analysis of Variance (ANOVA) and Tukey's comparison test for TS of faba bean–chitosan curcumin cross-linked films

Method

Null hypothesis	All means are equal
Alternative hypothesis	Not all means are equal
Significance level	$\alpha = 0,05$

Equal variances were assumed for the analysis.

Factor Information

Factor	Levels	Values
samples	7	FC-0.5C; FC-1.5C; FC-120GLU; FC-1C; FC-30GLU; FC-60GLU; FC-C

Analysis of Variance

Source	DF	Adj SS	Adj MS	F-Value	P-Value
samples	6	6,36956	1,06159	213,36	0,000
Error	7	0,03483	0,00498		
Total	13	6,40439			

Model Summary

S	R-sq	R-sq(adj)	R-sq(pred)
0,0705376	99,46%	98,99%	97,82%

Means

samples	N	Mean	StDev	95% CI
FC-0.5C	2	1,7755	0,0710	(1,6576; 1,8935)
FC-1.5C	2	1,5725	0,1333	(1,4546; 1,6904)
FC-120GLU	2	1,6381	0,0685	(1,5201; 1,7560)
FC-1C	2	1,4528	0,0318	(1,3348; 1,5707)
FC-30GLU	2	0,17489	0,00231	(0,05694; 0,29283)
FC-60GLU	2	1,7637	0,0777	(1,6458; 1,8817)
FC-C	2	0,1546	0,0165	(0,0367; 0,2725)

Pooled StDev = 0,0705376

Tukey Pairwise Comparisons

Grouping Information Using the Tukey Method and 95% Confidence

samples	N	Mean	Grouping		
FC-0.5C	2	1,7755	A		
FC-60GLU	2	1,7637	A		
FC-120GLU	2	1,6381	A	B	
FC-1.5C	2	1,5725	A	B	
FC-1C	2	1,4528		B	
FC-30GLU	2	0,17489			C
FC-C	2	0,1546			C

Means that do not share a letter are significantly different.

Table 3.10 One way Analysis of Variance (ANOVA) and Tukey's comparison test for EAB of faba bean–chitosan curcumin cross-linked films

Method

Null hypothesis	All means are equal
Alternative hypothesis	Not all means are equal
Significance level	α = 0,05

Equal variances were assumed for the analysis.

Factor Information

Factor	Levels	Values
samples	7	FC-0.5C; FC-1.5C; FC-120GLU; FC-1C; FC-30GLU; FC-60GLU; FC-C

Analysis of Variance

Source	DF	Adj SS	Adj MS	F-Value	P-Value
samples	6	204,531	34,0884	105,41	0,000
Error	7	2,264	0,3234		
Total	13	206,794			

Model Summary

S	R-sq	R-sq(adj)	R-sq(pred)
0,568667	98,91%	97,97%	95,62%

Means

samples	N	Mean	StDev	95% CI
FC-0.5C	2	1,256	0,575	(0,305; 2,207)
FC-1.5C	2	12,938	1,061	(11,987; 13,888)
FC-120GLU	2	1,7125	0,1061	(0,7617; 2,6633)
FC-1C	2	4,231	0,663	(3,280; 5,182)
FC-30GLU	2	2,619	0,486	(1,668; 3,570)
FC-60GLU	2	2,438	0,177	(1,487; 3,388)
FC-C	2	1,675	0,301	(0,724; 2,626)

Pooled StDev = 0,568667

Tukey Pairwise Comparisons

Grouping Information Using the Tukey Method and 95% Confidence

samples	N	Mean	Grouping		
FC-1.5C	2	12,938	A		
FC-1C	2	4,231		B	
FC-30GLU	2	2,619		B	C
FC-60GLU	2	2,438		B	C
FC-120GLU	2	1,7125			C
FC-C	2	1,675			C
FC-0.5C	2	1,256			C

Means that do not share a letter are significantly different.

Table 3.11 One way Analysis of Variance (ANOVA) and Tukey's comparison test for onset melting temperature of faba bean chitosan crosslinked films

Method

Null hypothesis	All means are equal
Alternative hypothesis	Not all means are equal
Significance level	$\alpha = 0{,}05$

Equal variances were assumed for the analysis.

Factor Information

Factor	Levels	Values
samples	7	FC-0.5C; FC-1.5C; FC-120GLU; FC-1C; FC-30GLU; FC-60GLU; FC-C

Analysis of Variance

Source	DF	Adj SS	Adj MS	F-Value	P-Value
samples	6	58,42	9,737	3,88	0,050
Error	7	17,56	2,508		
Total	13	75,98			

Model Summary

S	R-sq	R-sq(adj)	R-sq(pred)
1,58366	76,89%	57,09%	7,57%

Means

samples	N	Mean	StDev	95% CI
FC-0.5C	2	173,560	1,004	(170,912; 176,208)
FC-1.5C	2	173,06	1,46	(170,41; 175,70)
FC-120GLU	2	174,95	2,88	(172,31; 177,60)
FC-1C	2	171,22	1,61	(168,57; 173,86)
FC-30GLU	2	169,100	0,424	(166,452; 171,748)
FC-60GLU	2	173,23	1,66	(170,58; 175,87)
FC-C	2	169,460	0,778	(166,812; 172,108)

Pooled StDev = 1,58366

Tukey Pairwise Comparisons

Grouping Information Using the Tukey Method and 95% Confidence

samples	N	Mean	Grouping
FC-120GLU	2	174,95	A
FC-0.5C	2	173,560	A
FC-60GLU	2	173,23	A
FC-1.5C	2	173,06	A
FC-1C	2	171,22	A
FC-C	2	169,460	A
FC-30GLU	2	169,100	A

Means that do not share a letter are significantly different.

Table 3.11 One way Analysis of Variance (ANOVA) and Tukey's comparison test for peak temperature of faba bean chitosan crosslinked films

Method

Null hypothesis	All means are equal
Alternative hypothesis	Not all means are equal
Significance level	$\alpha = 0{,}05$

Equal variances were assumed for the analysis.

Factor Information

Factor	Levels	Values
samples	7	FC-0.5C; FC-1.5C; FC-120GLU; FC-1C; FC-30GLU; FC-60GLU; FC-C

Analysis of Variance

Source	DF	Adj SS	Adj MS	F-Value	P-Value
samples	6	77,54	12,924	4,33	0,038
Error	7	20,91	2,987		
Total	13	98,45			

Model Summary

S	R-sq	R-sq(adj)	R-sq(pred)
1,72819	78,76%	60,56%	15,06%

Means

samples	N	Mean	StDev	95% CI
FC-0.5C	2	177,815	1,407	(174,925; 180,705)
FC-1.5C	2	178,93	1,55	(176,04; 181,81)
FC-120GLU	2	179,230	1,146	(176,340; 182,120)
FC-1C	2	176,23	1,80	(173,34; 179,12)
FC-30GLU	2	172,831	1,201	(169,941; 175,721)
FC-60GLU	2	178,05	2,84	(175,16; 180,93)
FC-C	2	173,67	1,58	(170,78; 176,56)

Pooled StDev = 1,72819

Tukey Pairwise Comparisons

Grouping Information Using the Tukey Method and 95% Confidence

samples	N	Mean	Grouping
FC-120GLU	2	179,230	A
FC-1.5C	2	178,93	A
FC-60GLU	2	178,05	A
FC-0.5C	2	177,815	A
FC-1C	2	176,23	A
FC-C	2	173,67	A
FC-30GLU	2	172,831	A

Means that do not share a letter are significantly different.

Table 3.11 One way Analysis of Variance (ANOVA) and Tukey's comparison test for end temperature of faba bean chitosan crosslinked films

Method

Null hypothesis	All means are equal
Alternative hypothesis	Not all means are equal
Significance level	$\alpha = 0,05$

Equal variances were assumed for the analysis.

Factor Information

Factor	Levels	Values
samples	7	FC-0.5C; FC-1.5C; FC-120GLU; FC-1C; FC-30GLU; FC-60GLU; FC-C

Analysis of Variance

Source	DF	Adj SS	Adj MS	F-Value	P-Value
samples	6	274,40	45,733	18,14	0,001
Error	7	17,65	2,521		
Total	13	292,05			

Model Summary

S	R-sq	R-sq(adj)	R-sq(pred)
1,58792	93,96%	88,78%	75,83%

Means

samples	N	Mean	StDev	95% CI
FC-0.5C	2	191,640	0,693	(188,985; 194,295)
FC-1.5C	2	200,10	2,66	(197,44; 202,76)
FC-120GLU	2	192,26	1,76	(189,61; 194,92)
FC-1C	2	193,540	1,032	(190,885; 196,195)
FC-30GLU	2	185,170	1,202	(182,515; 187,825)
FC-60GLU	2	193,24	1,73	(190,58; 195,90)
FC-C	2	187,430	1,230	(184,775; 190,085)

Pooled StDev = 1,58792

Tukey Pairwise Comparisons

Grouping Information Using the Tukey Method and 95% Confidence

samples	N	Mean	Grouping		
FC-1.5C	2	200,10	A		
FC-1C	2	193,540		B	
FC-60GLU	2	193,24		B	
FC-120GLU	2	192,26		B	
FC-0.5C	2	191,640		B	
FC-C	2	187,430		B	C
FC-30GLU	2	185,170			C

Means that do not share a letter are significantly different.

Table 3.11 One way Analysis of Variance (ANOVA) and Tukey's comparison test for melting enthalpy of faba bean chitosan crosslinked films (transformed)

Method

Null hypothesis	All means are equal
Alternative hypothesis	Not all means are equal
Significance level	$\alpha = 0.05$

Equal variances were assumed for the analysis.

Factor Information

Factor	Levels	Values
sample	7	FC-0.5C; FC-1.5C; FC-120GLU; FC-1C; FC-30GLU; FC-60GLU; FC-C

Analysis of Variance

Source	DF	Adj SS	Adj MS	F-Value	P-Value
sample	6	0.000000	0.000000	240.04	0.000
Error	7	0.000000	0.000000		
Total	13	0.000000			

Model Summary

S	R-sq	R-sq(adj)	R-sq(pred)
0.0000031	99.52%	99.10%	98.07%

Means

sample	N	Mean	StDev	95% CI
FC-0.5C	2	0.000079	0.000002	(0.000074; 0.000084)
FC-1.5C	2	0.000025	0.000000	(0.000019; 0.000030)
FC-120GLU	2	0.000095	0.000004	(0.000090; 0.000100)
FC-1C	2	0.000036	0.000001	(0.000031; 0.000041)
FC-30GLU	2	0.000095	0.000002	(0.000089; 0.000100)
FC-60GLU	2	0.000116	0.000005	(0.000111; 0.000121)
FC-C	2	0.000092	0.000004	(0.000087; 0.000097)

Pooled StDev = 3.080241E-06

Tukey Pairwise Comparisons

Grouping Information Using the Tukey Method and 95% Confidence

sample	N	Mean	Grouping			
FC-60GLU	2	0.000116	A			
FC-120GLU	2	0.000095		B		
FC-30GLU	2	0.000095		B		
FC-C	2	0.000092		B		
FC-0.5C	2	0.000079			C	
FC-1C	2	0.000036				D
FC-1.5C	2	0.000025				D

Means that do not share a letter are significantly different.

Table 3.12 One way Analysis of Variance (ANOVA) and Tukey's comparison test for DPPH of faba bean chitosan crosslinked films

Method

Null hypothesis	All means are equal
Alternative hypothesis	Not all means are equal
Significance level	α = 0,05

Equal variances were assumed for the analysis.

Factor Information

Factor	Levels	Values
samples	7	FC-0.5C; FC-1.5C; FC-120GLU; FC-1C; FC-30GLU; FC-60GLU; FC-C

Analysis of Variance

Source	DF	Adj SS	Adj MS	F-Value	P-Value
samples	6	216,710	36,118	34,74	0,000
Error	7	7,278	1,040		
Total	13	223,988			

Model Summary

S	R-sq	R-sq(adj)	R-sq(pred)
1,01965	96,75%	93,97%	87,00%

Means

samples	N	Mean	StDev	95% CI
FC-0.5C	2	9,41	1,82	(7,70; 11,11)
FC-1.5C	2	11,73	0,00	(10,02; 13,43)
FC-120GLU	2	10,299	1,186	(8,594; 12,004)
FC-1C	2	15,206	0,911	(13,501; 16,911)
FC-30GLU	2	10,898	0,169	(9,193; 12,603)
FC-60GLU	2	8,563	0,254	(6,858; 10,268)
FC-C	2	20,747	1,276	(19,043; 22,452)

Pooled StDev = 1,01965

Tukey Pairwise Comparisons

Grouping Information Using the Tukey Method and 95% Confidence

samples	N	Mean	Grouping		
FC-C	2	20,747	A		
FC-1C	2	15,206		B	
FC-1.5C	2	11,73		B	C
FC-30GLU	2	10,898			C
FC-120GLU	2	10,299			C
FC-0.5C	2	9,41			C
FC-60GLU	2	8,563			C

Means that do not share a letter are significantly different.

Table 3.12 One way Analysis of Variance (ANOVA) and Tukey's comparison test for ABTS of faba bean chitosan crosslinked films

Method

Null hypothesis	All means are equal
Alternative hypothesis	Not all means are equal
Significance level	$\alpha = 0,05$

Equal variances were assumed for the analysis.

Factor Information

Factor	Levels	Values
samples	7	FC-0.5C; FC-1.5C; FC-120GLU; FC-1C; FC-30GLU; FC-60GLU; FC-C

Analysis of Variance

Source	DF	Adj SS	Adj MS	F-Value	P-Value
samples	6	6257,87	1042,98	198,51	0,000
Error	7	36,78	5,25		
Total	13	6294,65			

Model Summary

S	R-sq	R-sq(adj)	R-sq(pred)
2,29218	99,42%	98,91%	97,66%

Means

samples	N	Mean	StDev	95% CI
FC-0.5C	2	33,016	0,384	(29,184; 36,849)
FC-1.5C	2	34,579	0,288	(30,746; 38,411)
FC-120GLU	2	28,20	3,64	(24,37; 32,04)
FC-1C	2	60,80	3,55	(56,97; 64,63)
FC-30GLU	2	27,66	2,88	(23,83; 31,50)
FC-60GLU	2	25,868	1,016	(22,036; 29,701)
FC-C	2	86,549	1,153	(82,716; 90,382)

Pooled StDev = 2,29218

Grouping Information Using the Tukey Method and 95% Confidence

samples	N	Mean	Grouping		
FC-C	2	86,549	A		
FC-1C	2	60,80		B	
FC-1.5C	2	34,579			C
FC-0.5C	2	33,016			C
FC-120GLU	2	28,20			C
FC-30GLU	2	27,66			C
FC-60GLU	2	25,868			C

Means that do not share a letter are significantly different.

Table 3.13 One way Analysis of Variance (ANOVA) and Tukey's comparison test for MC of chickpea flour–chitosan curcumin cross-linked films

Method

Null hypothesis	All means are equal
Alternative hypothesis	Not all means are equal
Significance level	$\alpha = 0,05$

Equal variances were assumed for the analysis.

Factor Information

Factor	Levels	Values
samples	4	0- CUR/CF/CS; 0.5- CUR/CF/CS; 1- CUR/CF/CS; 1.5- CUR/CF/CS

Analysis of Variance

Source	DF	Adj SS	Adj MS	F-Value	P-Value
samples	3	51,6260	17,2087	187,93	0,000
Error	4	0,3663	0,0916		
Total	7	51,9923			

Model Summary

S	R-sq	R-sq(adj)	R-sq(pred)
0,302605	99,30%	98,77%	97,18%

Means

samples	N	Mean	StDev	95% CI
0- CUR/CF/CS	2	16,686	0,566	(16,092; 17,280)
0.5- CUR/CF/CS	2	9,7483	0,1241	(9,1542; 10,3424)
1- CUR/CF/CS	2	12,257	0,156	(11,663; 12,851)
1.5- CUR/CF/CS	2	11,6693	0,0752	(11,0752; 12,2634)

Pooled StDev = 0,302605

Tukey Pairwise Comparisons

Grouping Information Using the Tukey Method and 95% Confidence

samples	N	Mean	Grouping	
0- CUR/CF/CS	2	16,686	A	
1- CUR/CF/CS	2	12,257	B	
1.5- CUR/CF/CS	2	11,6693	B	
0.5- CUR/CF/CS	2	9,7483		C

Means that do not share a letter are significantly different.

Table 3.13 One way Analysis of Variance (ANOVA) and Tukey's comparison test for WS of chickpea flour–chitosan curcumin cross-linked films

Method

Null hypothesis	All means are equal
Alternative hypothesis	Not all means are equal
Significance level	$\alpha = 0{,}05$

Equal variances were assumed for the analysis.

Factor Information

Factor	Levels	Values
samples	4	0- CUR/CF/CS; 0.5- CUR/CF/CS; 1- CUR/CF/CS; 1.5- CUR/CF/CS

Analysis of Variance

Source	DF	Adj SS	Adj MS	F-Value	P-Value
samples	3	20,150	6,7166	16,98	0,010
Error	4	1,582	0,3955		
Total	7	21,732			

Model Summary

S	R-sq	R-sq(adj)	R-sq(pred)
0,628891	92,72%	87,26%	70,88%

Means

samples	N	Mean	StDev	95% CI
0- CUR/CF/CS	2	19,5896	0,0071	(18,3549; 20,8242)
0.5- CUR/CF/CS	2	22,248	0,250	(21,013; 23,482)
1- CUR/CF/CS	2	24,017	1,224	(22,782; 25,251)
1.5- CUR/CF/CS	2	22,389	0,147	(21,155; 23,624)

Pooled StDev = 0,628891

Tukey Pairwise Comparisons

Grouping Information Using the Tukey Method and 95% Confidence

samples	N	Mean	Grouping
1- CUR/CF/CS	2	24,017	A
1.5- CUR/CF/CS	2	22,389	A
0.5- CUR/CF/CS	2	22,248	A
0- CUR/CF/CS	2	19,5896	B

Means that do not share a letter are significantly different.

Table 3.13 One way Analysis of Variance (ANOVA) and Tukey's comparison test for SD of chickpea flour–chitosan curcumin cross-linked films

Method

Null hypothesis	All means are equal
Alternative hypothesis	Not all means are equal
Significance level	$\alpha = 0{,}05$

Equal variances were assumed for the analysis.

Factor Information

Factor	Levels	Values
samples	4	0- CUR/CF/CS; 0.5- CUR/CF/CS; 1- CUR/CF/CS; 1.5- CUR/CF/CS

Analysis of Variance

Source	DF	Adj SS	Adj MS	F-Value	P-Value
samples	3	12814,8	4271,60	87,72	0,000
Error	4	194,8	48,70		
Total	7	13009,6			

Model Summary

S	R-sq	R-sq(adj)	R-sq(pred)
6,97831	98,50%	97,38%	94,01%

Means

samples	N	Mean	StDev	95% CI
0- CUR/CF/CS	2	133,60	11,85	(119,90; 147,30)
0.5- CUR/CF/CS	2	66,79	1,97	(53,09; 80,49)
1- CUR/CF/CS	2	41,30	7,08	(27,60; 55,00)
1.5- CUR/CF/CS	2	30,726	0,622	(17,025; 44,426)

Pooled StDev = 6,97831

Tukey Pairwise Comparisons

Grouping Information Using the Tukey Method and 95% Confidence

samples	N	Mean	Grouping	
0- CUR/CF/CS	2	133,60	A	
0.5- CUR/CF/CS	2	66,79	B	
1- CUR/CF/CS	2	41,30	B	C
1.5- CUR/CF/CS	2	30,726		C

Means that do not share a letter are significantly different.

Table 3.14 One way Analysis of Variance (ANOVA) and Tukey's comparison test for WVP of chickpea flour–chitosan curcumin cross-linked films

Method

Null hypothesis	All means are equal
Alternative hypothesis	Not all means are equal
Significance level	$\alpha = 0{,}05$

Equal variances were assumed for the analysis.

Factor Information

Factor	Levels	Values
samples	4	0- CUR/CF/CS; 0.5- CUR/CF/CS; 1- CUR/CF/CS; 1.5- CUR/CF/CS

Analysis of Variance

Source	DF	Adj SS	Adj MS	F-Value	P-Value
samples	3	11,7975	3,93248	40,41	0,002
Error	4	0,3893	0,09733		
Total	7	12,1868			

Model Summary

S	R-sq	R-sq(adj)	R-sq(pred)
0,311972	96,81%	94,41%	87,22%

Means

samples	N	Mean	StDev	95% CI
0- CUR/CF/CS	2	5,7024	0,1330	(5,0899; 6,3148)
0.5- CUR/CF/CS	2	7,048	0,505	(6,436; 7,661)
1- CUR/CF/CS	2	7,23936	0,00324	(6,62688; 7,85184)
1.5- CUR/CF/CS	2	9,112	0,341	(8,499; 9,724)

Pooled StDev = 0,311972

Tukey Pairwise Comparisons

Grouping Information Using the Tukey Method and 95% Confidence

samples	N	Mean	Grouping	
1.5- CUR/CF/CS	2	9,112	A	
1- CUR/CF/CS	2	7,23936	B	
0.5- CUR/CF/CS	2	7,048	B	
0- CUR/CF/CS	2	5,7024		C

Means that do not share a letter are significantly different.

Table 3.14 One way Analysis of Variance (ANOVA) and Tukey's comparison test for TS of chickpea flour–chitosan curcumin cross-linked films

Method

Null hypothesis	All means are equal
Alternative hypothesis	Not all means are equal
Significance level	$\alpha = 0,05$

Equal variances were assumed for the analysis.

Factor Information

Factor	Levels Values
samples	4 0- CUR/CF/CS; 0.5- CUR/CF/CS; 1- CUR/CF/CS; 1.5- CUR/CF/CS

Analysis of Variance

Source	DF	Adj SS	Adj MS	F-Value	P-Value
samples	3	25,842	8,6141	34,43	0,003
Error	4	1,001	0,2502		
Total	7	26,843			

Model Summary

S	R-sq	R-sq(adj)	R-sq(pred)
0,500199	96,27%	93,48%	85,09%

Means

samples	N	Mean	StDev	95% CI
0- CUR/CF/CS	2	7,8320	0,0806	(6,8500; 8,8140)
0.5- CUR/CF/CS	2	7,169	0,745	(6,187; 8,151)
1- CUR/CF/CS	2	4,378	0,631	(3,396; 5,361)
1.5- CUR/CF/CS	2	3,584	0,201	(2,602; 4,566)

Pooled StDev = 0,500199

Tukey Pairwise Comparisons

Grouping Information Using the Tukey Method and 95% Confidence

samples	N	Mean	Grouping	
0- CUR/CF/CS	2	7,8320	A	
0.5- CUR/CF/CS	2	7,169	A	
1- CUR/CF/CS	2	4,378		B
1.5- CUR/CF/CS	2	3,584		B

Means that do not share a letter are significantly different.

Table 3.14 One way Analysis of Variance (ANOVA) and Tukey's comparison test for EAB of chickpea flour–chitosan curcumin cross-linked films

Method

Null hypothesis   All means are equal
Alternative hypothesis Not all means are equal
Significance level $\alpha = 0,05$
Equal variances were assumed for the analysis.

Factor Information

Factor	Levels Values
samples	4 0- CUR/CF/CS; 0.5- CUR/CF/CS; 1- CUR/CF/CS; 1.5- CUR/CF/CS

Analysis of Variance

Source	DF	Adj SS	Adj MS	F-Value	P-Value
samples	3	133,222	44,4072	63,73	0,001
Error	4	2,787	0,6968		
Total	7	136,009			

Model Summary

S	R-sq	R-sq(adj)	R-sq(pred)
0,834720	97,95%	96,41%	91,80%

Means

samples	N	Mean	StDev	95% CI
0- CUR/CF/CS	2	1,6438	0,1326	(0,0050; 3,2825)
0.5- CUR/CF/CS	2	2,350	0,371	(0,711; 3,989)
1- CUR/CF/CS	2	8,881	1,069	(7,242; 10,520)
1.5- CUR/CF/CS	2	11,100	1,220	(9,461; 12,739)

Pooled StDev = 0,834720

Tukey Pairwise Comparisons

Grouping Information Using the Tukey Method and 95% Confidence

samples	N	Mean	Grouping
1.5- CUR/CF/CS	2	11,100	A
1- CUR/CF/CS	2	8,881	A
0.5- CUR/CF/CS	2	2,350	B
0- CUR/CF/CS	2	1,6438	B

Means that do not share a letter are significantly different.

Table 3.15 One way Analysis of Variance (ANOVA) and Tukey's comparison test for onset melting temperature of chickpea flour–chitosan curcumin cross-linked films

Method

Null hypothesis	All means are equal
Alternative hypothesis	Not all means are equal
Significance level	$\alpha = 0,05$

Equal variances were assumed for the analysis.

Factor Information

Factor	Levels	Values
samples	4	0- CUR/CF/CS; 0.5- CUR/CF/CS; 1- CUR/CF/CS; 1.5- CUR/CF/CS

Analysis of Variance

Source	DF	Adj SS	Adj MS	F-Value	P-Value
samples	3	3,741	1,247	0,07	0,975
Error	4	75,247	18,812		
Total	7	78,988			

Model Summary

S	R-sq	R-sq(adj)	R-sq(pred)
4,33724	4,74%	0,00%	0,00%

Means

samples	N	Mean	StDev	95% CI
0- CUR/CF/CS	2	166,70	2,03	(158,19; 175,22)
0.5- CUR/CF/CS	2	165,69	1,94	(157,17; 174,21)
1- CUR/CF/CS	2	166,92	4,32	(158,40; 175,43)
1.5- CUR/CF/CS	2	165,28	6,98	(156,76; 173,79)

Pooled StDev = 4,33724

Tukey Pairwise Comparisons

Grouping Information Using the Tukey Method and 95% Confidence

samples	N	Mean	Grouping
1- CUR/CF/CS	2	166,92	A
0- CUR/CF/CS	2	166,70	A
0.5- CUR/CF/CS	2	165,69	A
1.5- CUR/CF/CS	2	165,28	A

Means that do not share a letter are significantly different.

Table 3.15 One way Analysis of Variance (ANOVA) and Tukey's comparison test for peak melting temperature of chickpea flour–chitosan curcumin cross-linked films

Method

Null hypothesis	All means are equal
Alternative hypothesis	Not all means are equal
Significance level	$\alpha = 0,05$

Equal variances were assumed for the analysis.

Factor Information

Factor	Levels	Values
samples	4	0- CUR/CF/CS; 0.5- CUR/CF/CS; 1- CUR/CF/CS; 1.5- CUR/CF/CS

Analysis of Variance

Source	DF	Adj SS	Adj MS	F-Value	P-Value
samples	3	7,319	2,440	0,15	0,924
Error	4	64,768	16,192		
Total	7	72,087			

Model Summary

S	R-sq	R-sq(adj)	R-sq(pred)
4,02392	10,15%	0,00%	0,00%

Means

samples	N	Mean	StDev	95% CI
0- CUR/CF/CS	2	170,25	1,79	(162,36; 178,15)
0.5- CUR/CF/CS	2	168,06	1,90	(160,17; 175,96)
1- CUR/CF/CS	2	169,58	3,99	(161,68; 177,48)
1.5- CUR/CF/CS	2	168,06	6,48	(160,17; 175,96)

Pooled StDev = 4,02392

Tukey Pairwise Comparisons

Grouping Information Using the Tukey Method and 95% Confidence

samples	N	Mean	Grouping
0- CUR/CF/CS	2	170,25	A
1- CUR/CF/CS	2	169,58	A
1.5- CUR/CF/CS	2	168,06	A
0.5- CUR/CF/CS	2	168,06	A

Means that do not share a letter are significantly different.

Table 3.15 One way Analysis of Variance (ANOVA) and Tukey's comparison test for end melting temperature of chickpea flour–chitosan curcumin cross-linked films

Method

Null hypothesis	All means are equal
Alternative hypothesis	Not all means are equal
Significance level	$\alpha = 0,05$

Equal variances were assumed for the analysis.

Factor Information

Factor	Levels Values
samples	4 0- CUR/CF/CS; 0.5- CUR/CF/CS; 1- CUR/CF/CS; 1.5- CUR/CF/CS

Analysis of Variance

Source	DF	Adj SS	Adj MS	F-Value	P-Value
samples	3	24,26	8,087	1,31	0,388
Error	4	24,77	6,191		
Total	7	49,03			

Model Summary

S	R-sq	R-sq(adj)	R-sq(pred)
2,48826	49,49%	11,60%	0,00%

Means

samples	N	Mean	StDev	95% CI
0- CUR/CF/CS	2	181,065	0,417	(176,180; 185,950)
0.5- CUR/CF/CS	2	176,30	1,72	(171,41; 181,18)
1- CUR/CF/CS	2	179,58	2,23	(174,69; 184,47)
1.5- CUR/CF/CS	2	178,44	4,08	(173,56; 183,33)

Pooled StDev = 2,48826

Tukey Pairwise Comparisons

Grouping Information Using the Tukey Method and 95% Confidence

samples	N	Mean	Grouping
0- CUR/CF/CS	2	181,065	A
1- CUR/CF/CS	2	179,58	A
1.5- CUR/CF/CS	2	178,44	A
0.5- CUR/CF/CS	2	176,30	A

Means that do not share a letter are significantly different.

Table 3.15 One way Analysis of Variance (ANOVA) and Tukey's comparison test for melting enthalpy of chickpea flour–chitosan curcumin cross-linked films

Method

Null hypothesis	All means are equal
Alternative hypothesis	Not all means are equal
Significance level	$\alpha = 0,05$

Equal variances were assumed for the analysis.

Factor Information

Factor	Levels	Values
samples	4	0- CUR/CF/CS; 0.5- CUR/CF/CS; 1- CUR/CF/CS; 1.5- CUR/CF/CS

Analysis of Variance

Source	DF	Adj SS	Adj MS	F-Value	P-Value
samples	3	6686,2	2228,75	73,57	0,001
Error	4	121,2	30,30		
Total	7	6807,4			

Model Summary

S	R-sq	R-sq(adj)	R-sq(pred)
5,50419	98,22%	96,88%	92,88%

Means

samples	N	Mean	StDev	95% CI
0- CUR/CF/CS	2	81,18	5,78	(70,37; 91,99)
0.5- CUR/CF/CS	2	99,98	6,98	(89,17; 110,79)
1- CUR/CF/CS	2	144,33	6,06	(133,52; 155,13)
1.5- CUR/CF/CS	2	149,17	1,55	(138,36; 159,97)

Pooled StDev = 5,50419

Tukey Pairwise Comparisons

Grouping Information Using the Tukey Method and 95% Confidence

samples	N	Mean	Grouping	
1.5- CUR/CF/CS	2	149,17	A	
1- CUR/CF/CS	2	144,33	A	
0.5- CUR/CF/CS	2	99,98		B
0- CUR/CF/CS	2	81,18		B

Means that do not share a letter are significantly different.

Table 3.16 One way Analysis of Variance (ANOVA) and Tukey's comparison test for DPPH scavenging activity of chickpea flour–chitosan curcumin cross-linked films

Method

Null hypothesis	All means are equal
Alternative hypothesis	Not all means are equal
Significance level	α = 0,05

Equal variances were assumed for the analysis.

Factor Information

Factor	Levels	Values
samples	4	0- CUR/CF/CS; 0.5- CUR/CF/CS; 1- CUR/CF/CS; 1.5- CUR/CF/CS

Analysis of Variance

Source	DF	Adj SS	Adj MS	F-Value	P-Value
samples	3	0,130462	0,043487	133,63	0,000
Error	4	0,001302	0,000325		
Total	7	0,131764			

Model Summary

S	R-sq	R-sq(adj)	R-sq(pred)
0,0180399	99,01%	98,27%	96,05%

Means

samples	N	Mean	StDev	95% CI
0- CUR/CF/CS	2	0,3265	0,0170	(0,2910; 0,3619)
0.5- CUR/CF/CS	2	0,52125	0,00997	(0,48583; 0,55667)
1- CUR/CF/CS	2	0,2308	0,0301	(0,1954; 0,2663)
1.5- CUR/CF/CS	2	0,19050	0,00297	(0,15508; 0,22592)

Pooled StDev = 0,0180399

Tukey Pairwise Comparisons

Grouping Information Using the Tukey Method and 95% Confidence

samples	N	Mean	Grouping		
0.5- CUR/CF/CS	2	0,52125	A		
0- CUR/CF/CS	2	0,3265		B	
1- CUR/CF/CS	2	0,2308			C
1.5- CUR/CF/CS	2	0,19050			C

Means that do not share a letter are significantly different.

Table 3.16 One way Analysis of Variance (ANOVA) and Tukey's comparison test for ABTS scavenging activity of chickpea flour–chitosan curcumin cross-linked films

Method

Null hypothesis	All means are equal
Alternative hypothesis	Not all means are equal
Significance level	$\alpha = 0,05$

Equal variances were assumed for the analysis.

Factor Information

Factor	Levels	Values
samples	4	0- CUR/CF/CS; 0.5- CUR/CF/CS; 1- CUR/CF/CS; 1.5- CUR/CF/CS

Analysis of Variance

Source	DF	Adj SS	Adj MS	F-Value	P-Value
samples	3	0,232962	0,077654	237,11	0,000
Error	4	0,001310	0,000328		
Total	7	0,234272			

Model Summary

S	R-sq	R-sq(adj)	R-sq(pred)
0,0180972	99,44%	99,02%	97,76%

Means

samples	N	Mean	StDev	95% CI
0- CUR/CF/CS	2	0,3300	0,0341	(0,2945; 0,3655)
0.5- CUR/CF/CS	2	0,42845	0,00898	(0,39292; 0,46398)
1- CUR/CF/CS	2	0,05385	0,00799	(0,01832; 0,08938)
1.5- CUR/CF/CS	2	0,03680	0,00198	(0,00127; 0,07233)

Pooled StDev = 0,0180972

Tukey Pairwise Comparisons

Grouping Information Using the Tukey Method and 95% Confidence

samples	N	Mean	Grouping		
0.5- CUR/CF/CS	2	0,42845	A		
0- CUR/CF/CS	2	0,3300		B	
1- CUR/CF/CS	2	0,05385			C
1.5- CUR/CF/CS	2	0,03680			C

Means that do not share a letter are significantly different.

CURRICULUM VITAE

Surname, Name: Yıldız, Eda

EDUCATION

Degree	Institution	Year of Graduation
MS	METU Food Engineering	2016
BS	METU Food Engineering	2014
High School	Ankara Lisesi (Anadolu), Ankara	2009

FOREIGN LANGUAGES

Advanced English,

PUBLICATIONS

Emir, A. A., Yildiz, E., Aydogdu, Y., Sumnu, G. (2022). Active films based on faba bean (Vicia faba L.) flour incorporated sumac (Rhus coriaria): Assessment of antioxidant and antimicrobial performances of packaging for shelf life of chicken breast. Food and Bioproduct processing. (Accepted Manuscript)

Yildiz, E., Emir, A. A., Sumnu, G. & Kahyaoglu, L. N. (2022). Citric acid cross-linked curcumin/chitosan/chickpea flour film: An active packaging for chicken breast storage. Food Bioscience, 50(PA), 102121. https://doi.org/10.1016/j.fbio.2022.102121

Yildiz, E., Sumnu, G. & Kahyaoglu, L. N. (2022). Assessment of curcumin incorporated chickpea flour / PEO (polyethylene oxide) based electrospun nanofiber as an antioxidant and antimicrobial food package. Food and Bioproducts

Processing, 135, 205–216. https://doi.org/10.1016/j.fbp.2022.08.002

Yildiz, E., İlhan, E., Kahyaoglu, L. N., Sumnu, G. & Oztop, M. H.(2021). The effects of crosslinking agents on faba bean flour–chitosan- curcumin films and their characterization. Legume Science, 1–13.

Aydogdu Emir, A., Yildiz, E., Aydogdu, Y., Sumnu, G., & Sahin, S. (2021). Gallic acid encapsulated pea flour-based nanofibers produced by electrospinning as a potential active food packaging material. Legume Science, (February), 1–10. https://doi.org/10.1002/leg3.90

Yildiz, E., Sumnu, G., & Kahyaoglu, L. N. (2021). Monitoring freshness of chicken breast by using natural halochromic curcumin loaded chitosan / PEO nano fibers as an intelligent package. International Journal of Biological Macromolecules, 170, 437–446. https://doi.org/10.1016/j.ijbiomac.2020.12.160

Yildiz, E., Bayram, I., Sumnu, G., Sahin, S., & Ibis, O. I. (2021). Development of pea flour based active films produced through different homogenization methods and their effects on lipid oxidation. Food Hydrocolloids, 111(August 2020), 106238. https://doi.org/10.1016/j.foodhyd.2020.106238

Uygun, E., Yildiz, E., Sumnu, G., & Sahin, S. (2020). Microwave Pretreatment for the improvement of physicochemical properties of carob flour and rice starch-based electrospun nanofilms. Food and Bioprocess Technology. https://doi.org/10.1007/s11947-020-02440-x

Yildiz, E., Sumnu, G., & Sahin, S. (2019). Effects of microwave-assisted baking on quality of gluten-free cakes and breads. Cereal Foods World, 64(4), 51–63.

Aydogdu, A., Yildiz, E., Aydogdu, Y., Sumnu, G., Sahin, S., & Ayhan, Z. (2019). Enhancing oxidative stability of walnuts by using gallic acid loaded lentil flour based electrospun nanofibers as active packaging material. Food Hydrocolloids, 95(April), 245–255. https://doi.org/10.1016/j.foodhyd.2019.04.020

Aydogdu, A., Yildiz, E., Ayhan, Z., Aydogdu, Y., Sumnu, G., & Sahin, S. (2019). Nanostructured poly(lactic acid)/soy protein/HPMC films by electrospinning for

potential applications in food industry. European Polymer Journal, 112(December 2018), 477–486. https://doi.org/10.1016/j.eurpolymj.2019.01.006

Yildiz, E., Guner, S., Sumnu, G., Sahin, S., & Oztop, M. H. (2018). Monitoring the effects of ingredients and baking methods on quality of gluten-free cakes by Time-Domain (TD) NMR Relaxometry. Food and Bioprocess Technology, 11(10), 1923–1933. https://doi.org/10.1007/s11947-018-2152-z

Yildiz, E., Şumnu, S. G., & Şahin, S. (2018). Effects of buckwheat flour, gums and proteins on rheological properties of gluten-free batters and structure of cakes. Quality Assurance and Safety of Crops and Foods, 10(3), 245–254. https://doi.org/10.3920/QAS2017.1221

Berk (Yildiz), E., Sumnu, G., & Sahin, S. (2017). Usage of carob bean flour in gluten free cakes. Chemical Engineering Transactions, 57, 1909–1914. https://doi.org/10.3303/CET1757319

Berk, (Yildiz) E., Şumnu, S. G., & Şahin, S. (2017). Effects of hydrocolloids and carob bean flour on rheological properties of batter and cake quality. Gida/The Journal of Food, 42(6), 754–762. https://doi.org/10.15237/gida.GD17079